OTOLITH AGE VALIDATION AND MICROCHEMICAL INVESTIGATION OF THE NORTHERN STOCK OF ATLANTIC BLACK SEA BASS (*CENTROPRISTIS STRIATA*)

A Thesis Presented

by

ELISE R. KOOB

Submitted to the Office of Graduate Studies,
University of Massachusetts Boston,
in partial fulfillment of the requirements for the degree of

MASTER OF SCIENCE

December 2020

Intercampus Marine Science Program

OTOLITH AGE VALIDATION AND MICROCHEMICAL INVESTIGATION OF THE NORTHERN STOCK OF ATLANTIC BLACK SEA BASS (*CENTROPRISTIS STRIATA*)

A Thesis Presented

by

ELISE R. KOOB

Approved as to style and content by:

_____
John Mandelman, Research Faculty
Chairperson of Committee

_____
Michael Armstrong, Adjunct Faculty
University of Massachusetts Amherst
Member

_____
Robyn Hannigan, Provost
Clarkson University
Member

_____
Ron Etter, Professor
Member

_____
Juanita Urban-Rich, Program Director
Environmental Sciences and Marine Science & Technology Program

_____
Robert Chen, Dean
School for the Environment

ABSTRACT

OTOLITH AGE VALIDATION AND MICROCHEMICAL INVESTIGATION OF THE NORTHERN STOCK OF ATLANTIC BLACK SEA BASS (*CENTROPRISTIS STRIATA*)

December 2020

Elise R. Koob, B.S., University of New Hampshire Durham
M.S., University of Massachusetts Boston

Directed by Dr. John Mandelman

Black sea bass (*Centropristis striata*) is a demersal marine species that supports extensive commercial and recreational fisheries along the Atlantic coast. A recent expansion into the Gulf of Maine raises questions about this species' movement and population dynamics in the region. Additionally, the 2016 catch-at-age stock assessment model for the northern stock incorporated a population split at the Hudson Canyon. Though this model better accounts for differences in populations, several issues remain. First, validation of the otolith ageing technique for this stock is incomplete; and, second, the origin of fish that moved into the northern ranges of the Gulf of Maine (GOM) remains unclear.

Error stemming from inaccurate age determinations can have serious effects on age-structured calculations (e.g. growth rate) leading to stock assessments that do not correctly reflect the population. In this study, I validated the black sea bass otolith ageing method

using marginal increment analysis and young-of-year annulus measurements. Samples spanned the spatial distribution and age range of the northern stock. Results indicated black sea bass otoliths complete an annual increment, one translucent and one opaque band, in the late spring or early summer. Additionally, the first annulus was validated, an important step in verifying total age that is not present in the current literature for this species.

The natal origin of black sea bass caught in the northern ranges of the GOM was assessed by otolith core trace element and stable isotope microchemistry. Analysis of spawning adult otoliths identified unique chemical fingerprints for the regions north and south of the Hudson Canyon: Southern New England (SNE) and the mid-Atlantic Bight (MAB), respectively. Black sea bass caught in Maine waters were assigned to a spawning region by matching chemical fingerprints. Overall, 87% were assigned to SNE and 13% to the MAB.

This project helps to improve the accuracy and precision of black sea bass otolith ageing practices by validating the method used by agencies and organizations across its distribution. Additionally, this project confirms hypotheses that SNE spawned fish moved north, and further elucidates population composition of the GOM, an area where little is known about this species.

ACKNOWLEDGEMENTS

I would like to begin by thanking my advisors, John Mandelman and Michael Armstrong, for mentoring me from the development of this project and applying to the University of Massachusetts Boston (UMB), to writing and defending this thesis. I would also like to thank my committee members, Robyn Hannigan and Ron Etter, for their guidance and invaluable insights along the way. Additionally, I would like to thank Lisa Kerr, whose collaboration on this project I could not have gone without.

A huge thank you to the Age and Growth laboratory at the Massachusetts Division of Marine Fisheries (MA DMF), particularly Scott Elzey and Kim Trull, for helping me develop ideas for this study, process and age over 1,000 black sea bass otoliths, and analyze results. I could not have accomplished this without you!

This project could not have been completed without the generous support of collaborators along the Atlantic coast. I would like to thank MA DMF, the Northeast Fisheries Science Center, Rutgers University, Northeastern University, the North Carolina Department of Environment and Natural Resources, and the Rhode Island Department of Environmental Management in collaboration with the Commercial Fisheries Research Foundation and the Virginia Institute for Marine Science for providing me with black sea bass otoliths from Maine to Cape Hatteras throughout all months of the year. The archived otolith sample these agencies helped me collect for this project was incredible. I would also like to thank the following individuals from each of these institutions for their guidance and eagerness to help, from answering a plethora of my questions and connecting me to new collaborators to supplying and transporting samples: Eric Robillard, Sandy Sutherland, Gary

Shepherd, Richard McBride, Doug Zemeckis, Mattea Burglund, Marissa McMahan, Todd VanMiddlesworth, Nicole Lengyel, Thomas Heimann, James Garland, and Jeff Kneebone. I would also like to thank Lisa Kerr and Zach Whitener at the Gulf of Maine Research Institute for access to instrumentation and help processing samples for the microchemical analyses I conducted. The Environmental Analytics Facility at UMB, particularly Alan Christian, Alan Stebbins, and Amy Johnson, also deserve a huge thank you for assistance in processing microchemistry samples and data.

Thank you to the Atlantic Coastal Cooperative Statistics Program for funding this project as part of the FY2017 award period. An additional thank you to MA DMF and its Education Policy for the opportunity to pursue a graduate degree while continuing my work for the agency.

I'd like to express an abundance of appreciation to those who helped read and edit this thesis many times over: Joseph Koob, Kathy Furman, Anna Webb, Scott Elzey, and Christy Draghetti. Finally, many thanks to all my friends and family for their love, encouragement, and support over the past few years. I am extremely grateful to have such a wonderful group of people by my side. I would also like to thank my husband, Patrick, for his unrelenting love and support, and for always motivating me to achieve my goals.

TABLE OF CONENTS

CHAPTER Page

LIST OF FIGURES

Figure Page

LIST OF TABLES

CHAPTER 1

INTRODUCTION

Fisheries management often involves a multi-disciplinary approach to the sustainable allocation of marine resources. Managers implement fisheries regulations using information from biological stock assessments, socio-economic influences, sustainability goals, and stakeholder inputs (Cochrane and Garcia 2009). Stock assessments evaluate the status of a fish stock by utilizing information gathered about a species, such as behavior, migration, and stock structure, as well as measured or calculated biological parameters, like age, growth, mortality, and maturity (Jennings et al. 2001). Changes to distributions, a misunderstanding of basic life history, or an overall lack of data for a species can undermine stock assessments and fisheries management, leading to overexploitation of a fish stock (Campana 2001; Pilling et al. 2008; Kleisner et al. 2017). Thus, collecting accurate information is imperative to the successful management of a species and its continued, sustainable exploitation.

The black sea bass *(Centropristis striata)* is a demersal, marine bony fish that is found in the Gulf of Mexico and along the Atlantic coast, from Florida to the Gulf of Maine (GOM). These populations are split into three distinct stocks: Gulf of Mexico, northern Atlantic stock, and southern Atlantic stock; originally based on meristic, morphometric, and growth differences (Miller 1959; Mercer 1978) and more recently confirmed by genetics (Bowen and Avise 1990; Roy et al. 2012; Mccartney et al. 2013; Lewandowski 2014). The

Gulf of Mexico stock is a separate subspecies, *Centropristis striata melana*, from the Atlantic populations, both of which are designated *Centropristis striata striata* (Miller 1959). Atlantic black sea bass are separated into two distinct stocks north and south of Cape Hatteras, North Carolina based on differing behavioral and growth characteristics (Mercer 1978; Wenner et al. 1986). Data suggests occasional mixing from north to south during the overwintering period; however, Cape Hatteras largely acts as a biogeographical boundary that inhibits significant migration and larval transport (Roy et al. 2012; Mccartney et al. 2013). The northern Atlantic stock of black sea bass is the focus of this research project and the basis of discussion for the remainder of this work.

Black sea bass in the north Atlantic most commonly reside in structured habitats, rock piles, reefs, and wrecks (Kendall 1977; Fabrizio et al. 2014; Cullen and Stevens 2017) but also were documented feeding in sandy habitats (Steimle et al. 1999; Cullen and Stevens 2017). Black sea bass are opportunistic bottom feeders consuming a large array of prey, though the majority of their diet is made up of crustaceans (crabs and shrimp), small fish, and mollusks (Bigelow and Schroeder 1953; Mercer 1989; Hood et al. 1994; Steimle et al. 1999; McMahan et al. 2020). This species can live to approximately 12 years of age (Mercer 1978; Shepherd and Lambert 1996); and reach 65cm in length (Bigelow and Schroeder 1953; Kendall 1977). Black sea bass not only have an important commercial fishery along the Atlantic coast (Musick and Mercer 1977; Able et al. 1995), but also an extremely valued recreational fishery that equates to about half the total annual landings of the species (Cadrin et al. 2016; NEFSC 2017). Inshore fisheries (primarily pots and hook-and-line) occur

between May and October, while the offshore trawl fishery occurs from November to March (Shepherd and Terceiro 1994; Miller et al. 2016b).

Black sea bass are protogynous hermaphrodites, meaning they typically change sexes from female to male (Lavenda 1949; Kendall 1977). They mature between 1 to 3 years of age and transition between 2 to 5 years of age (Mercer 1978; O'Brien et al. 1993; Shepherd and Idoine 1993). Atypical reproductive characteristics are also occasionally observed in this species, such as prematurational transformation (Wuenschel et al. 2011), maturation as young, small males (Provost et al. 2017), or they forgo transition resulting in older, large females (Blaylock and Shepherd 2016). Transition from female to male primarily happens after the spawning period (Mercer 1978; Wuenschel et al. 2011; Provost et al. 2017), which occurs near shore from late spring through the summer. Populations in the mid-Atlantic Bight have a protracted spawning period from April through October and peak in July (Mercer 1978; Able et al. 1995; Drohan et al. 2007); whereas populations north of New York typically spawn from May to July (Kolek 1990; Caruso 1995; Wuenschel et al. 2013; McBride et al. 2018).

The northern stock of black sea bass undergo seasonal migratory movements, offshore in the fall and returning inshore in the spring (Kendall 1977; Musick and Mercer 1977; Mercer 1978; Shepherd and Lambert 1996; Moser and Shepherd 2009). Water temperatures trigger these movements, dropping below 10-12°C in the fall and returning to approximately 7°C for the spring migration (Kolek 1990; Drohan et al. 2007; Moser and Shepherd 2009). Fish from regions north of the Hudson Canyon tend to move south and east in the fall, toward the outer continental shelf; whereas individuals originating in the mid-

Atlantic Bight tend to migrate directly east, with little to no southerly movements (Able et al. 1995; Moser and Shepherd 2009). This difference results in disparate distances traveled to overwintering grounds for black sea bass originating from these two regions. Additionally, more northerly fish tend to begin the fall migration sooner due to an earlier decline in water temperatures, meaning they also spend more time offshore than their southern counterparts (Moser and Shepherd 2009; Miller et al. 2016a). During their first fall, young-of-year (YOY) black sea bass move offshore later than larger, older fish (Musick and Mercer 1977; Able et al. 1995; Able and Hales 1997), needing extra time for growth to survive migration and overwintering (Miller et al. 2016a). Temperature and salinity are importance factors for overwintering sites, with most fish found in areas over 8°C and with salinity between 33–35 practical salinity units (Bigelow and Schroeder 1953; Miller et al. 2016a). This species' return inshore in the spring is characterized by homing to previous spawning grounds (Kolek 1990; Moser and Shepherd 2009; Fabrizio et al. 2013), though Moser and Shepherd (2009) noted that fish traveling longer distances were less likely to return to the exact inshore tagging location, with some individuals exhibiting "occasional straying" to the north.

Historically, black sea bass were rarely encountered north of the Cape Cod islands (Bigelow and Schroeder 1953; Kendall 1977) but are now observed in much higher numbers. Analysis of recreational catch and fishery-independent survey data from the past 15 years showed increasing trends in juvenile and adult black sea bass north of the Hudson Canyon (Miller et al. 2016a; SARC 2016). Additionally, commercial and recreational fishermen reported increasing abundance and expanded distributions of this species in northern regions (Cadrin et al. 2016; McMahan 2017). Black sea bass larval distributions have also moved

northward. Able et al. (1995) found YOY off eastern Long Island, Rhode Island, and Massachusetts (North and South Cape Cod), areas in which YOY were not documented prior to 1987. McBride et al. (2018) analyzed fishery-independent survey data (1978-2016) and noted that YOY are now seen along the entire north Atlantic coast in the fall and that nursery grounds are moving northward by 0.021 degrees of latitude annually (total of 1 degree north over the last 40 years). They also note developing females were documented, for the first time, in the southern GOM (McBride et al. 2018).

Changes observed in the northern stock of black sea bass may be in response to warming ocean waters. The GOM is warming faster than most places on Earth (Pershing et al. 2015), with an average rate of warming that increased from 0.026°C yr^{-1} since the early 1980's to 0.26°C yr^{-1} since 2004 (Mills et al. 2013). Many species along the Atlantic coast have exhibited poleward distribution shifts, as well as earlier and faster seasonal migrations due to increased ocean temperatures (Murawski 1993; Nye et al. 2009; Mills et al. 2013; Pinsky et al. 2013). Bell et al. (2015) and Kleisner et al. (2016) demonstrated similar behavior in black sea bass, observing northerly distribution trends associated with temperature. McBride et al. (2018) and Miller et al. (2016a) also correlated the northward expansion and abundance of YOY, juveniles, and adults with warmer temperatures.

An alternative hypothesis indicates the apparent distribution shift of black sea bass may be a product of increased reproductive productivity in the northern region of the stock as opposed to fish moving from south to north in large numbers (McBride et al. 2018). As discussed, catches have increased north of Hudson Canyon, but have remained the same or slightly reduced in the mid-Atlantic Bight (Miller et al. 2016a). This increase in productivity

could be forcing individuals to seek alternative habitat in the GOM due to density overflow. Other hypotheses regarding the success of black sea bass colonization in the GOM include enhanced recruitment due to improved nursery conditions (Bell et al. 2015) or an open predator niche has allowed black sea bass to thrive (McMahan 2017). Regardless of the influencing factors, the GOM's rapidly warming waters have provided a new habitat that was previously inaccessible or too energetically taxing for the species to survive and proliferate. Moser and Shepherd (2009) explained that the benefit of moving to a new habitat must be higher than the costs associated with the added migration or changes to life history. Thus, black sea bass' movement north into the GOM indicates there must be optimal habitat, or a benefit to life history, now available that once was not.

Nevertheless, little is known about this species' movement, interactions, and potential for long-term success in the GOM. Distribution shifts can have cascading effects and major implications for management (Fogarty et al. 2007; Bell et al. 2015; Pershing et al. 2015). Since black sea bass were long considered "a rare stray to the north" (Bigelow and Schroeder 1953), there is limited data available to advise management decisions in the GOM.

The Atlantic States Marine Fisheries Commission and the mid-Atlantic Fishery Management Council jointly manage the northern stock of Atlantic black sea bass (NEFSC 2004). Concerns of insufficient age data, as well as unknowns regarding spatial structure and population mixing, led to the rejection of a catch-at-age stock assessment model in 2012 (NEFSC 2012; ASMFC 2013). The recommendations following this rejection prioritized the collection of information on growth, age, migration patterns, and stock structure and signified black sea bass as a species of importance (NEFSC 2012; ASMFC 2014). In

response, agencies along the Atlantic coast began to collect and age black sea bass samples to supplement data for future stock assessments (ASMFC 2013). Additionally, the investigation of tagging studies, fisheries independent trawl surveys, commercial and recreational fisheries data, and oceanographic conditions of the region provided support for a geographical separation of the northern stock at the Hudson Canyon (Cadrin et al. 2016; Miller et al. 2016b; SARC 2016). As a result, an age-based statistical catch-at-age model was accepted at the 62nd Northeast Regional Stock Assessment Workshop in 2016 using spatial sub-units north and south of the Hudson Canyon (NEFSC 2017).

Although the new stock assessment better represents the status and movement patterns of black sea bass in the northern stock, several issues remain. One concern involves the age data supplied to the stock assessment. Black sea bass age determination is predominantly completed using otoliths, which are often considered the most accurate ageing structure (Beamish and McFarlane 1983; Casselman 1983). Otoliths, or ear stones, accrete calcium carbonate layers daily that are visually differentiated between seasons as opaque or translucent bands (Pannella 1971). These bands are counted to determine age, using the assumption that one opaque band and one translucent band equate to one year in a fish's life. This assumption, however, must be validated. Despite the increase in direct ageing effort by agencies across the north Atlantic coast, there has been little effort to complete a large-scale age validation study for black sea bass in the northern stock. Mercer (1978) included validation work in their study but the samples were limited in spatial area, age range, and sample size. Robillard et al. (2016) described an age validation study for otoliths and scales; however, the oxytetracycline tagging and marginal increment analysis completed on otoliths

involved a small sample size (n = 55) and age range (2-5 years old), and the capture location for otolith samples was not defined.

Age data is vital to estimating parameters for stock assessments such as age at maturity, mortality, size at age, growth functions, and spawning stock biomass (Beamish and McFarlane 1983; Campana and Thorrold 2001; Natanson et al. 2002). Inaccurate age data can undermine fisheries management and lead to overexploitation (Campana 2001). Additionally, any shift in otolith deposition patterns or timing due to recent changes in the northern stock have not yet been explored. These issues highlight the need for a large-scale, directed age validation study for the northern stock of black sea bass to ensure that accurate age data are submitted to future stock assessments.

Another issue concerning black sea bass in the north Atlantic is the unknown origin of fish now captured in the GOM, particularly in the northern GOM. One argument is that fish or larvae are transported through the Cape Cod Canal into Cape Cod Bay and advected north; however, there is little evidence thus far to support this hypothesis (G. Shepherd, personal communication, 2017; McBride et al. 2018). Alternatively, individuals could be migrating around Cape Cod, but there are no published tagging studies targeting fish caught in the GOM to confirm. Previous tagging studies show that black sea bass exhibited site fidelity and homing to spawning grounds when returning from seasonal migrations; however, individuals farther north exhibited straying behavior (Kolek 1990; Moser and Shepherd 2009). Regardless, GOM-caught individuals are most likely fish from the southern New England region, rather than mass migration from the mid-Atlantic. Confirmation of this

hypothesis is imperative, though, as this type of migration change could greatly impact stock assessments and management regulations.

Otolith microchemical analysis is an alternative to physically tagging and releasing live fish, which is extremely time and resource intensive. Otolith calcium carbonate layers used for age determinations can also be analyzed for compounds incorporated from the surrounding environment. Microchemical analysis is used in a variety of applications including: identifying separate stocks (Campana et al. 1994), discerning migration patterns (Elsdon et al. 2008), classifying nursery grounds (Kerr et al. 2007) and inferring environmental history (Thorrold et al. 1997b). Natal origin is assessed by analyzing the chemical composition of otolith cores (i.e. the region within the first few months of a fish's life) to create unique 'chemical fingerprints' of natal regions (Campana and Neilsson 1985; Kalish 1989). Comparing the core chemical fingerprints from black sea bass caught in the GOM to regions of known spawning could clarify where these fish originated and provide novel information about the population composition in this area.

The purpose of this thesis is to validate the otolith age determination methods used for black sea bass and employ otolith microchemical analyses to answer questions about this species' movement into the GOM. In Chapter 2, I use marginal increment analysis to identify the timing of annulus deposition and confirm they occur once per year. In addition, I verify the location of the first annulus with YOY measurements and modal length frequency analysis. In Chapter 3, I analyze otolith cores from black sea bass caught in three regions: GOM (Maine), southern New England (SNE; northern Massachusetts to the Hudson Canyon) and the mid-Atlantic Bight (MAB; Hudson Canyon to Cape Hatteras, North Carolina) to

glean natal origin information for GOM caught samples. My hypotheses are that (1) black sea bass complete an annual increment, one translucent and one opaque band, in the late spring or early summer, (2) YOY black sea bass measurements and modal length frequency will verify identification of the first annulus, (3) the otolith core elemental fingerprints between SNE and MAB will be significantly different, and (4) classification of GOM black sea bass will result in samples matching the core fingerprint of SNE and not MAB.

References

Able, K. W., M. P. Fahay, and G. R. Shepherd. 1995. Early life history of black sea bass, Centropristis striata, in the mid-Atlantic Bight and a New Jersey estuary. Fishery Bulletin 93:429–445.

Able, K. W., and L. S. Hales. 1997. Movements of juvenile black sea bass Centropristis striata (Linnaeus) in a southern New Jersey estuary. Journal of Experimental Marine Biology and Ecology 213:153–167.

ASMFC. 2013. Proceedings of the 2013 black sea bass ageing workshop. Atlantic States Marine Fisheries Commission:1–18.

ASMFC. 2014. 2015 Action Plan. Atlantic States Marine Fisheries Commission:1–28.

Beamish, R. J., and G. A. McFarlane. 1983. The forgotten requirement for age validation in fisheries biology. Transactions of the American Fisheries Society 112(6):735–743.

Bell, R. J., D. E. Richardson, J. A. Hare, P. D. Lynch, and P. S. Fratantoni. 2015. Disentangling the effects of climate, abundance, and size on the distribution of marine fish: an example based on four stocks from the Northeast US shelf. ICES Journal of Marine Science 72(5):1311–1322.

Bigelow, H. B., and W. C. Schroeder. 1953. Black sea bass, Centropristis striata. Pages 407–409 Fishes of the Gulf of Maine. Vol 53. Fishery Bulletin of the Fish and Wildlife Service.

Blaylock, J., and G. R. Shepherd. 2016. Evaluating the vulnerability of an atypical protogynous hermaphrodite to fishery exploitation: results from a population model for black sea bass (Centropristis striata). Fishery Bulletin 114:476–489. National Marine Fisheries Service.

Bowen, B. W. W., and J. C. C. Avise. 1990. Genetic structure of Atlantic and Gulf of Mexico populations of sea bass, menhaden, and sturgeon: influence of zoogeographic factors and life-history patterns. Marine Biology 107:371–381.

Cadrin, S., R. Leaf, and O. Jensen. 2016. Contributions to the SAW62 black sea bass stock assessment. Science Center for Marine Fisheries:1–6.

Campana, S. E. 2001. Accuracy, precision and quality control in age determination, including a review of the use and abuse of age validation methods. Journal of Fish Biology 59:197–242.

Campana, S. E., A. J. Fowler, and C. M. Jones. 1994. Otolith elemental fingerprinting for stock identification of Atlantic Cod (Gadus morhua) using laser ablation ICPMS. Canadian Journal of Fisheries & Aquatic Sciences 51:1942–1950.

Campana, S. E., and D. Neilsson. 1985. Microstructure of fish otoliths. Canadian Journal of Fisheries & Aquatic Sciences 42:1014–1032.

Campana, S. E., and S. R. Thorrold. 2001. Otoliths, increments, and elements: keys to a comprehensive understanding of fish populations? Canadian Journal of Fisheries & Aquatic Sciences 58(1):30–38.

Caruso, P. G. 1995. The age, growth, and spawning of black sea bass (Centropristis striata, Linneaus) in Massachusetts waters. MADMF Black Sea Bass Investigations Internal Report:11–25.

Casselman, J. M. 1983. Age and growth assessment of fish from their calcified structures-techniques and tools. Pages 1–17 in E. D. Prince and L. M. Pulos, editors. Proceedings of the International Workshop on Age Determination of Oceanic Pelagic Fishes: Tunas, Billfishes, and Sharks. NOAA Technical Report NMFS 8. Miami, Florida.

Cochrane, K. L., and S. M. Garcia. 2009. A Fishery Manager's Guidebook: Second. The Food and Agriculture Organization of the United Nations and Wiley-Blackwell, United Kingdom.

Cullen, D. W., and B. G. Stevens. 2017. Use of an underwater video system to record observations of black sea bass (Centropristis striata) in waters off the coast of Maryland. Fishery Bulletin 115:408–418.

Drohan, A. F., J. P. Manderson, and D. B. Packer. 2007. Essential fish habitat source document: black sea bass, Centropristis striata, life history and habitat characteristics. NOAA Technical Memorandum NMFS-NE-200. Woods Hole, MA.

Elsdon, T. S., B. K. Wells, S. E. Campana, B. M. Gillanders, C. M. Jones, K. E. Limburg, D. H. Secor, S. R. Thorrold, and B. D. Walther. 2008. Otolith chemistry to describe movements and life-history parameters of fishes: hypotheses, assumptions, limitations and inferences. Oceanography and Marine Biology 46:297–330.

Fabrizio, M. C., J. P. Manderson, and J. P. Pessutti. 2013. Habitat associations and dispersal of black sea bass from a mid-Atlantic Bight reef. Marine Ecology Progress Series 482:241–253.

Fabrizio, M. C., J. P. Manderson, and J. P. Pessutti. 2014. Home range and seasonal movements of black sea bass (Centropristis striata) during their inshore residency at a reef in the mid-Atlantic Bight. Fishery Bulletin 112:82–97.

Fogarty, M., L. Incze, R. Wahle, D. Mountain, A. Robinson, A. Pershing, K. Hayhoe, A. Richards, and J. Manning. 2007. Potential climate change impacts on marine resources of the northeastern United States. Climate Change and Marine Resources Impacts:1–33.

Hood, P. B., M. F. Godcharles, and R. S. Barco. 1994. Age, growth, reproduction, and the feeding ecology of black sea bass (Centropristis striata) in the eastern Gulf of Mexico. Bulletin of Marine Science 54(1):24–37.

Jennings, S., M. J. Kaiser, and J. D. Reynolds. 2001. Marine fisheries ecology. Blackwell Science Ltd, Malden, MA.
Kalish, J. M. 1989. Otolith microchemistry: validation of the effects of physiology, age and environment on otolith composition. Journal of Experimental Marine Biology and Ecology 132:151–178.
Kendall, A. W. 1977. Biological and fisheries data on black sea bass, Centropristis striata (Linnaeus). Highlands, NJ.
Kerr, L. A., D. H. Secor, and R. T. Kraus. 2007. Stable isotope (δ13C and δ18O) and Sr/Ca composition of otoliths as proxies for environmental salinity experienced by an estuarine fish. Marine Ecology Progress Series 349:245–253.
Kleisner, K. M., M. J. Fogarty, S. McGee, A. Barnett, P. Fratantoni, J. Greene, J. A. Hare, S. M. Lucey, C. McGuire, J. Odell, V. S. Saba, L. Smith, K. J. Weaver, and M. L. Pinsky. 2016. The effects of sub-regional climate velocity on the distribution and spatial extent of marine species assemblages. PLoS ONE 11(2):1–21.
Kleisner, K. M., M. J. Fogarty, S. McGee, J. A. Hare, S. Moret, C. T. Perretti, and V. S. Saba. 2017. Marine species distribution shifts on the U.S. Northeast Continental Shelf under continued ocean warming. Progress in Oceanography 153:24–36.
Kolek, D. 1990. Homing of black sea bass, Centropristis striata, in Nantucket Sound, with comments on seasonal distribution, growth rates, and fisheries of the species. MADMF Black Sea Bass Investigations Internal Report:2–9.
Lavenda, N. 1949. Sexual differences and normal protogynous hermaphroditism in the Atlantic sea bass, Centropristes striatus. Copeia 3:185–194.
Lewandowski, J. F. 2014. Genetic stock identification and migration in black sea bass (Centropristis striata) along the western Atlantic coast and Gulf of Mexico. University of South Carolina.
McBride, R. S., M. K. Tweedie, and K. Oliveira. 2018. Reproduction, first-year growth, and expansion of spawning and nursery grounds of black sea bass (Centropristis striata) into a warming Gulf of Maine. Fishery Bulletin 116:323–336.
Mccartney, M. A., M. L. Burton, and T. G. Lima. 2013. Mitochondrial DNA differentiation between populations of black sea bass (Centropristis striata) across Cape Hatteras, North Carolina (USA). Journal of Biogeography 40:1386–1398.
McMahan, M. D. 2017. Ecological and socioeconomic implications of a northern range expansion of black sea bass, Centropristis striata. Northeastern University.
McMahan, M. D., G. D. Sherwood, and J. H. Grabowski. 2020. Geographic variation in life-history traits of black sea bass (Centropristis striata) during a rapid range expansion. Frontiers in Marine Science 7(567758):1–15.
Mercer, L. P. 1978. The reproductive biology and population dynamics of black sea bass, Centropristis striata. The College of William and Mary.
Mercer, L. P. 1989. Species profiles: life histories and environmental requirements of coastal fishes and invertebrates (South Atlantic): Black Sea Bass. U.S. Fish Wildlife Service Biological Report 82, Morehead City, NC.
Miller, A. S., G. R. Shepherd, and P. S. Fratantoni. 2016a. Offshore habitat preference of overwintering juvenile and adult black sea bass, Centropristis striata, and the relationship to year-class success. PLoS ONE 11(1):1–19.

Miller, R. J. 1959. A review of the sea basses of the genus Centropristis (Serranidae). Tulane Studies in Zoology and Botany 7(2):35–68.
Miller, T. J., R. J. Latour, K. Drew, and J. Wiedenmann. 2016b. Proposed partitioning of northern black sea bass stock for purposes of developing spatial stock assessment models. Report to the Mid-Atlantic Fishery Management Council's Scientific and Statistical Committee:1–5.
Mills, K. E., A. J. Pershing, C. J. Brown, Y. Chen, F.-S. Chiang, D. S. Holland, S. Lehuta, J. A. Nye, J. C. Sun, A. C. Thomas, and R. A. Wahle. 2013. Fisheries management in a changing climate: lessons from the 2012 ocean heat wave in the Northwest Atlantic. Oceanography 26(2):191–195.
Moser, J., and G. R. Shepherd. 2009. Seasonal distribution and movement of black sea bass (Centropristis striata) in the northwest Atlantic as determined from a mark-recapture experiment. Journal of Northwest Atlantic Fishery Science 40:17–28. Northwest Atlantic Fisheries Organization.
Murawski, S. A. 1993. Climate change and marine fish distributions: forecasting from historical analogy. Transactions of the American Fisheries Society 122(5):647–658.
Musick, J. A., and L. P. Mercer. 1977. Seasonal distribution of black sea bass, Centropristis striata, in the Mid-Atlantic Bight with comments on the ecology and fisheries of the species. Transactions of the American Fisheries Society 106(1):12–25.
Natanson, L. J., J. J. Mello, and S. E. Campana. 2002. Validated age and growth of the porbeagle shark (Lamna nasus) in the western North Atlantic Ocean. Fisheries Bulletin 100:266–278.
NEFSC. 2004. 39th assessment of the northern stock of black sea bass consensus assessment report. Northeast Fisheries Science Center SARC 39:9–86.
NEFSC. 2012. 53rd Northeast regional stock assessment workshop. Northeast Fisheries Science Center Reference Assessment Summary Report:1–33.
NEFSC. 2017. 62nd Northeast regional stock assessment workshop. Northeast Fisheries Science Center Reference Assessment Summary Report:1–36.
Nye, J. A., J. S. Link, J. A. Hare, and W. J. Overholtz. 2009. Changing spatial distribution of fish stocks in relation to climate and population size on the Northeast United States continental shelf. Marine Ecology Progress Series 393:111–129.
O'Brien, L., J. Burnett, and R. K. Mayo. 1993. Maturation of nineteen species of finfish off the Northeast coast of the United States, 1985-1990. NOAA Technical Report NMFS 113:1–66.
Pannella, G. 1971. Fish otoliths: daily growth layers and periodical patterns. Science 173:1124–1127.
Pershing, A. J., M. A. Alexander, C. M. Hernandez, L. A. Kerr, A. Le Bris, K. E. Mills, J. A. Nye, N. R. Record, H. A. Scannell, J. D. Scott, G. D. Sherwood, and A. C. Thomas. 2015. Slow adaptation in the face of rapid warming leads to collapse of the Gulf of Maine cod fishery. Science 350(6262):809–812.
Pilling, G. M., P. Apostolaki, P. Failler, C. Floros, P. A. Large, B. Morales-Nin, P. Reglero, K. I. Stergiou, and A. C. Tsikliras. 2008. Assessment and management of data-poor fisheries. Pages 280–305 Advances in Fisheries Science: 50 years on from Beverton and Holt.

Pinsky, M. L., B. Worm, M. J. Fogarty, J. L. Sarmiento, and S. A. Levin. 2013. Marine taxa track local climate Velocities. Science 341:1239–1242.

Provost, M. M., O. P. Jensen, and D. L. Berlinsky. 2017. Influence of size, age, and spawning season on sex change in black sea bass. Marine and Coastal Fisheries 9(1):126–138. Taylor & Francis.

Robillard, E., J. W. Gregg, J. Dayton, and J. Gartland. 2016. Validation of black sea bass, Centropristis striata, ages using oxytetracycline marking and scale margin increments. Appendix A1, Stock Assessment Report of Black Sea Bass. Woods Hole, MA.

Roy, E. M., J. M. Quattro, and T. W. Greig. 2012. Genetic management of black sea bass: influence of biogeographic barriers on population structure. Marine and Coastal Fisheries 4(1):391–402.

SARC. 2016. Proposed partitioning of northern black sea bass stock for purposes of developing spatial stock assessment models. Black Sea Bass Benchmark Stock Assessment Review Term of Reference - Spatial Issues:1–40.

Shepherd, G. R., and J. S. Idoine. 1993. Length-based analyses of yield and spawning biomass per recruit for black sea bass Centropristis striata, a protogynous hermaphrodite. Fishery Bulletin 91:328–337.

Shepherd, G. R., and M. C. Lambert. 1996. Assessment of black sea bass north of Cape Hatteras, North Carolina. Northeast Fisheries Science Center Reference Document 95-17:1–15.

Shepherd, G. R., and M. Terceiro. 1994. The summer flounder, scup, and black sea bass fishery of the middle Atlantic Bight and Southern New England waters. NOAA Technical Report NMFS 122:1–13, Woods Hole, MA.

Steimle, F. W., C. A. Zetlin, P. L. Berrien, and S. Chang. 1999. Essential fish habitat source document: life history and habitat characteristics. NOAA Technical Memorandum NMFS-NE-143:1–42.

Thorrold, S. R., C. M. Jones, and S. E. Campana. 1997. Response of otolith microchemistry to environmental variations experienced by larval and juvenile Atlantic croaker (Micropogonias undulatus). Limnology and Oceanography 42(1):102–111.

Wenner, C. A., W. A. Roumillat, and C. W. Waltz. 1986. Contributions to the life history of black sea bass, Centropristis striata, off the Southeastern United States. Fishery Bulletin 84(3):723–741.

Wuenschel, M. J., R. S. McBride, and G. R. Fitzhugh. 2013. Relations between total gonad energy and physiological measures of condition in the period leading up to spawning: results of a laboratory experiment on black sea bass (Centropristis striata). Fisheries Research 138:110–119.

Wuenschel, M. J., G. R. Shepherd, R. S. McBride, R. Jorgensen, K. Oliverira, E. Robillard, and J. Dayton. 2011. Sex and maturity of black sea bass collected in Massachusetts and Rhode Island waters; preliminary results based on macroscopic staging of gonads with a comparison to survey data. Working Paper for SARC 53-Black Sea Bass Meeting:529–559.

CHAPTER 2

AGE VALIDATION OF THE NORTHERN STOCK OF ATLANTIC BLACK SEA BASS USING MARGINAL INCREMENT ANALYSIS AND FIRST ANNULUS VALIDATION

Introduction

The northern Atlantic stock of black sea bass *(Centropristis striata)* extends from Cape Hatteras, North Carolina to the Gulf of Maine (GOM; Mercer 1978). This species can live approximately 12 years of age (Mercer 1978; Shepherd and Lambert 1996) and reach 65cm in length (Bigelow and Schroeder 1953; Kendall 1977). Black sea bass support an important commercial fishery (Musick and Mercer 1977; Able et al. 1995), as well as a valued recreational fishery that equates to about half the total annual landings (Cadrin et al. 2016; NEFSC 2017). This stock experienced a recent range expansion into Maine waters, a region in which this species was rarely seen historically (Bigelow and Schroeder 1953; Kendall 1977), and has been linked to warming ocean trends (Bell et al. 2015; Kleisner et al. 2016; Miller et al. 2016a; McBride et al. 2018). Reliance on this fishery, combined with data gaps regarding growth, age, migration patterns, and stock structure, led to the designation of black sea bass as a species of importance and a push for additional research (ASMFC 2014).

A catch-at-age stock assessment model for the north Atlantic stock of black sea bass was rejected in 2012, in part due to insufficient age data (NEFSC 2012; ASMFC 2013). Age data are used to calculate a variety of parameters, such as age at recruitment, age at maturity,

growth rates, age structure, productivity estimations, and mortality rates (Beamish and McFarlane 1983; Penttila and Dery 1988; Natanson et al. 2002). In response, agencies along the Atlantic coast began to collect and age black sea bass samples and a statistical catch-at-age model was accepted in 2016 (NEFSC 2017). Despite the increase in direct ageing, there has been little effort to complete a large-scale age validation study for this stock.

Current black sea bass age determinations are primarily completed using otoliths, or ear stones, which are considered the most accurate ageing structure in many species (Beamish and McFarlane 1983; Casselman 1983). Calcium carbonate layers are accreted onto otoliths daily and a seasonal banding pattern is formed, differentiated as opaque or translucent (Campana and Thorrold 2001). Age is determined by counting paired bands from otolith core (birth) to otolith edge (capture), making the assumption that one opaque band and one translucent band equals one year in a fish's life (Beamish and McFarlane 1983). Error occurs when growth layers identified as annuli (yearly growth bands) do not truly correspond to one year of growth and can lead to fisheries overexploitation (Campana 2001; McBride 2015). Validation of an ageing method is a process that verifies assumed annuli occur once per year. These studies also help identify checks, or false annuli, which are regions of growth that can be difficult to differentiate from a true annulus (Penttila and Dery 1988). Though there have been several attempts to validate black sea bass otolith ageing methods, these studies have been limited by small spatial ranges, few age classes, and/or modest sample sizes (Mercer 1978; Robillard et al. 2016). Thus far, there has not been a large-scale age validation study for the northern Atlantic stock of black sea bass, using

samples representative of those included in the stock assessment process, i.e. from a variety of gear types, locations, sources, and age classes.

The most common method of age validation is marginal increment analysis (MIA), which measures growth from the last fully completed annulus to the edge of the ageing structure (i.e. the marginal increment) at different times throughout the year (Campana 2001). Marginal increments are then expressed as a proportion of the previous year's growth and plotted as means by month (Hood et al. 1994; Fowler and Short 1998; Franks et al. 1999; Winner et al. 2017). If annuli are formed once per year and growth continues throughout the year, these plots should form a sinusoidal pattern with only one minimum per year (when annulus formation is complete and new growth begins), confirming the annual periodicity of the growth band (Mercer 1978; Wenner et al. 1986; Fowler 1990; Lehodey and Grandperrin 1996; Vilizzi and Walker 1999; Pilling et al. 2000). Additionally, marginal increment measurements help to determine the timing of annulus formation which can then clarify many ageing errors (VanderKooy et al. n.d.).

Verifying the location of the first annulus is also an imperative step in validating ageing methods, otherwise, age estimates could err by a consistent amount (Campana 2001). Assessment of the first annulus can be completed by (1) measuring the completed first annulus of young-of-year (YOY) in the season of annulus formation, and (2) tracking the modal length frequency of the smallest fish in the population to confirm that measured samples are YOY (Campana 2001; Carvalho et al. 2017b).

The lack of a comprehensive age validation study, recent implementation of an age-based stock assessment model, and issues identifying the first annulus (Dery and Mayo 1988;

ASMFC 2013; Robillard et al. 2016) highlight the need to conduct a large-scale otolith age validation study for this stock. The goal of this study was to identify the timing of annulus deposition and validate the current otolith ageing method for the entire spatial range and observed age classes of the northern Atlantic stock of black sea bass, using MIA and first annulus validation of YOY. I hypothesized that (1) black sea bass complete an annual increment, one translucent and one opaque band, in the late spring or early summer, and (2) YOY black sea bass measurements and modal length frequency analysis will verify identification of the first annulus.

Methodology

Sample Collection and Selection

MIA requires samples to be collected across an entire year, preferably monthly, as well as across the observed age-range of the selected species (Beamish and McFarlane 1983; Campana 2001). Black sea bass samples in this study were split up into three age bins: ages 1-2 (AB 1), ages 3-4 (AB 2) and ages 5 and older (AB 3), to account for growth differences. These bins were chosen based on a combination of visual differences in growth across this species' lifetime and sampling likelihood. For example, AB 3 was chosen to encompass ages 5 and above due to a slowed growth pattern and similarity in band widths at these ages. Additionally, obtaining the goal sample size at the largest ages in order to constitute a separate bin would be difficult. Likewise, obtaining enough samples for ages 1 and 2 to be separate bins was unlikely; therefore, these were binned together despite rapid growth within each age. To capture potential growth variability among regions due to the large spatial scale

covered (i.e. Cape Hatteras to Maine), a goal of 40 samples per age bin was chosen. Black sea bass sagittal otolith samples were acquired from collaborators across the northeastern United States from both fishery dependent and independent sources (Table 2.1).

Age determinations supplied by collaborative institutions were used to bin samples to begin processing. Otoliths without age estimates were binned based on an age-length key created from previously aged samples. An initial subsample (n = 1008) was created with available otoliths by randomly selecting approximately 30 samples within each age bin and month. A second subsample (n = 432) was taken after remaining otoliths were received from collaborators to fill the 40 samples per age bin per month goal.

Samples for the first annulus validation measurements required YOY sample collection from the MA-DMF fall Resource Assessment Survey (2017; n = 30), as well as YOY from the NEFSC Winter Bottom Trawl Survey archive (2016; n = 3). Age 1 samples that had growth at the edge of the otolith, i.e. new translucent growth deposited after the first annulus, were also needed for comparison. Age 1+ otolith selection was completed after this information was acquired from the MIA. Subsequently, age 1+ otoliths selected for first annulus measurements were from July-August in Massachusetts waters (2015-2016; n = 36).

A reference collection (n = 100) spanning ages 0 to 10 was also created using MA-DMF archived otoliths. These samples were used to assess reader error before and after completing otolith ageing for this project and were independent of the samples used in MIA.

Sample Preparation

Sectioned otoliths were used in this study. Whole otoliths tend to underestimate fish age and sectioning results in higher accuracy (Mercer 1978; Hyndes et al. 1992; Fowler and

Short 1998). Additionally, completing marginal increment measurements on whole otoliths is difficult due to their curvature and presence of broad, diffuse bands; whereas, sectioned otoliths have a crisp line at the edge of an annulus from which to measure. Left-sided otoliths were selected preferentially for consistency in subsequent microchemistry studies. All otolith preparation followed these methods including those samples for the MIA, first annulus analysis, and reference collection.

Prior to sectioning, black sea bass whole otoliths were photographed under reflected light at 1.42x magnification using a camera-microscope system and Image Pro® Premier software V9.1 (Media Cybernetics, Inc., Rockville, MD). Otoliths not previously sectioned (n = 1,365) were embedded using West System® epoxy resin and hardener in silicone molds. Transverse sections (0.5mm) along the dorsoventral plane, containing the otolith core (Figure 2.1) were removed using a low speed Buehler® Iso-Met™ diamond blade saw and stored in labeled Fisherbrand® 1.5 mL plastic vials.

Otolith Ageing and Measurements

Black sea bass annuli are considered to be the winter growth zone (opaque band) and a date of January 1 was used for year class advancement (Dery and Mayo 1988). Age determinations were made under a compound microscope (100x) by placing sectioned samples on a glass slide with mineral oil. Each sample was aged by two independent readers without knowledge of fish size, capture location, or any previous age interpretations. Ages that differed between readers required a third, consensus, determination before analyses were performed. These ages were used to group samples into the three age bins for analysis, in lieu of the initial determination used to bin samples during the sample selection. Age

determinations for the reference collection samples were made following these methods. Each reader completed the reference collection (randomized prior to each reading) before and after MIA samples were read.

Annulus measurements were made using Image Pro® Premier and a compound microscope-camera system. A straight line was drawn along the dorsal side of the sulcal groove, from the otolith core to otolith edge (radius), and the distal edge of each opaque band was marked (Figure 2.2). Margin codes were also assigned for use in an accompanying analysis to confirm the timing of annulus deposition (Supplemental Materials).

Statistical Analysis

All analyses and visualizations for this project were run using R software version 3.6.1 (R Core Team 2019). Black sea bass otolith paired ages were evaluated for precision and ageing bias using Chang's coefficient of variation (CV; Chang 1982) and a modification of the Bland-Altman bias plot (BAbble plot; Mcbride 2015). Additionally, within-reader precision was assessed by comparing each reader's reference collection session and the agreed reference collection ages. CV statistics were produced using the *'FSA'* package, version 0.8.26 (Ogle et al. 2019).

The marginal increment ratio (MIR) was used in the MIA to assess otolith growth throughout the year (Hood et al. 1994; Morales-Nin et al. 1998; Vilizzi and Walker 1999; Zlokovitz et al. 2003). The MIR was calculated by dividing the marginal increment (completed edge growth) by the distance between the distal edges of the two previous opaque bands (presumed penultimate annulus):

$$MIR = (R_t - R_{t-1}) / (R_{t-1} - R_{t-2})$$ (Condini et al. 2014)

Where R_t was the otolith radius (core to edge); R_{t-1} was the measurement from otolith core to the distal edge of the last opaque band; and, R_{t-2} was the measurement from otolith core to the distal edge of the penultimate opaque band (Figure 2.2).

A two-way analysis of variance (ANOVA) was used to assess average MIRs between different times of year and among age bins, as recommended by Campana (2001). Akaike's information criteria (AIC) was used to identify the best model for analysis, varying predictors (Month Bin, Age Bin, Region), additivity, and interactions. Month bins (e.g. January-February, March-April, etc.) were used instead of individual months because of missing data that would preclude interactive models from running. Missing data was also the reason that region (i.e. capture location) could only be included as an additive predictor and not interactive. Regions designated for this analysis were north and south of the Hudson Canyon, the recent population split as described in NEFSC (2017). Additionally, monthly MIR averages were used to visually assess the timing of annulus formation for each age bin.

Although not the direct purpose of this study, the possibility of growth differences between regions (Dery and Mayo 1988), as well as the recent separation of the northern stock into two sub-units, motivated an analysis to include Region as an interactive predictor variable. A three-way ANOVA used seasons instead of month bins due to missing data. Season groupings were chosen based on information available about black sea bass migration (arrive inshore by April and leave by October/November; Drohan et al. 2007), and were as follows: Winter = January, February, March; Spring = April, May, June; Summer = July, August, September; Fall = October, November, December.

Assumptions for each of the above models were checked by visual inspection of diagnostic plots. Type III sums of squares were used for both ANOVA's due to the unbalanced data. Post-hoc multiple comparison analyses were conducted using Tukey's Honestly Significant Differences (HSD; alpha = 0.05) and estimated marginal means (emmeans) due to unbalanced sample sizes among factor levels (Mangiafico 2016; Lenth 2019). Model selection, ANOVA's, post-hoc analyses, and visualizations were conducted using base R, as well as the following packages: 'car' version 3.0-3 (Fox and Weisberg 2019), 'emmeans' version 1.4.1 (Lenth 2019), 'multcomp' version 1.4-10 (Hothorn et al. 2008), and 'ggplot2' version 3.2.1 (Wickham 2016).

An ANOVA does not account for the cyclical nature of MIR data and is a noted source of concern for MIA studies based solely on this statistical test (Okamura et al. 2013). A circular-linear model proposed by Okamura et al. (2013) was applied to the data from this study to analyze how many cycles (i.e. annuli) exist in a one-year timespan. This method assesses AIC values for three models: whether no cycle (model N), one cycle (model A), or two cycles (model B) are present in the MIR data. This method was used for each age bin separately and for separate regions (age bins combined). This analysis was completed in R, using code included in the supplemental material (SIII) of Okamura et al. (2013).

Measurements of fall age 0 (September-October; n = 33) and summer age 1+ (July-August; n = 36) black sea bass otoliths were compared using Welch's two sample t-test for first annulus validation. Summer age 1+ measurements were also compared to the first annulus measurements of all MIA samples to confirm proper identification in the study samples. MA-DMF fall Resource Assessment Survey (September, 2015-2017) and summer

Massachusetts Ventless Trap Survey (July-August, 2015-2017) length-frequency plots of the smallest fish captured (first two length modes) were evaluated to confirm identification of the fall age 0 and summer age 1+ samples as YOY. Diagnostics to evaluate test assumptions were assessed visually.

Results

Ageing Precision

A total of 1,440 black sea bass otoliths were initially subsampled for this study. Forty-nine of those samples were excluded due to issues with broken or poorly sectioned otoliths and could not be reliably aged or measured for MIA. Additionally, MIRs could not be calculated for fish that were age 1 prior to annulus formation (as a result of using the January 1 advancement date) and were removed from analysis (n = 23).

Otoliths used in MIA and first annulus identification (n = 1,368) were from black sea bass captured across the north Atlantic stock (Figure 2.3). These samples were collected from every month of the year, ranging from 35mm to 605mm in total length (TL) and 0 to 12 years in age (Table 2.2; Figure 2.4). Sex data was available for 856 of the aged samples: 491 females (TL = 100mm to 500mm) and 365 males (TL = 80mm to 546mm). Age determinations were agreed upon for 1,222 otoliths (89.33%) between two independent readers; the remaining samples required a third, consensus, reading. A CV below 5% is recommended for precision among readers for age determinations (Campana 2001; McBride 2015). Examination of a BAbble plot of age differences between readers (Figure 2.5) as well as a low CV (2.20%) revealed low bias and high precision for age determinations between

readers. Additionally, there was high within reader precision for both individuals from the reference collection, before and after study samples were examined (CVs < 2%).

Marginal Increment Analysis

Measurements of 1,335 otoliths were used for MIA. The Month Bin model with the lowest AIC value was selected for further analysis (model 4; Table 2.3). Diagnostic plots conformed to model assumptions of normality and heteroskedasticity. The two-way ANOVA indicated a statistically significant interaction between Month Bin and Age Bin on the MIR ($F = 13.795$, $df = 10$, $p < 0.0001$). Tukey's HSD post hoc analysis shows that the ratio of growth at the edge of an otolith for a particular month bin differs between age bins (Figure 2.6). Month bins Jan-Feb, Mar-Apr and May-Jun show a pattern of the lowest mean MIR occurring in AB 1, followed by AB 2, and lastly AB 3 ($p < 0.01$); however, the remaining month bins show slightly different patterns. AB 1 and AB 2 were not significantly different in Jul-Aug ($p = 0.3143$) and Nov-Dec ($p = 0.3178$) but were significantly different from AB 3 ($p < 0.001$). Also, AB 2 and AB 3 were not significantly different in Sep-Oct ($p = 0.8206$) but were significantly different from AB 1 ($p < 0.001$).

Campana (2001) noted that a minimum in the MIR should occur once per year and be significantly different from other times of the year. Figure 2.7 shows the minimum mean MIR in each age bin (letter 'a') occurred once per year and was significantly different from other month bins ($p < 0.0001$). The only exception was for AB 3, which appeared to have a minimum that extended from Jul-Aug to Sep-Oct ($p = 0.9849$); whereas, the minimums for AB 1 and AB 2 were both in Jul-Aug only. Plotting raw data showed the monthly mean MIR for AB 3 declined in July prior to a minimum in August (Figure 2.12). Similarly, this

occurred in May-Jun of AB 1, where a depression in mean MIR was observed (Figures 2.7 and 2.12). All age bins exhibit a gradual increase in mean MIR throughout the year following the minimum.

A two-way interaction model between Age Bin, Season, and Region had the lowest AIC value and was selected for further analysis (Model 8; Table 2.4). A three-way interaction model was included in the AIC test (model 9); however, the only difference between this model and model 8 were three data points and resulted in a non-significant three-way interaction when testing with an ANOVA ($F = 1.801$, $df = 6$, $p = 0.0954$). Therefore, the difference between the two models was negligible and the two-way interaction model was analyzed further. ANOVA results indicated no significant interaction between Age Bin and Region ($F = 1.717$, $df = 2$, $p = 0.1800$); however, there was a significant interaction between Season and Region ($F = 3.593$, $df = 3$, $p = 0.0132$). Tukey's HSD results indicated that there was a higher mean MIR in the winter, spring, and fall in the south ($p < 0.01$, $p < 0.05$, and $p < 0.0001$, respectively), but regions were not significantly different in the summer ($p = 0.4486$; Figure 2.8).

Figure 2.9 shows that there was one minimum in mean MIR per year for each region, which occurred in the summer and was significantly different from all other seasons ($p < 0.0001$). Figure 2.12 shows that annulus deposition completion occurred in June in the north, prior to the minimum mean MIR in July and August. Missing data for the southern region in May-Jun precludes a thorough comparison of the timing of annulus deposition between regions; however, a MIR peak occurred in April and a minimum in July (the next available month of data).

A significant interaction was also detected between Season and Age Bin ($F = 16.602$, $df = 6$, $p < 0.0001$) which corroborated results from the first model analyzed. Tukey's HSD indicated significant differences between age bins in each season ($p < 0.01$; Figure 2.10). The only variant was that AB 1 and AB 2 in Summer were not significantly different ($p = 0.4830$), which was also seen in the previous model (Jun-Jul in Figure 2.6). Additionally, one minimum in mean MIR (Summer) was observed per year for each age bin increase growth throughout the year (Figure 2.11).

AIC results from the Okamura et al. (2013) circular-linear models (hereinafter referred to as the Okamura analysis) showed that one cycle was completed within a one-year timespan for all age bins and each region (Model A; Table 2.5). This confirmed previous results of one minimum in mean MIR per year (Tukey's HSD), as well as visual inspection of monthly mean MIRs (Figure 2.12).

YOY Measurements & Length-Frequency Analysis

Welch's two sample t-test between otolith radius measurements of fall age 0+ samples compared to the first annulus measurements of age 1+ samples were significantly different ($t = -11.923$, $df = 67$, $p = < 0.0001$). Age 0+ radii were smaller than the annulus counted in age 1+ samples (Figure 2.13). This indicated first annulus deposition in age 1+ samples that was not present in the age 0+ fish. Welch's two sample t-test between first annulus measurements of summer age 1+ samples compared to the first annulus measurements from all MIA samples ($n = 1,299$) was not significantly different ($t = 1.007$, $df = 37$, $p = 0.3205$; Figure 2.14), indicating that the first annulus in the MIA study was identified correctly. Measurements of the first annulus (all MIA samples) ranged from

0.41mm to 0.92mm with a mean of 0.61mm. First annulus measurements were similar between regions and were within the upper and lower 95% confidence intervals of the mean (0.62mm and 0.61mm, respectively).

Modal length frequency analysis using MA-DMF Resource Assessment Survey and Ventless Trap Survey data confirmed samples used for first annulus validation were YOY (Figures 2.15 and 2.16). A distinct modal separation between ages was apparent in the MIA samples and overlapping length modes with the smallest fish in each survey was observed. Measured fall age 0+ fish lengths in this study were from 35mm to 120mm (TL), which was comparable to length ranges from the first mode of captured fish in fall Resource Assessment survey data of 20mm to approximately 125mm. Measured summer age 1+ fish lengths in this study ranged from 110mm to 207mm; whereas, survey lengths of the smallest mode of black sea bass in the summer Ventless Survey data were 60mm to approximately 180mm.

Discussion

Annulus Periodicity

This study verified that one opaque and one translucent band were deposited per year for each age bin. One clear minimum in mean MIR was observed in each age bin and otolith growth continued throughout the year (Figures 2.7 and 2.12). This sinusoidal pattern is indicative of MIA studies confirming one annulus deposited per year (Mercer 1978; Wenner et al. 1986; Fowler 1990; Lehodey and Grandperrin 1996; Vilizzi and Walker 1999; Pilling et al. 2000). Additionally, the Okamura analysis used in this study confirmed these results, indicating one cycle occurred per year for each age group (Table 2.5).

Timing of Annulus Deposition

Annulus deposition is considered finished when new translucent growth is observed at the otolith edge. In other words, the opaque annulus is being completed when mean MIR values are at a maximum before dropping to a minimum, which indicates new growth. The timing of annulus deposition in this study was dependent on age. Maximum mean MIR for AB 1 was observed in March-April; however, a decline in the mean in May-June (prior to the minimum in July-August) indicated some fish were completing the annulus in these months (Figures 2.7 and 2.12). Thus, annulus completion occurred between April and June for this age group. This variability was not surprising given the extensive spatial range from which these samples were collected (Maine to Virginia). Miller et al. (2016a) showed that over-wintering adult black sea bass gathered along a defined shelf contour, whereas juveniles were scattered across the shelf and experienced a wider range of temperatures and salinities. Individual variation in this youngest age group, therefore, may be magnified by the environmental conditions experienced while over-wintering.

Maximum mean MIR for AB 2 was observed in June, followed by a stark decline to a minimum in July and August, and a continuation of growth thereafter (Figures 2.7 and 2.12). Annulus completion clearly occurred in June for this age bin. Reduced variability in the timing of annulus deposition in this age group, compared to AB 1, was likely due to a more consistent growth rate between ages and regions.

Maximum and minimum mean MIRs for AB 3 occurred in June and August, respectively (Figure 2.12). The mean MIR in July fell between these extremes, like the pattern observed in May-June in AB 1. This indicated that some otoliths exhibited new,

translucent growth in July (small amount of growth at the otolith margin); whereas, others were still depositing the opaque annulus (large amount of growth at the otolith margin). The delay in annulus deposition for some samples in this age group (August minimum as compared to July for AB 1 and AB 2) could be related to energy allocated to spawning rather than growth during this period. Morales-Nin and Ralston (1990) observed a decline in otolith growth as spawning season progressed and stated, "during the maturity period the metabolic energy seems to be diverted from growth, causing the formation of thin increments [as] seasonal growth rings." The northern stock of black sea bass typically spawns between April and October, peaking in June-July (Mercer 1978; Wuenschel et al. 2013; McBride et al. 2018). Of the forty-four fish measured in July for AB 3, twenty-five were classified as spawning condition fish (i.e. 'ripe' or 'ripe and running'). Other studies of black sea bass in the northern stock have noted that annulus formation appears to be associated with spawning period (Mercer 1978; Alexander 1981; Caruso 1995); however, this connection may be coincidental (Beckman and Wilson 1995). Instead annulus deposition timing is likely the result of a combination of environmental and physiological processes (Fowler and Short 1998). Additionally, black sea bass exhibit a variety of reproductive strategies, including maturation as young, small males (Provost et al. 2017), that could also impact otolith growth in younger age groups. Instead, the variability in annulus deposition for AB 3 could be due to the difficulty of accurately measuring growth at the otolith edge of older fish. The decline in otolith growth with increasing age made it challenging to discern the start of translucent edge growth; therefore, an apparent delay in annulus deposition could be an artifact of the measurement methodology.

Age Bin Separation

This study confirmed that separate age bins were necessary for accurate validation of this species because of differences in otolith deposition rates with age. As a fish ages, somatic growth slows and otolith growth bands become closer together (Beamish and McFarlane 1983). Otolith growth in the fish's first year is expected to be larger than growth in the second year, which will be larger than the third, and so on until a certain size or age where otolith growth will become more consistent. Significant differences in mean MIR between age bins throughout the year demonstrated this variance in the otolith deposition with age. For example, AB 1 had the lowest overall mean MIR throughout the year (Figure 2.6) and did not come close to approaching 1.0 (Figure 2.7). Mean MIR values that approach 1.0 would indicate the completed edge growth on an otolith equals the growth of the penultimate annulus. The patterns observed in AB 1 confirmed there was rapid growth in the first years of life followed by a slight decline in growth the following year. AB 3 has the highest mean MIR values throughout the year and comes closer to approaching 1.0 at the time of annulus completion (emmean MIR = 0.78 in May-June). Otoliths in this age bin have a higher proportion of edge growth compared to the penultimate annulus, because growth has slowed, and annuli measurements were more consistent. As expected, overall mean MIR values for AB 2 fall between the values of AB 1 and AB 3 throughout the year.

First Annulus Validation

First annulus validation must be completed in conjunction with MIA to validate absolute age (Campana 2001). MIA verifies annual banding deposition patterns in an ageing structure; however, if the first annulus was not validated, ageing methods could be incorrect

by a consistent amount. Additionally, the identification of the first annulus is often a primary source of error in ageing practices (Penttila and Dery 1988; Campana 2001). This is particularly important for black sea bass due to reported discrepancies between identification of age 0 versus age 1 fish in the fall months that contributed to the exclusion of these indices in the latest stock assessment (ASMFC 2016).

This study validated the location of the first annulus by measuring YOY, age 0 fish in the fall and age 1+ fish shortly after the time of annulus formation (spring/early summer as indicated above). Figure 2.13 shows the disparate measurements between each age. Although there was slight overlap in the extremes, the first annulus in most age 1+ samples was significantly larger than the expected total radius of an age 0 fish in the previous fall. Additionally, no significant differences were found between the first annulus measurements from age 1+ fish and the first annulus measured on all MIA samples, indicating it was identified correctly in this study (Figure 2.14). The first annulus for all MIA samples occurred between 0.41mm and 0.92mm from the core, with a mean measurement of 0.61mm.

The samples used for age 0 and age 1+ fish were confirmed as YOY by comparing their modal length frequencies to the length frequencies of the smallest black sea bass caught in the MA-DMF Resource Assessment (fall survey) and Ventless Trap surveys (summer survey; Figures 2.15 and 2.16). The similarities between the length frequencies was clear, and the designation of the samples in this study as YOY was appropriate. It should be noted that the samples measured for first annulus validation were all from Massachusetts waters. The similarity in first annulus size of these samples compared to all MIA samples (Figure 2.14), as well as the previously mentioned similarity in mean first annulus measurements

between regions north and south of the Hudson Canyon, suggest that these results are applicable to the whole northern stock.

Regional Differences

The documented variability of black sea bass otolith growth by location (Dery and Mayo 1988), as well as the recent separation of the northern stock into two sub-units, motivated an analysis of possible differences between these regions. The interaction between Age Bin and Season corroborated findings from the Month Bin model in that: (1) differences between age bins by season supported the separation of the black sea bass age range for validation (Figure 2.10), and (2) there appeared to be one minimum per year in mean MIR for each age bin (Figure 2.11). Additionally, no significant interaction between Age Bin and Region revealed no significant regional difference in otolith edge growth within age bins.

The significant interaction between Season and Region in this model indicated that there were some differences in edge growth between regions throughout the year. The non-significant difference in mean MIR values in the summer was not surprising because otolith growth is minimal following annulus deposition (Mercer 1978; Robillard et al. 2016; Figure 2.8). Higher mean MIRs for the south in the winter, spring, and fall indicated that fish from this region were depositing more material at these times than fish from the north. A large amount of otolith edge growth for both regions occurred in the fall months (Figures 2.8 and 2.9); however, there was also a large amount of edge growth in the northern region from fall to winter that was not as apparent in the southern region. MIR emmeans in fall and winter in the north were 0.42 and 0.54, respectively, versus 0.54 and 0.60 in the south. The finding that fish from the north achieved a large proportion of their otolith edge growth from January

through March is in line with previous research, but additional work is needed. Several studies report that black sea bass were larger and had faster growth rates throughout the year in higher latitudes (Alexander 1981; Dery and Mayo 1988; Kolek 1990; Caruso 1995; McMahan et al. 2020). McMahan et al. (2020) postulated that more northerly black sea bass may be adapted to grow in lower temperatures or that they exhibit countergradient variation, with more growth achieved in the shorter growing season. This could explain the results observed in this study; however, a closer look at growth is needed to address this topic, which was outside the purview of this project.

Though there were slight differences in otolith deposition rates between regions at certain times of the year, one mean MIR minimum is observed for each region (summer) with growth continuing throughout the year (Figure 2.9). Additionally, the Okamura analysis confirmed that one MIR cycle occurred each year for both regions (Table 2.5). Deposition was completed in June for the northern region, with some fish lagging into July (Figure 2.12). Missing data prevented a full comparison of timing between regions; however, annulus deposition for the south was completed on or after April but before July, suggesting a similar timing of late spring or early summer for this region.

Differences in sample size between regions should also be noted. A larger proportion of samples were captured from north of the Hudson Canyon, in part due to the number of collaborators and projects from which samples were collected in this region, but also due to the subsampling procedure used in this study. An initial subsample (n = 1,008) was taken to begin processing before all samples were acquired from collaborators, and many of the samples captured south of the Hudson Canyon were received after this initial subsample. The

objective of this study was not to analyze regional differences; however, due to the recent sub-unit distinction and expanse of samples used in this study, exploring differences that could impact the validation between regions was warranted. The slight differences in mean MIR values observed between regions do not impact the validation of annuli in this study and the otolith ageing method for black sea bass was validated for both regions.

Literature Comparison

Annulus deposition in previous black sea bass otolith age validation studies is slightly inconsistent. Mercer (1978) concluded that opaque deposition occurred in April and May for black sea bass in the mid-Atlantic Bight (MAB). This was, however, highly variable for the ages examined (1 through 5). Mercer (1978) states "the mean marginal increment should drop to near zero at the time of annulus formation…this occurs from March through June." These results can only be clearly seen for the ages 1 through 3. Age 4 shows a very slight depression in marginal increment during these months, and age 5 samples appeared to have a minimum in July and August, though sample sizes were low. Additionally, in-depth comparisons between this study and the current work were difficult to make because Mercer (1978) measured whole otoliths. The accretion of growth on whole otoliths is much more difficult to distinguish than it is for sectioned otoliths. Annuli on whole otoliths appear broader and more diffuse, making measurements less precise; whereas, a crisp line at the distal edge of annuli on otolith sections makes measurements easier and more consistent. Additionally, the curvature of whole otoliths could impact increment measurements and likely contributed to the variability observed between age groups. The timing of deposition between these two studies was expected to be slightly different due to these disparities;

however, both studies reported annulus deposition in late spring or early summer, with a possible delay for older age groups.

Alexander (1981) conducted marginal increment analysis on black sea bass whole otoliths from the New York Bight. Though each age group was analyzed separately (ages 2-5), only the months of June, July, August, and October were represented. In addition to the difficulty of measuring whole otoliths mentioned above, conclusions made from these measurements were questionable. Alexander notes that "because the marginal increments…indicate little increase until after August, I suspect that annulus formation probably occurs during August." An increase in the marginal increment, though, does not necessarily indicate annulus formation. There was no mention of opaque material observed at the otolith edge; however, if it was present, this would indicate the start of annulus formation, not completion. Dery and Mayo (1988) note that annulus completion occurs in May or June, though also mentions that opaque material can be present into the early autumn months. Robillard et al. (2016) described an oxytetracycline tagging and MIA study completed on black sea bass otoliths in 1990 and reported that annulus formation occurred during the summer. This study was completed using sectioned otoliths but was severely limited in sample size and sampling area was not noted.

The timing of annulus deposition for black sea bass otoliths in this thesis appears to generally agree with reports from previous studies (spring or early summer). Detailed comparisons were difficult due to issues with sampling (limited locations, gear types, represented ages, and sample sizes), as well as use of whole otoliths in some studies. Additionally, none of the above published studies included validation of the first annulus, a

necessary step in validating an ageing method. Hales and Able (1995) and McBride et al. (2018) conducted studies to validate the daily ageing method for black sea bass otoliths; however, both studies used fish less than 1 year old.

Recommendations

Age determinations for black sea bass in the northern stock are currently supplied by several agencies along the northeastern Atlantic coast. Each organization has their own protocols for ageing methods; however, scales have largely been phased out in preference to otoliths. Variation between the use of whole, sectioned, or a combination of the two exists (ASMFC 2018). The recommendation following this study is to use sectioned otoliths for future black sea bass ageing. Not only has this ageing structure been validated by this study, but sectioned otoliths tend to be clearer, easier to interpret, and provide more accurate age determinations (Mercer 1978).

Conclusion

This study demonstrated that black sea bass otoliths lay down one opaque annulus per year in the late spring or early summer. Younger fish completed annulus formation earlier in the season than older fish. It is possible that this was due to a greater amount of energy diverted to reproduction in older fish; however, this species exhibits a wide variety of reproductive strategies, where young mature fish are also common. Therefore, the apparent delay in opaque annulus completion could be an artifact of measuring difficulty in the older age groups. In all age groups, annulus formation was completed by July or August and new translucent material had begun. Additionally, although there were slight differences in the

rate of material deposition between regions, the otolith ageing method was validated for samples captured from both stock subunits (north and south of the Hudson Canyon).

Accurate age data is crucial; error stemming from inaccurate age determinations can have critical impacts on age-structured calculations, e.g. growth rate, mortality rate, and productivity parameters. This is especially important due to the recent application of an age-based stock assessment for the northern stock of black sea bass (NEFSC 2017). Furthermore, it was imperative to evaluate possible changes to seasonal timing or annulus formation due to recent changes to distribution and/or productivity of this species in the northern stock. This project helps ensure the accuracy and precision of black sea bass ageing practices by validating the otolith ageing method used by agencies and organizations across the north Atlantic coast. Previous attempts at otolith age validation were constrained by sample sizes, restricted age ranges, and/or were only applied to a small subset of the stock (Mercer 1978; Robillard et al. 2016). Additionally, there has been no published work up to this point validating the first annulus on otoliths, which was completed in this study. This project utilized samples representing the entire spatial range of the northern stock, included a variety of capture methods and fishery types, and spanned the observed age range of this species. Completing such a validation study representative of the stock will increase confidence in the quality of data used in the stock assessment.

References

Able, K. W., M. P. Fahay, and G. R. Shepherd. 1995. Early life history of black sea bass, Centropristis striata, in the mid-Atlantic Bight and a New Jersey estuary. Fishery Bulletin 93:429–445.

Alexander, M. S. 1981. Population response of the sequential hermaphrodite black sea bass, Centropristis striata, to fishing. State University of New York at Stony Brook.
ASMFC. 2013. Proceedings of the 2013 black sea bass ageing workshop. Atlantic States Marine Fisheries Commission:1–18.
ASMFC. 2014. 2015 Action Plan. Atlantic States Marine Fisheries Commission:1–28.
ASMFC. 2016. 62nd SAW assessment report black sea bass terms of reference. Atlantic States Marine Fisheries Commission:1–261.
ASMFC. 2018. Report of the quality assurance/quality control fish ageing workshop. Atlantic States Marine Fisheries Commission:1–53.
Beamish, R. J., and G. A. McFarlane. 1983. The forgotten requirement for age validation in fisheries biology. Transactions of the American Fisheries Society 112(6):735–743.
Beckman, D. W., and C. A. Wilson. 1995. Seasonal timing of opaque zone formation in fish otoliths. Pages 27–43 in D. H. Secor, J. M. Dean, and S. E. Campana, editors. Recent Developments in Fish Otolith Research. University of South Carolina Press, Columbia, South Carolina.
Bell, R. J., D. E. Richardson, J. A. Hare, P. D. Lynch, and P. S. Fratantoni. 2015. Disentangling the effects of climate, abundance, and size on the distribution of marine fish: an example based on four stocks from the Northeast US shelf. ICES Journal of Marine Science 72(5):1311–1322.
Bigelow, H. B., and W. C. Schroeder. 1953. Black sea bass, Centropristis striata. Pages 407–409 Fishes of the Gulf of Maine. Vol 53. Fishery Bulletin of the Fish and Wildlife Service.
Cadrin, S., R. Leaf, and O. Jensen. 2016. Contributions to the SAW62 black sea bass stock assessment. Science Center for Marine Fisheries:1–6.
Campana, S. E. 2001. Accuracy, precision and quality control in age determination, including a review of the use and abuse of age validation methods. Journal of Fish Biology 59:197–242.
Campana, S. E., and S. R. Thorrold. 2001. Otoliths, increments, and elements: keys to a comprehensive understanding of fish populations? Canadian Journal of Fisheries & Aquatic Sciences 58(1):30–38.
Caruso, P. G. 1995. The age, growth, and spawning of black sea bass (Centropristis striata, Linneaus) in Massachusetts waters. MADMF Black Sea Bass Investigations Internal Report:11–25.
Carvalho, M. G., C. Moreira, H. Queiroga, P. T. Santos, and A. T. Correia. 2017. Age, growth and sex of the shanny, Lipophrys pholis (Linnaeus, 1758) (Teleostei, Blenniidae), from the NW coast of Portugal. Journal of Applied Ichthyology 33:242–251.
Casselman, J. M. 1983. Age and growth assessment of fish from their calcified structures-techniques and tools. Pages 1–17 in E. D. Prince and L. M. Pulos, editors. Proceedings of the International Workshop on Age Determination of Oceanic Pelagic Fishes: Tunas, Billfishes, and Sharks. NOAA Technical Report NMFS 8. Miami, Florida.
Chang, W. Y. B. 1982. A statistical method for evaluating the reproducibility of age determination. Canadian Journal of Fisheries and Aquatic Sciences 39:1208–1210.

Dery, L. M., and J. P. Mayo. 1988. Black Sea Bass, Centropristis striata. Pages 59–69 in J. Pentilla and L. M. Dery, editors. Age Determination Methods for Northwest Atlantic Species. NOAA Technical Report NMFS 72.

Drohan, A. F., J. P. Manderson, and D. B. Packer. 2007. Essential fish habitat source document: black sea bass, Centropristis striata, life history and habitat characteristics. NOAA Technical Memorandum NMFS-NE-200. Woods Hole, MA.

Fowler, A. J. 1990. Validation of annual growth increments in the otoliths of a small, tropical coral reef fish. Marine Ecology Progress Series 64:25–38.

Fowler, A. J., and D. A. Short. 1998. Validation of age determination from otoliths of the King George whiting Sillaginodes punctata (Perciformes). Marine Biology 130:577–587.

Fox, J., and S. Weisberg. 2019. An {R} Companion to Applied Regression.

Franks, J. S., J. R. Warren, and M. V Buchanan. 1999. Age and growth of cobia, Rachycentron canadum, from the northeastern Gulf of Mexico. Fishery Bulletin 97(3):459–471.

Hales, L. S., and K. W. Able. 1995. Effects of oxygen concentration on somatic and otolith growth rates of juvenile black sea bass, Centropristis striata. Pages 135–153 in D. H. Secor, J. M. Dean, and S. E. Campana, editors. Recent Developments in Fish Otolith Research. University of South Carolina Press, Columbia, South Carolina.

Hood, P. B., M. F. Godcharles, and R. S. Barco. 1994. Age, growth, reproduction, and the feeding ecology of black sea bass (Centropristis striata) in the eastern Gulf of Mexico. Bulletin of Marine Science 54(1):24–37.

Hothorn, T., F. Bretz, and P. Westfall. 2008. Simultaneous inference in general parametric models. Biometrical Journal 50(3):346–363.

Hyndes, G. A., N. R. Loneragan, and I. C. Potter. 1992. Influence of sectioning otoliths on marginal increment trends and age and growth estimates for the flathead Platycephalus speculator. Fishery Bulletin 90:276–284.

Kendall, A. W. 1977. Biological and fisheries data on black sea bass, Centropristis striata (Linnaeus). Highlands, NJ.

Kleisner, K. M., M. J. Fogarty, S. McGee, A. Barnett, P. Fratantoni, J. Greene, J. A. Hare, S. M. Lucey, C. McGuire, J. Odell, V. S. Saba, L. Smith, K. J. Weaver, and M. L. Pinsky. 2016. The effects of sub-regional climate velocity on the distribution and spatial extent of marine species assemblages. PLoS ONE 11(2):1–21.

Kolek, D. 1990. Homing of black sea bass, Centropristis striata, in Nantucket Sound, with comments on seasonal distribution, growth rates, and fisheries of the species. MADMF Black Sea Bass Investigations Internal Report:2–9.

Lehodey, P., and R. Grandperrin. 1996. Age and growth of the alfonsino Beryx splendens over the seamounts off New Caledonia. Marine Biology 125:249–258.

Lenth, R. 2019. Emmeans: estimated marginal means, aka least-squares means. R package version 1.4.3.01.

Mangiafico, S. S. 2016. Summary and analysis of extension program evaluation in RVersion 1. New Brunswick, NJ.

McBride, R. S. 2015. Diagnosis of paired age agreement: a simulation of accuracy and precision effects. ICES Journal of Marine Science 72(7):2149–2167.

McBride, R. S., M. K. Tweedie, and K. Oliveira. 2018. Reproduction, first-year growth, and expansion of spawning and nursery grounds of black sea bass (Centropristis striata) into a warming Gulf of Maine. Fishery Bulletin 116:323–336.
McMahan, M. D., G. D. Sherwood, and J. H. Grabowski. 2020. Geographic variation in life-history traits of black sea bass (Centropristis striata) during a rapid range expansion. Frontiers in Marine Science 7(567758):1–15.
Mercer, L. P. 1978. The reproductive biology and population dynamics of black sea bass, Centropristis striata. The College of William and Mary.
Miller, A. S., G. R. Shepherd, and P. S. Fratantoni. 2016. Offshore habitat preference of overwintering juvenile and adult black sea bass, Centropristis striata, and the relationship to year-class success. PLoS ONE 11(1):1–19.
Morales-Nin, B., and S. Ralston. 1990. Age and growth of Lutjanus kasmira (Forskal) in Hawaiian waters. Journal of Fish Biology 36:191–203.
Morales-Nin, B., G. J. Torres, A. Lombarte, and L. Recasens. 1998. Otolith growth and age estimation in the European hake. Journal of Fish Biology 53:1155–1168.
Musick, J. A., and L. P. Mercer. 1977. Seasonal distribution of black sea bass, Centropristis striata, in the Mid-Atlantic Bight with comments on the ecology and fisheries of the species. Transactions of the American Fisheries Society 106(1):12–25.
Natanson, L. J., J. J. Mello, and S. E. Campana. 2002. Validated age and growth of the porbeagle shark (Lamna nasus) in the western North Atlantic Ocean. Fisheries Bulletin 100:266–278.
NEFSC. 2012. 53rd Northeast regional stock assessment workshop. Northeast Fisheries Science Center Reference Assessment Summary Report:1–33.
NEFSC. 2017. 62nd Northeast regional stock assessment workshop. Northeast Fisheries Science Center Reference Assessment Summary Report:1–36.
Ogle, D. H., P. Wheeler, and A. Dinno. 2019. FSA: fisheries stock analysis. R package version 0.8.26.
Okamura, H., A. E. Punt, Y. Semba, and M. Ichinokawa. 2013. Marginal increment analysis: a new statistical approach of testing for temporal periodicity in fish age verification. Journal of Fish Biology 82:1239–1249.
Penttila, J., and L. M. Dery. 1988. Age determination methods for Northwest Atlantic species. NOAA Technical Report NMFS 72:1–135.
Pilling, G. M., R. S. Millner, M. W. Easey, C. C. Mees, S. Rathacharen, and R. Azemia. 2000. Validation of annual growth increments in the otoliths of the lethrinid Lethrinus mahsena and the lutjanid Aprion virescens from sites in the tropical Indian Ocean, with notes on the nature of growth increments in Pristipomoides filamentosus. Fishery Bulletin 98:600–611.
Provost, M. M., O. P. Jensen, and D. L. Berlinsky. 2017. Influence of size, age, and spawning season on sex change in black sea bass. Marine and Coastal Fisheries 9(1):126–138. Taylor & Francis.
R Core Team. 2019. R: a language and environment for statistical computing. R Foundation for Statistical Computing. Vienna, Austria.

Robillard, E., J. W. Gregg, J. Dayton, and J. Gartland. 2016. Validation of black sea bass, Centropristis striata, ages using oxytetracycline marking and scale margin increments. Appendix A1, Stock Assessment Report of Black Sea Bass. Woods Hole, MA.

Shepherd, G. R., and M. C. Lambert. 1996. Assessment of black sea bass north of Cape Hatteras, North Carolina. Northeast Fisheries Science Center Reference Document 95-17:1–15.

VanderKooy, S., S. Elzey, J. Gilmore, and J. Kipp. (n.d.). A practical handbook for determining the ages of Gulf of Mexico and Atlantic coast fishes: Third Edition. Gulf States Marine Fisheries Commission, Ocean Springs, MS.

Vilizzi, L., and K. F. Walker. 1999. Age and growth of the common carp, Cyprinus carpio, in the River Murray, Australia: validation, consistency of age interpretation, and growth models. Environmental Biology of Fishes 54:77–106.

Wenner, C. A., W. A. Roumillat, and C. W. Waltz. 1986. Contributions to the life history of black sea bass, Centropristis striata, off the Southeastern United States. Fishery Bulletin 84(3):723–741.

Wickham, H. 2016. ggplot2: elegant graphics for data analysis. Springer-Verlag, New York.

Winner, B. L., T. C. MacDonald, and K. B. Amendola. 2017. Age and growth of sheepshead (Archosargus probatocephalus) in Tampa Bay, Florida. Fishery Bulletin 115(2):155–166.

Wuenschel, M. J., R. S. McBride, and G. R. Fitzhugh. 2013. Relations between total gonad energy and physiological measures of condition in the period leading up to spawning: results of a laboratory experiment on black sea bass (Centropristis striata). Fisheries Research 138:110–119.

Zlokovitz, E. R., D. H. Secor, and P. M. Piccoli. 2003. Patterns of migration in Hudson River striped bass as determined by otolith microchemistry. Fisheries Research 63:245–259.

Figures

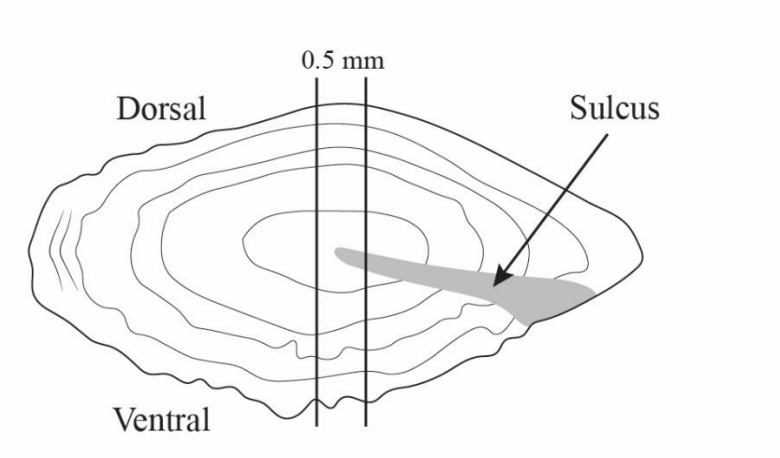

Figure 2.1: Positioning of the transverse dorsoventral section (0.5mm) taken through the core of a whole black sea bass otolith.

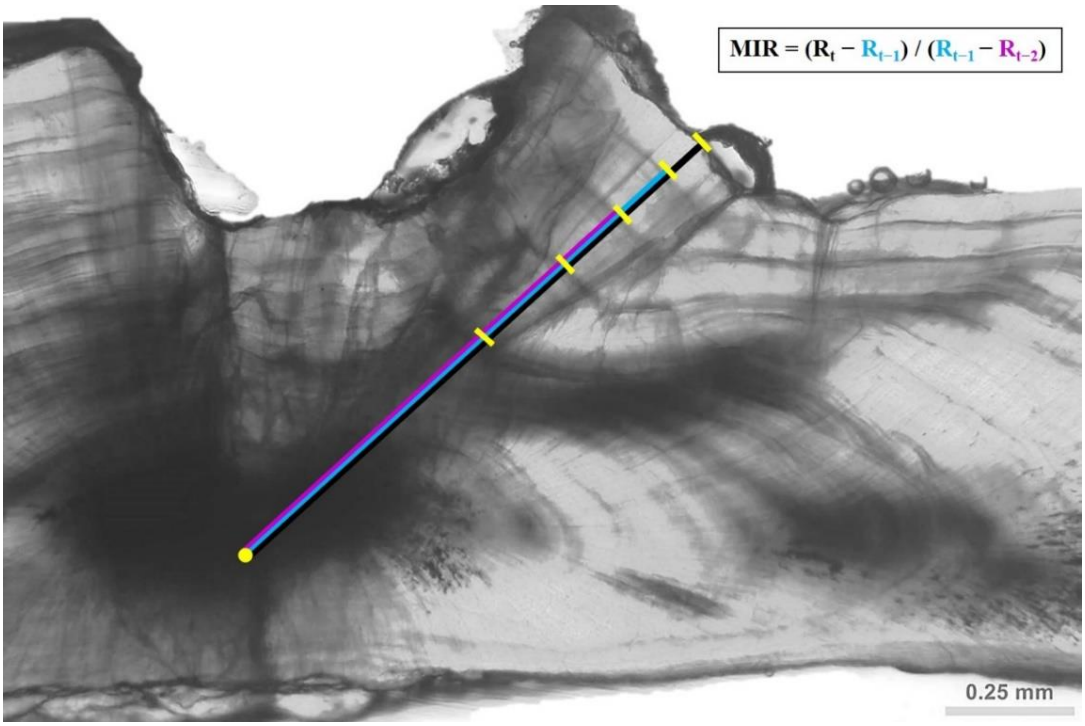

Figure 2.2: Measurements on a sectioned black sea bass otolith for MIA. Yellow dot: otolith core, yellow bars: markers for annulus measurements (distal edge of each opaque band), black bar: Rt (radius), blue bar: Rt-1 (core to last opaque band), purple bar: Rt-2 (core to penultimate opaque band).

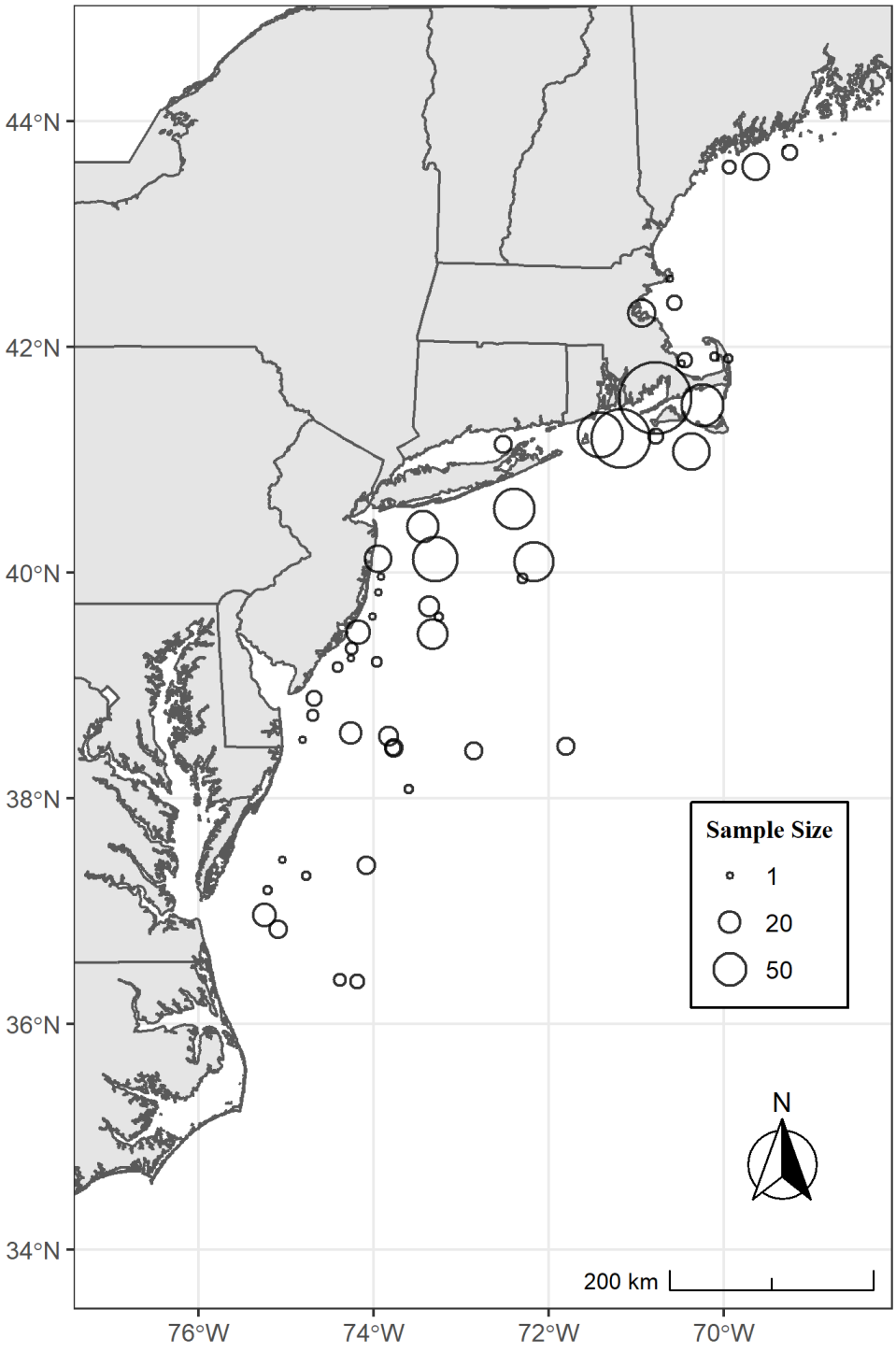

Figure 2.3: Map of black sea bass samples used in MIA and first annulus validation. Size of circle scaled to sample sizes at that location.

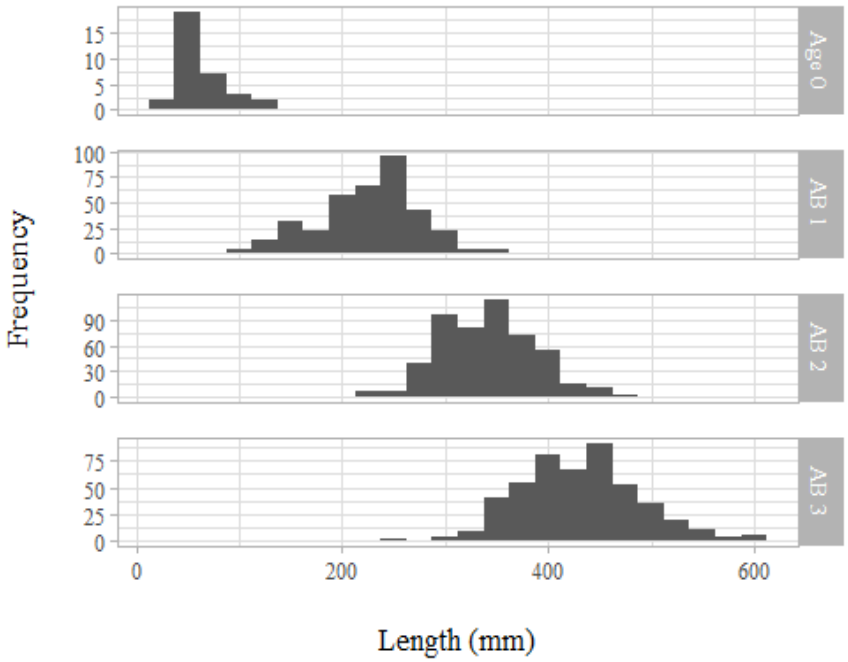

Figure 2.4: Black sea bass length frequency histograms for samples used in MIA and first annulus validation.

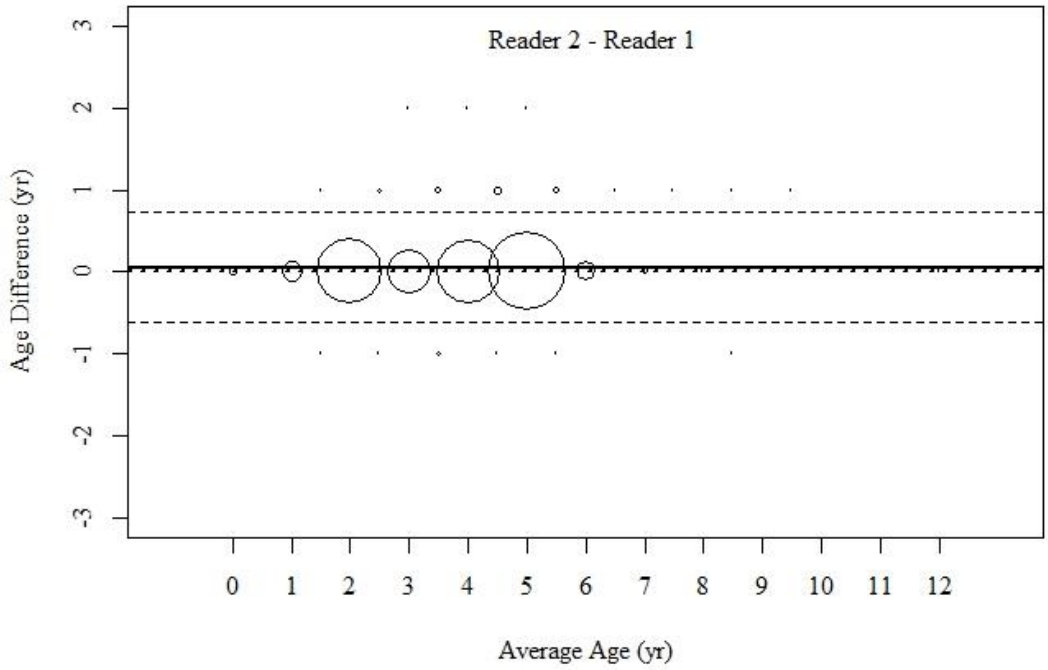

Figure 2.5: BAbble plot (McBride 2015) of differences in age determinations (Reader 2 – Reader 1). Dotted black line indicates no bias (located at 0), solid black line indicates degree and direction of bias and the thin dashed black lines are 95% confidence limits.

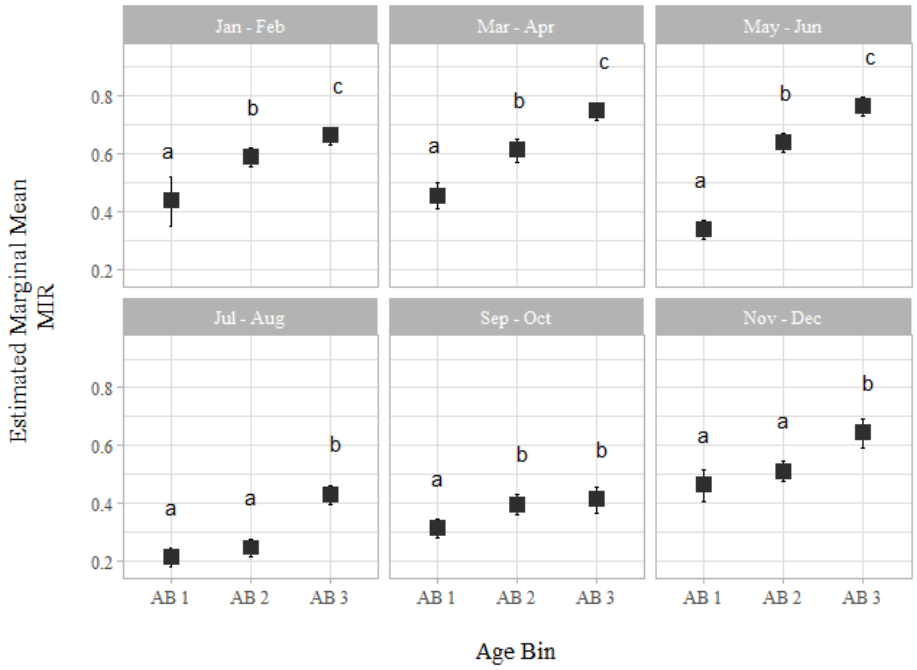

Figure 2.6: Estimated marginal means of MIR for Age Bin by Month Bin. Letters denote significant differences (Tukey's HSD; alpha = 0.05). Error bars represent two standard errors of the estimated marginal mean.

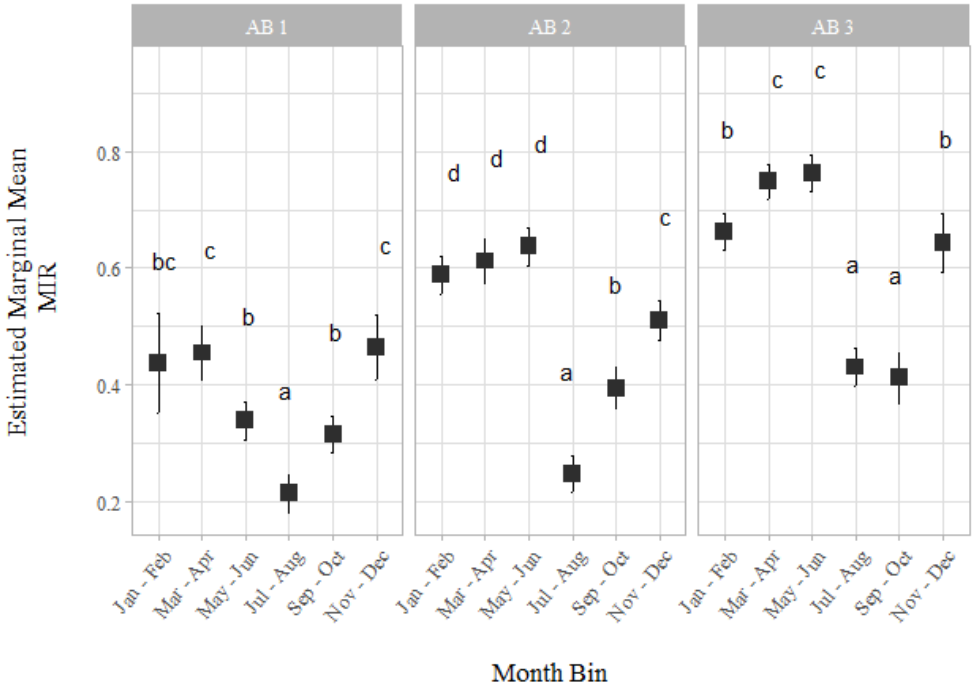

Figure 2.7: Estimated marginal means of MIR for Month Bin by Age Bin. Letters denote significant differences (Tukey's HSD; alpha = 0.05). Error bars represent two standard errors of the estimated marginal mean.

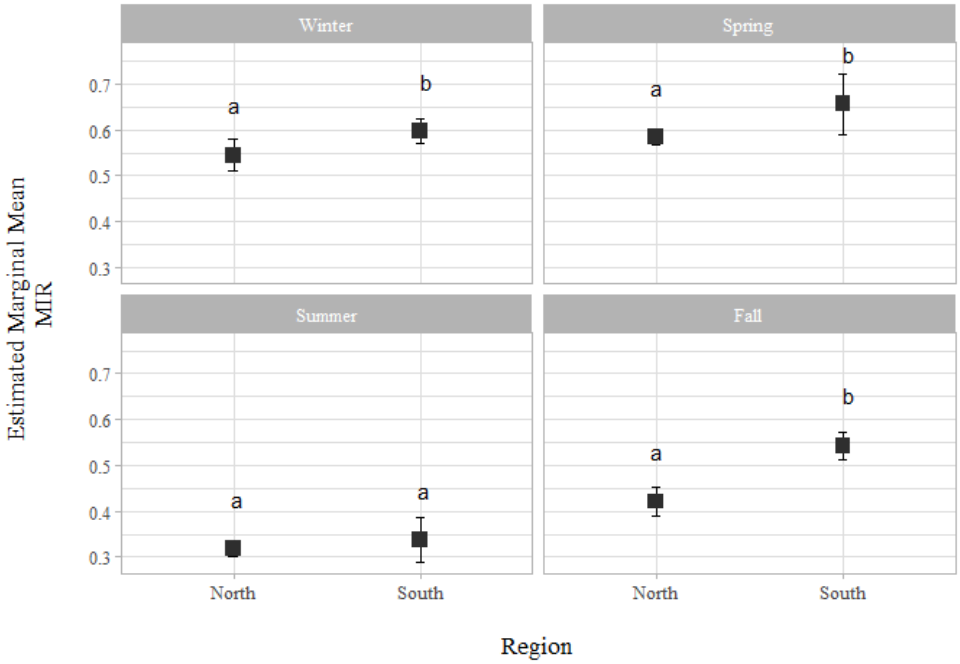

Figure 2.8: Estimated marginal means of MIR for Region by Season. Letters denote significant differences (Tukey's HSD; alpha = 0.05). Error bars represent two standard errors of the estimated marginal mean.

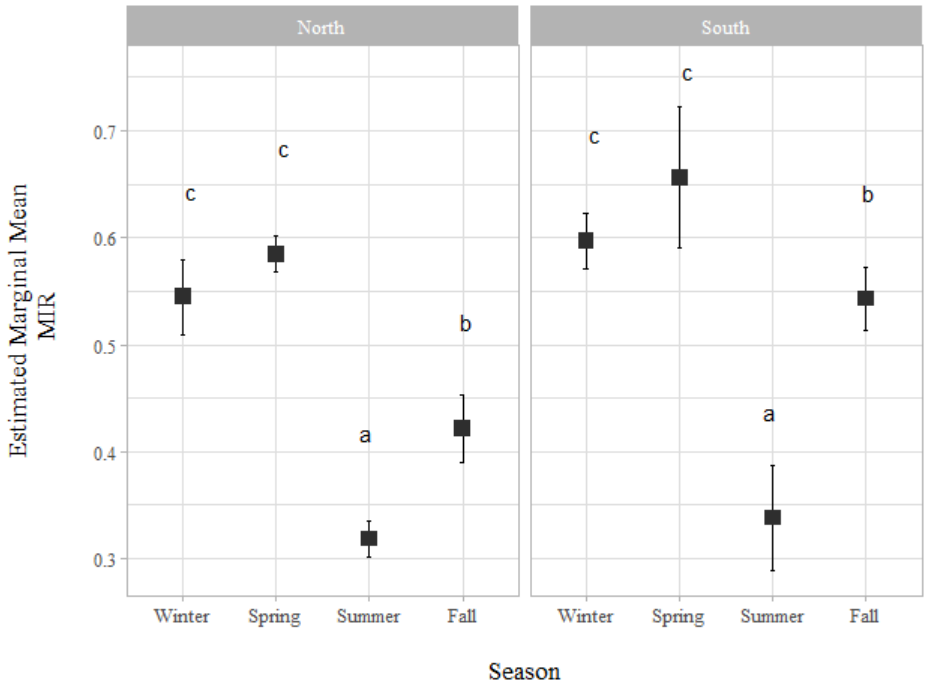

Figure 2.9: Estimated marginal means of MIR for Season by Region. Letters denote significant differences (Tukey's HSD; alpha = 0.05). Error bars represent two standard errors of the estimated marginal mean.

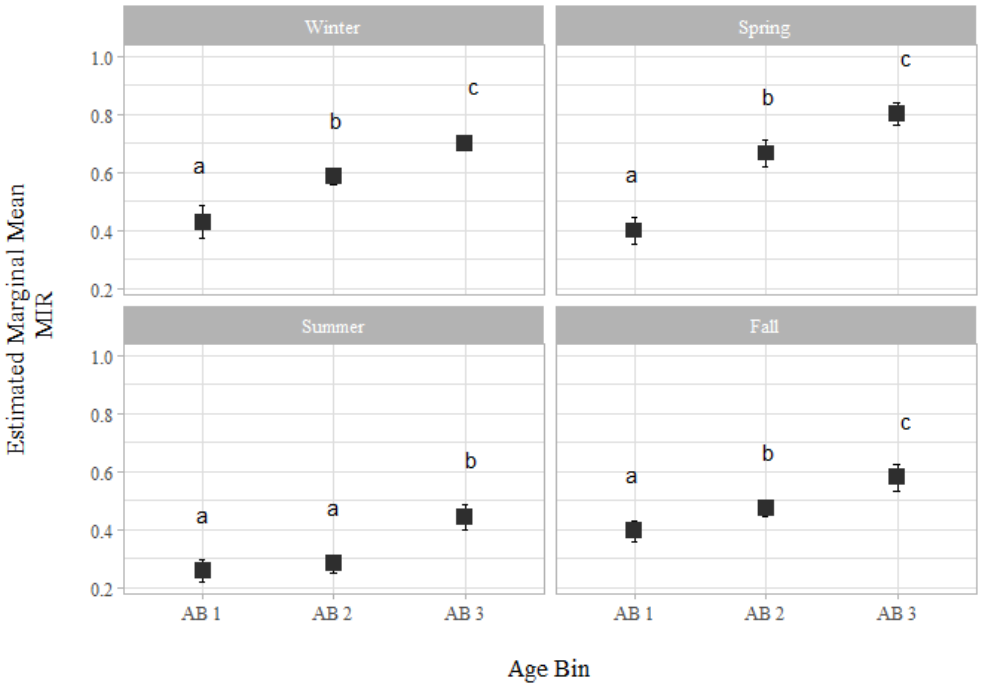

Figure 2.10: Estimated marginal means of MIR for Age Bin by Season. Letters denote significant differences (Tukey's HSD; alpha = 0.05). Error bars represent two standard errors of the estimated marginal mean.

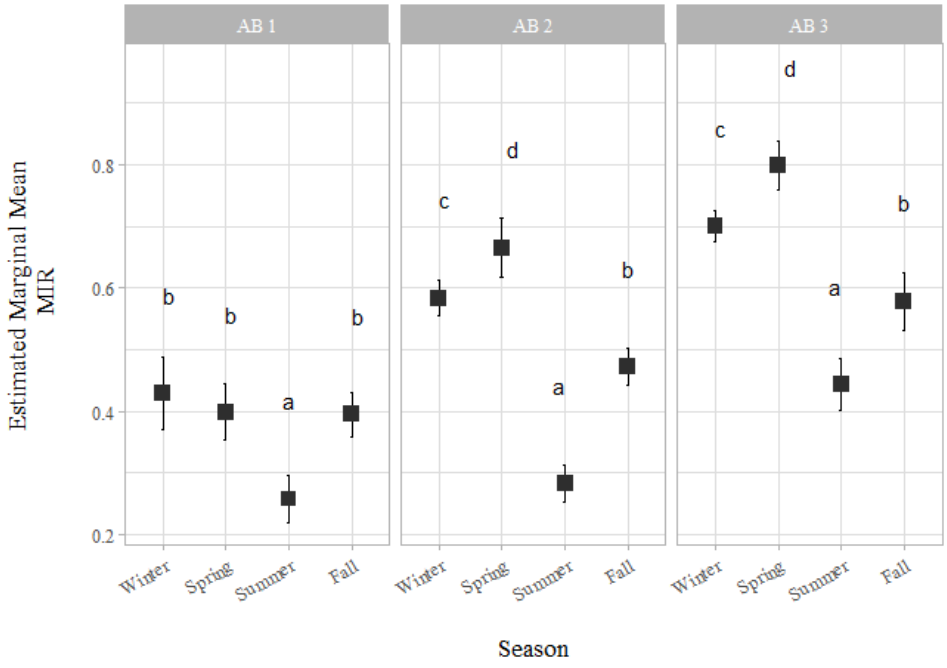

Figure 2.11: Estimated marginal means of MIR for Season by Age Bin. Letters denote significant differences (Tukey's HSD; alpha = 0.05). Error bars represent two standard errors of the estimated marginal mean.

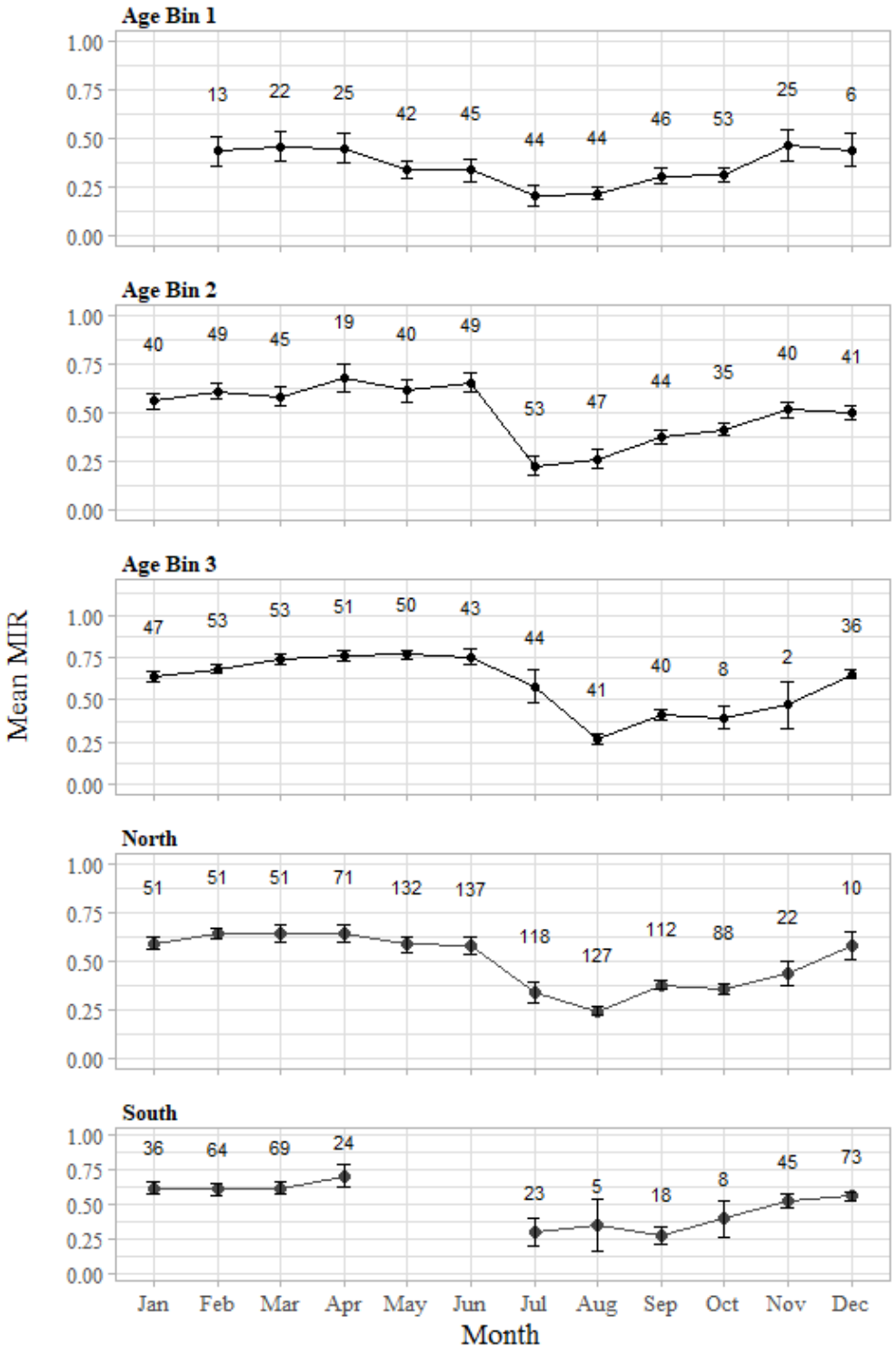

Figure 2.12: Monthly mean MIRs (raw data) for each age bin and region. Error bars are two standard errors of the mean. Numbers denote sample size.

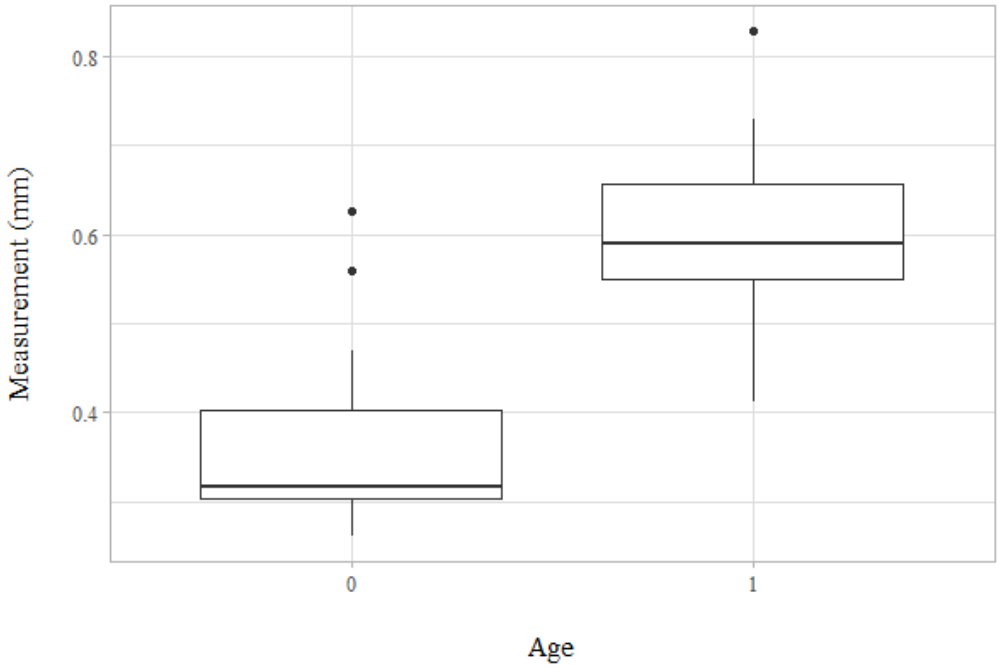

Figure 2.13: Boxplot of fall (Sept/Oct) age 0 radius measurements (n = 33) and summer (July/Aug) age 1+ first annulus measurements (n = 36).

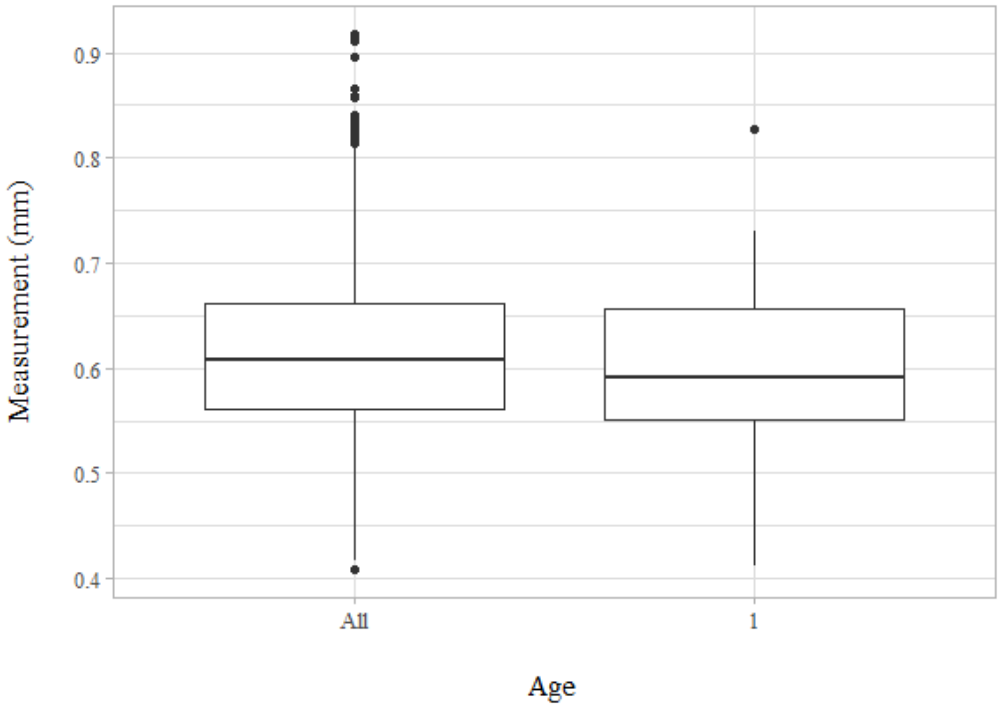

Figure 2.14: Boxplot of all first annulus measurements from MIA (n = 1,299) and summer (July/Aug) age 1+ first annulus measurements (n = 36).

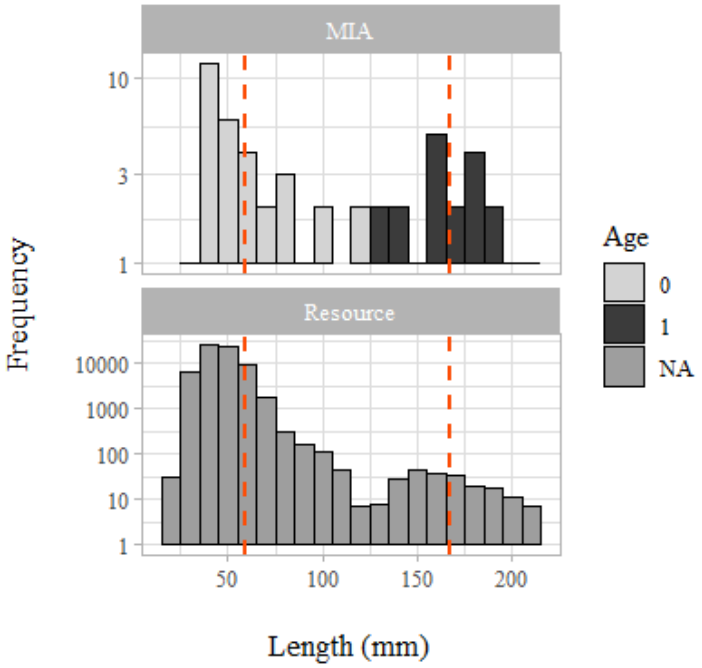

Figure 2.15: Length-frequency distributions of MIA data for ages 0 and 1 in the fall (Sept/Oct) and MA-DMF Resource Assessment Survey data for fish ≤ 220mm. Red dashed lines denote age 0 and age 1 means from MIA data.

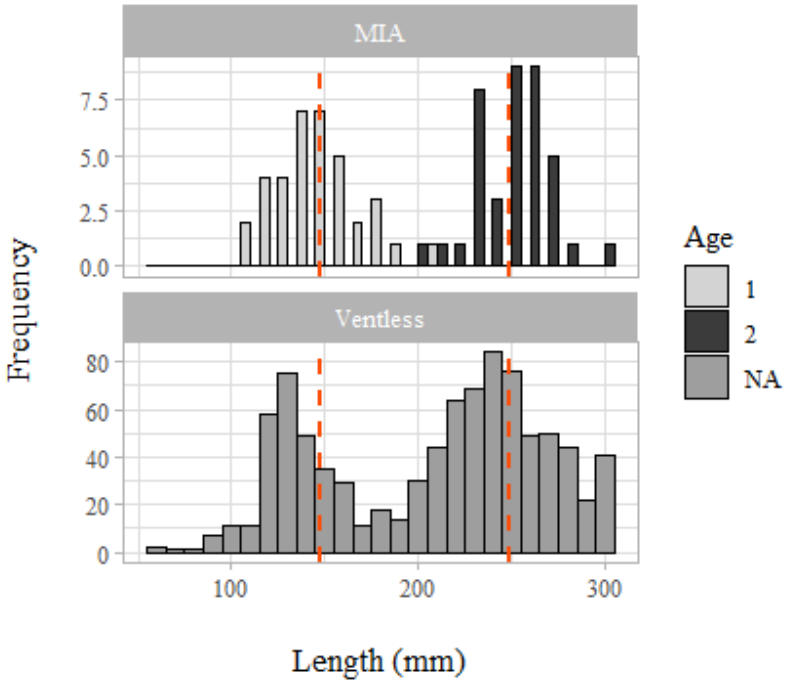

Figure 2.16: Length-frequency distributions of MIA data for ages 1 and 2 in the summer (July/Aug) and Ventless Trap Survey data for fish ≤ 310mm. Red dashed lines denote age 1 and age 2 means from MIA data.

Tables

Table 2.1: Number of samples (n), sampling years, state waters where black sea bass were captured, fishery type and gear type for samples contributed by each source. Sources: Massachusetts Division of Marine Fisheries (MA-DMF), Northeastern University, Rhode Island Department of Environmental Management (RI-DEM) in collaboration with the Commercial Fisheries Research Foundation (CFRF) and Virginia Institute of Marine Science (VIMS), Northeast Fisheries Science Center (NEFSC), Rutgers University, and North Carolina Department of Environment and Natural Resources (NC-DENR).

Source	Samples (n)	Years	States	Fishery	Gear Type
MA-DMF	2387	2013-2017	MA	Independent	Trawl; trap
Northeastern University	147	2013-2016	ME, MA	Independent; Dependent	Trap; hook and line
RI-DEM; CFRF; VIMS	545	2017	RI	Dependent	Trap; gillnet; trawl
NEFSC	483	2015-2017	MA to NC	Independent; Dependent	Trawl
Rutgers University	152	2017	NJ	Independent	Trap; hook and line
NC-DENF	847	2013-2016	MA to NC	Dependent	Trawl

Table 2.2: Number of samples by month and age used for MIA and first annulus validation.

	Age	Jan	Feb	Mar	Apr	May	Jun	Jul	Aug	Sep	Oct	Nov	Dec	Total
	0									30	3			33
AB 1	1				1		2	15	21	17	21	7		84
	2		13	22	24	42	43	29	23	29	32	18	6	281
AB 2	3	15	17	20	7	24	13	21	20	22	15	10	16	200
	4	25	32	25	12	16	36	32	27	22	20	30	25	302
AB 3	5	42	46	39	41	27	27	27	28	27	7	2	19	332
	6	1	4	9	5	16	15	12	11	10	1		4	88
	7		2	4	1	6		4	1	2			7	27
	8	1			2	1	1	1	1	1			5	13
	9	3	1		2									6
	11												1	1
	12			1										1
	Total	87	115	120	95	132	137	141	132	160	99	67	83	1368

Table 2.3: AIC test of candidate Month Bin models.

No.	Candidate Model	df	AIC
1	MIR ~ 1 (null)	2	-105.21
2	MIR ~ Month Bin	7	-669.9
3	MIR ~ Month Bin + Age Bin	9	-1071.92
4	MIR ~ Month Bin * Age Bin	19	-1184.91
5	MIR ~ Month Bin + Region	8	-667.93
6	MIR ~ Month Bin + Age Bin + Region	10	-1076.36

Table 2.4: AIC test of candidate Season models.

No.	Candidate Model	df	AIC
1	MIR ~ 1 (null)	2	-105.21
2	MIR ~ Season	5	-601.12
3	MIR ~ Season + Age Bin	7	-1028.26
4	MIR ~ Season * Age Bin	13	-1106.91
5	MIR ~ Season + Region	6	-611.89
6	MIR ~ Season * Region	9	-637.8
7	MIR ~ Season + Age Bin + Region	8	-1052.17
8	MIR ~ Season:Age Bin + Season:Region + Age Bin:Region	19	-1141.43
9	MIR ~ Season * Age Bin * Region	25	-1140.39

Table 2.5: Okamura model results. AIC values for each model: each age bin and separate regions, age bins combined. Model N = no cycle, Model A = 1 cycle, Model B = 2 cycles.

Group	Model N	Model A	Model B
AB 1	-172.68	-181.71	-174.61
AB 2	-76.94	-309.51	17.31
AB 3	18.84	-393.42	199.00
North	-86.75	-415.07	39.80
South	-8.71	-221.74	64.89

Supplemental Materials

Margin Code Analysis

In addition to marginal increment analysis, margin codes (1-4; Table 2.6) were assigned to each otolith, visually interpreting the completion of otolith edge growth compared to the previous increment (following the guidelines of VanderKooy et al. n.d.). These codes were used in conjunction with plotting mean increment ratios for each month of the year to confirm timing of black sea bass otolith annulus deposition.

Margin code results were calculated as a proportion of each code occurring per month for all age bins combined. These data were plotted overlaying MIR raw data averages per month (all age bins combined) to corroborate the timing of band formation (Figure 2.17). Marginal increment measurements in this study were made to the distal edge of the opaque band; therefore, annulus completion occurs just prior to the minimum in mean MIR, when the growth zone is fully formed (i.e. MC1). Figure 2.17 shows that MC 1 peaked in June. This occurred just prior to the peak in MC 2, which indicates new growth at the otolith margin and corresponded with a minimum in MIR values (July and August). MC 3 and MC 4 peaks followed as growth at the otolith edge continued to accrete throughout the year.

This margin code data corroborated results observed in monthly mean MIR values and confirmed that annulus formation was completed in June, just prior to the minimum in mean MIR, for all age bins combined.

Table 2.6: Margin codes for assessing completeness of growth at otolith edge (VanderKooy et al. n.d.).

Margin Code	Description of Margin Growth
1	Annual growth zone on margin fully formed
2	Annual growth zone on margin less than 1/3 formed
3	Annual growth zone on margin 1/3 to 2/3 formed
4	Annual growth zone on margin more than 2/3 formed, but not fully formed

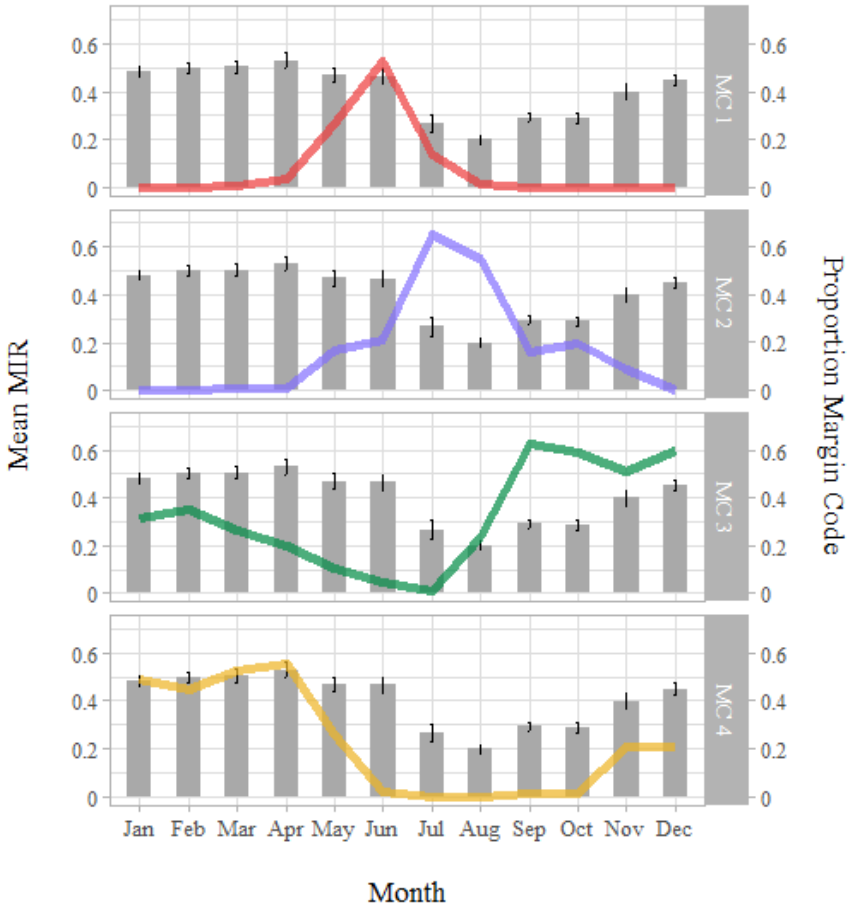

Figure 2.17: Line charts of the proportion of each margin code overlaid on monthly mean MIR bar charts, all age bins combined. Error bars are two standard errors of the mean. MC1 = margin code 1; MC2 = margin code 2; MC3 = margin code 3; MC4 = margin code 4.

CHAPTER 3

USING OTOLITH MICROCHEMISTRY TO DETERMINE NATAL ORIGIN OF BLACK SEA BASS IN THE GULF OF MAINE

Introduction

The northern stock of black sea bass *(Centropristis striata)* is an important commercial and recreational finfish species extending from Cape Hatteras, North Carolina to the Gulf of Maine (GOM; Musick and Mercer 1977; Cadrin et al. 2016). Total catch of this stock has exceeded 3,600 metric tons in recent years, over 70% of which is from north of the Hudson Canyon (NEFSC 2017). Prior to 2016, the northern stock was managed as one population; however, differences in catch and survey data, recruitment, and migration patterns between populations north and south of the Hudson Canyon (Cadrin et al. 2016; Miller et al. 2016a, 2016b; SARC 2016) led to the separation of this stock into two distinct sub-units (NEFSC 2017). Though this greater spatial detail allows for more nuanced stock assessment and management regulations, recent observations of black sea bass as far north as Maine (SARC 2016; McMahan et al. 2020) raise additional concerns about the structure and movement patterns of this species.

Once rare in the GOM (Bigelow and Schroeder 1953), commercial and recreational fishermen (Cadrin et al. 2016; McMahan 2017), as well as fishery-independent surveys (Miller et al. 2016a) report an increasing abundance of black sea bass in the region. This

recent expansion is poorly understood, and the origin of these fish is conjecture. Black sea bass from Southern New England (SNE; north of the Hudson Canyon) migrate south and east in the fall to the outer continental shelf; whereas, fish from the mid-Atlantic Bight (MAB; south of the Hudson Canyon) migrate directly east (Mercer 1978; Able et al. 1995; Moser and Shepherd 2009). These populations return in the spring and exhibit spawning site fidelity (Kolek 1990; Able and Hales 1997; Moser and Shepherd 2009; Fabrizio et al. 2013). Two suppositions for the origin of GOM black sea bass are: (1) fish or larvae are transported through the Cape Cod Canal and advected north, or (2) individuals are migrating farther north when returning to SNE spawning grounds and traveling past Cape Cod. It is also important, however, to explore the possibility that fish spawned in the MAB have begun migrating north. Changes in migration or species distribution can have major implications on survivability, resource availability, and management (Fogarty et al. 2007; Kleisner et al. 2017), and there have been no published tagging studies in the GOM to address these concerns.

Otolith microchemical analyses can help answer questions that would otherwise often require extensive amounts of time and money, such as tagging (Elsdon et al. 2008). Otoliths accrete calcium carbonate layers daily, incorporating elements from the environment into the carbonate matrix (Campana 1999). They are metabolically inert (Campana and Neilsson 1985); therefore, the layers are never absorbed, and elemental compositions are retained throughout a fish's life. Uptake and assimilation of elements into new otolith material can be influenced by environmental concentrations (Farrell and Campana 1996), water temperature or salinity (Radtke 1989; Townsend et al. 1992; Hoff and Fuiman 1995; Thorrold et al.

1997a), growth rate (Sadovy and Severin 1992, 1994; Fowler et al. 1995b), physiological regulation (Kalish 1989; Campana 1999), and diet (Farrell and Campana 1996). Consequently, fish encountering different environments will produce unique 'elemental fingerprints' (Campana et al. 2000; Campana and Thorrold 2001). These fingerprints can be used to distinguish between populations, examine environmental history, categorize nursery grounds, track migration, and determine natal origins (Edmonds et al. 1989; Kalish 1990, 1991; Campana et al. 1994, 2000; Townsend et al. 1995; Thorrold et al. 1997a, 1997b, 1998; Campana 1999, 2005; Gillanders 2002; Tanner et al. 2012, 2016). These techniques have never been used on black sea bass otoliths and provide an opportunity to elucidate this species' movement into the GOM.

Determining if GOM fish are originating from a single stock unit, or a combination of the two, is important for management and conservation practices (Steer et al. 2009; Loewen et al. 2015; Tanner et al. 2016). The natal origin of a group of fish is analyzed by targeting the otolith core, i.e. the time after hatch (Campana 1999, 2005; Arslan and Secor 2008), and matching the elemental fingerprint to those of known spawning regions (Thresher 1999; Kerr et al. 2020). McBride et al. (2018, Supplemental Material) noted spawning condition females occur along the Atlantic coast from Cape Hatteras through Massachusetts, but there is no evidence of spawning north of 43ºN. SNE and MAB populations of black sea bass should have unique otolith core elemental fingerprints due to differences in spawning behavior and migration (Campana et al. 1994, 2000). Thus, natal origin determination of GOM caught fish can occur by matching the elemental fingerprints to those from SNE or MAB.

Information gathered from otolith microchemistry enhances the understanding of a species' population dynamics, which is imperative to the successful management of an exploited stock (Secor 1999; Artetxe-Arrate et al. 2019). Black sea bass movement into the GOM is poorly understood and the resulting changes to their migration could impact allocation of proper management units and regulations. The goal of this study was to identify core elemental fingerprints of black sea bass spawning regions (SNE and MAB) and use these to classify natal origin of GOM caught fish. I hypothesized that (1) the otolith core elemental fingerprints between SNE and MAB would be significantly different; and, (2) classification of GOM black sea bass would result in samples matching the core fingerprint of SNE and not MAB.

Methodology

Sample Selection

Otoliths for microchemical analyses were selected from collaborative samples acquired for the study in Chapter 2. Samples were split into three regions based on capture location: upper GOM (Maine), SNE (Massachusetts to the Hudson Canyon), and MAB (Hudson Canyon to Cape Hatteras; Figure 3.1). The separation of SNE and MAB follows the recent partition of the stock into two populations at the Hudson Canyon, as described by SARC (2016). SNE and MAB samples were selected from fish with maturity codes of 'ripe' or 'ripe and running' at the time of capture. Fabrizio et al. (2014) observed that black sea bass exhibit home-ranges 0.05-2.8 square miles in size between feeding and spawning grounds. The relative limited movement of spawning condition fish (compared to size of

allocated regions) ensures that these samples represent black sea bass spawning locations for this study (Campana 1999; Campana et al. 2000). The criteria used between collaborators for maturity staging were comparable; all based off of standards set by Burnett et al. (1989).

Forty to fifty otoliths from each region were selected for analysis; sample sizes were limited by fish that included prerequisite maturity data. Collection of SNE and MAB young-of-year (YOY; age 0 juveniles) was intended to confirm natal elemental fingerprints and contribute to baseline data for classification analysis; however, these samples were not acquired from the MAB. Elemental comparisons between SNE YOY and SNE spawning adults were examined in the Supplemental Material. The SNE YOY collected represented years not accounted for in the other regions and, thus, were excluded from the mixed stock classification analysis.

Left side otoliths were selected when feasible, though some right-side otoliths were used (n = 20). This combination was not concerning as variation in otolith microchemistry between regions was expected to be greater than any noise created from differences between left and right side otoliths. Additionally, some studies have shown there were no significant differences between otoliths of the same fish (Thorrold et al. 1997b; Campana et al. 2000; Javor and Dorval 2014). All samples were randomized across sex and year class.

Otolith Preparation and Microchemical Analysis

Black sea bass otoliths have a central opaque region that Wenner et al. (1986) noted represents the first 1-4 months of life. Age 0 juveniles display a high degree of site fidelity (Able and Hales 1997), remaining in natal regions from 1 to 6 months until fall migration (Fabrizio et al. 2013). The central opaque region was targeted for analysis as it was believed

to represent the period prior to fall migration and avoids incorporating material associated with time spent outside natal regions, which could dilute the core chemical signature.

Otoliths (previously sectioned for analysis in Chapter 2) were mounted to standard glass slides using a small amount of Crystal Bond® adhesive. Eight samples were mounted to each slide to optimize space. Photographs of sections (100x) and measurements of the otolith core (opaque region only) prior to microchemical analyses were taken using a camera-microscope system and imaging software (Image Pro® Premier).

Trace elements are often seen as the most useful markers for elemental fingerprints in otoliths (Campana et al. 1997; Hamer and Jenkins 2007); however, adding stable isotope measurements produce more robust classification models (Thorrold et al. 1998; Tanner et al. 2016). Laser ablation inductively coupled mass spectrometry (LA-ICPMS) and gas bench isotope ratio mass spectrometry (GB-IRMS) were used in this study to measure trace elements and stable isotopes, respectively. These two methods allow for directed sampling of a small region of interest, versus analyzing whole otoliths in solution-based assays (Kalish 1989; Radtke 1989; Gallahar and Kingsford 1992; Fowler et al. 1995b, 1995a).

Trace Element Analysis: LA-ICPMS

Samples were analyzed using a PerkinElmer NexION 2000C Inductively Coupled Plasma Mass Spectrometer (ICPMS) with CETAC 213 G2+ (213 nm Nd:YAG) equipped with the HelEX II sample cell for solid sampling at the Environmental Analytical Facility (EAF) at the University of Massachusetts Boston. Samples were viewed under reflected light, and transect lines were drawn across the opaque core of the otoliths for analysis (Figure 3.2). A pre-ablation transect was run prior to elemental assay to remove any surface contaminants

(Campana et al. 1994; Thresher 1999). Otolith material along the drawn transect was vaporized by the laser and transported by argon gas to the ICPMS for isotopic composition analysis (Denoyer et al. 1991).

Laboratory recommendations for instrument specifications were used as follows: pre-ablation transect spot size of 50µm and a speed of 50 µms-1; sampling transect spot size at 30µm and a speed of 15µms-1; laser output at 20%. Three transects of MACS-3 pressed carbonate disc standard (US Geological Survey, Reston, VA) were run before and after each slide (eight samples). The isotopes analyzed were: Ca^{48}, Mg^{24}, Mg^{25}, Mg^{26}, Mn^{55}, Cu^{63}, Cu^{65}, Zn^{64}, Zn^{66}, Zn^{68}, Sr^{86}, Sr^{87}, Sr^{88}, Cd^{112}, Cd^{114}, Ba^{136}, Ba^{137} and Ba^{138}. Additionally, Si^{28} was monitored to confirm the laser was not ablating the glass slide below the sample section. Data reduction and processing were completed using Igor Pro 7® (WaveMetrics, Inc., Portland, OR) and Iolite® software (Iolite Software, University of Melbourne, AU) to correct for instrument drift and standardize to MACS-3. Isotopic abundances were converted to parts per million (ppm), reported relative to Ca48, and averaged across the entire transect. Cd^{112}, Cd^{114}, and Zn^{68} were removed from further analysis due to a large proportion of erroneous values produced during LA-ICPMS analysis. Limit of detection values (ppm) for each isotope, averaged across all samples were: Mg^{24} = 0.041, Mg^{25} = 0.130, Mg^{26} = 0.770, Mn^{55} = 0.195, Cu^{63} = 0.274, Cu^{65} = 0.425, Zn^{64} = 0.326, Zn^{66} = 0.473, Sr^{86} = 1.543, Sr^{87} = 0.373, Sr^{88} = 0.089, Ba^{136} = 1.458, Ba^{137} = 0.057, Ba^{138} = 0.018. All isotope measurements were consistently above the corresponding average limits of detection.

Stable Isotope Analysis: GB-IRMS

Following LA-ICPMS analysis, otolith cores were milled using a New Wave™ Research MicroMill (Electro Scientific Industries, Portland, OR) at the Gulf of Maine Research Institute in Portland, Maine. Micromill specifications were set to laboratory recommendations, as follows: scan speed of 55 μms^{-1}, 9 passes/sample, depth/pass at 55µm, and drill speed at 100%. The diameter of the carbide drill bit was 300µm. The entire opaque region of the otolith core was sampled for analysis (Figure 3.2). Milled sample material was collected onto weighing paper, folded, and placed in Fisherbrand® 1.5mL plastic vials. The micromill, drill bit, and sample slides were cleaned with pressurized air and 95% ethanol between each sample to prevent cross-contamination.

Milled otolith material was weighed using a microbalance and placed in clean glass instrument tubes at the EAF. Laboratory standards NBS-19, IA-R022, and $CaCO_3$ were weighed to match sample weights for each run (0.2-0.3mg) and placed in clean glass instrument tubes. Air was removed from sample and standards tubes by injecting helium gas, and powdered material was reacted with 100µl of 100% phosphoric acid and allowed to digest at 25 ºC for 24 hours. Sample tubes, now containing CO_2 gas, were analyzed for d13C and d18O using a Thermo Scientific™ Gas Bench II Isotope Ratio Mass Spectrometer (IRMS) for gas chromatography at the EAF. The $CaCO_3$ standard was run at the start of each analysis day; whereas, NBS-19 and IA-R022 standards were run at the start, after every 9-12 samples, and at the end of each analysis day. Isotope ratio measurements were calibrated based on repeated measurements of the standards and reported relative to the Vienna Pee Dee Belemnite standard for carbonate materials.

Statistical Analysis

Using the opaque region of otolith cores instead of a distinct measurement for each sample increases the likelihood of variation in the amount of material analyzed. Otolith core transect measurements were compared between regions using one-way analysis of variance (ANOVA) followed by Tukey's Honestly Significant Differences (Tukey's HSD). Additionally, due to a significant ANOVA result, Pearson's correlation coefficients were used to look at the effect of core measurements on isotope values in each region (Thorrold et al. 1998). The significance value for all test conducted in this study was alpha = 0.05.

Pearson's correlation coefficients between isotopes of the same element were also used to confirm relative abundance of those elements (Campana et al. 1994). All within-element correlations were high ($r \geq 0.79$; Table 3.1); therefore, the following isotopes were used in subsequent analyses: Mg^{24}, Mn^{55}, Cu^{63}, Zn^{64}, Sr^{86}, Ba^{137}, as well as d18O and d13C. All trace elements were expressed as element:Ca ratios. Data transformations were necessary for element:Ca distributions to satisfy normality assumptions. Mg:Ca, Mn:Ca, and Ba:Ca were log10 transformed (log10(1+X)); while, Cu:Ca and Zn:Ca required inverse transformations (1/(X+1)). Sr:Ca, d18O, and d13C were not transformed. Normality and homogeneity of variance and covariance were assessed using diagnostic plots, the Shapiro-Wilk test, and Levene's test. Values five standard deviations from the mean were removed as outliers (Campana 2005).

Multivariate analysis of variance (MANOVA) with Pillai's trace (robust to deviations in normality; Ateş et al. 2019) was used to identify significant differences in core chemical fingerprints between regions (Campana et al. 2000). Individual one-way ANOVA tests were

conducted for each significant isotope identified in the MANOVA with Region as the independent variable. Post-hoc analyses of isotopes with significant ANOVA results were followed with Tukey's HSD. Plots between regions were produced for each isotope using estimated marginal means (Lenth 2019) to help visualize regional differences.

Discrimination and classification of samples in this study were conducted using two supervised learning approaches: linear discriminant function analysis (LDFA) and random forest approach (RF). In each of these methods, discrimination functions for groups of known origin (i.e. SNE and MAB) were built using isotopic concentrations as discriminatory variables (James et al. 2013). These functions were then used to classify samples with unknown group membership (i.e. GOM) to the population with the highest probability of origin (Manel et al. 2005). LDFA creates a linear function from the supplied variables that best separates each group (Manel et al. 2005); whereas, RF uses bootstrap resampling with replacement to build classification trees for group prediction (Breiman 2001). LDFA can provide powerful discrimination between groups (Jones et al. 2017) and is the most frequently used method (Mercier et al. 2011). It can, however, be limited by assumptions of normality (Mercier et al. 2011), and its application to classify samples of unknown origins has been questioned (Campana 2005). RF is not limited by assumptions of normality (Mercier et al. 2011) and had the best performance among classification methods in otolith elemental fingerprint analyses (Mercier et al. 2011; Tournois et al. 2013; Artetxe-Arrate et al. 2019; Maguffee et al. 2019).

LDFA classification accuracy for SNE and MAB discrimination function was measured using leave-one-out cross-validation with equal prior probabilities (Venables and

Ripley 2002). Variable importance was evaluated based on the weight of standardized linear discriminant coefficients (Thomas and Zumbo 1996). Final variable selection was completed by comparing the accuracies of eight models: (1) all isotopes, (2) isotopes with significant differences between regions (ANOVA), (3-8) addition and subtraction of non-significant isotopes to model 2. The model with the highest accuracy was chosen for classification of unknown origin GOM samples.

RF classification error was assessed using the average 'out-of-bag' (OOB) error rate from the built in cross-validation procedure (Breiman 2001). The mean decrease in Gini coefficient was used as a proxy for variable importance (Breiman 2001) and final variable selection was completed by assessing the OOB error rate among models 1-8, as described above. The model with the lowest error rate was chosen for classification of unknown GOM samples. To avoid losing data due to low sample sizes, the probability threshold used for RF was 0.50 (the same as the default value for LDFA). Analysis of additional RF threshold levels is available in the Supplemental Materials. Functions to optimize RF parameters of *mtry* and *ntree* indicated that the default values produced the lowest error, as is described elsewhere (Liaw and Wiener 2002; Díaz-Uriarte and Alvarez de Andrés 2006).

Analyses and visualizations were conducted using base R (version 3.6.1; R Core Team, 2019), as well as the following packages: 'car' version 3.0-3 (Fox and Weisberg 2019), 'emmeans' version 1.4.1 (Lenth 2019), 'multcomp' version 1.4-10 (Hothorn et al. 2008), 'ggplot2' version 3.2.1 (Wickham 2016), 'MASS' version 7.3-51.1 (Venables and Ripley 2002), and 'randomForest' version 4.6-14 (Liaw and Wiener 2002).

Results

A total of 156 black sea bass otoliths were selected for microchemical analysis. Fifteen samples were removed due to issues of broken otolith sections, contamination, or instrumentation error. Three samples in New York waters were also removed due to their proximity to the MAB (Figure 3.1). These samples were assigned to SNE based on the NMFS statistical area Hudson Canyon separation described in SARC (2016); however, it is noted that this partition is not precise and there is overlap between groups. Consequently, these samples could obscure elemental contrasts between the two populations. Descriptive details for the final samples used for this study (n = 141) are in Table 3.2.

Measurements of otolith cores ranged from 0.48 mm to 1.02 mm, which were slightly smaller, though comparable, to measurements taken by Wenner et al. (1986) for black sea bass in the southern stock (0.56 mm to 1.54 mm). Core measurements differed significantly across regions ($F = 4.36$, $df = 2$, $p = 0.0148$). Tukey's HSD indicated the mean GOM core measurement was fairly similar to MAB ($p = 0.05$), but significantly smaller than SNE ($p < 0.05$). Mean core lengths for GOM, SNE, and MAB were 0.70 mm, 0.77 mm, and 0.76 mm, respectively. It is unlikely these differences between regions were contributing to systemic effects on isotope concentrations; however, additional analyses were examined to confirm. Pearson's correlation coefficients between core measurements and isotope values for each region were low, ranging between -0.33 to 0.36 (Figure 3.3). Additional plots used to assess any relationship between isotopes and core measurements for each region are available in the Supplemental Materials (Figure 3.5). No clear patterns were evident between measurements and isotope values. The ANOVA results preclude correcting for differences in core

measurements by using an analysis of covariance; however, there was very little correlation between these variables, and the differences seen in the ANOVA may not be biologically meaningful (i.e. a difference of 0.1mm between MAB and SNE that lead to statistical significance for GOM).

All elements passed Levene's test for homogeneity ($p < 0.05$). Shapiro-Wilk's test for normality was passed by all elements ($p < 0.05$) except d13C ($p = 0.0017$). Inspection of d13C diagnostic plots showed a very slight left-skewed distribution, not a large departure from normality; therefore, parametric tests were considered suitable for this isotope. Only one outlier from Mg:Ca was removed for MANOVA and ANOVA analyses (approximately 5 standard deviations above the mean).

Results of the MANOVA indicated statistically significant differences in core elemental fingerprints between regions: Pillai's Trace = 0.73, $F = 9.44$, $df = 2$, $p < 0.0001$. Individual element one-way ANOVA results are shown in Table 3.3. Levels of d18O, Mg:Ca, Mn:Ca, Cu:Ca, and Ba:Ca. differed significantly across regions; whereas, Sr:Ca and d13C did not. ANOVA results for Zn:Ca were unclear ($p = 0.0467$), but post-hoc analysis using Tukey's HSD indicated no significant differences ($p > 0.05$). Visual inspection of these results revealed regional variation, even though it was not statistically significant (Figure 3.4). Mean Zn:Ca concentrations were elevated in SNE, as compared to GOM and MAB. The remaining non-significant isotopes also displayed a slight pattern, where levels of d13C and Sr:Ca were higher in GOM and SNE than in MAB. Additional isotopes showing this pattern included, Mg:Ca and Ba:Ca, where mean MAB concentrations were significantly lower than GOM and SNE ($p < 0.01$). GOM and SNE were not significantly different for

these isotopes ($p = 0.107$ and $p = 0.9969$, respectively), though GOM had a higher concentration of Mg:Ca. Among the three regions, MAB had the highest means for d18O, Mn:Ca, and Cu:Ca. Mean d18O in the MAB was significantly higher than the GOM and SNE ($p < 0.001$), which were not significantly different from each other ($p = 0.3999$). Mn:Ca and Cu:Ca followed similar patterns for each region, where GOM had the lowest mean concentration, followed by SNE, then MAB as the highest. Post-hoc analysis indicated that GOM and SNE were not significantly different for Mn:Ca ($p = 0.1745$), and SNE and MAB were not significantly different for Cu:Ca ($p = 0.1962$).

The most influential elemental variables for discriminating SNE and MAB regions in the leave-one-out cross validation LDFA (full model) were Ba:Ca, d18O, d13C, Mn:Ca, Mg:Ca, and Cu:Ca (Table 3.4). Except for d13C, these were also the isotopes that varied significantly with location in the ANOVA analyses above (Table 3.3). Zn:Ca and Sr:Ca were not included in the LDFA coefficient output due to low contribution in separating these populations. Classification accuracies for each of the eight models analyzed using leave-one-out cross-validation LDFA are in Table 3.5. The model using significant isotopes plus d13C (model 4) resulted in the highest overall classification success (85%) and had regional classification accuracies of 88% and 82% for SNE and MAB, respectively. Assignment of GOM samples to a region of origin using this LDFA model resulted in 41 samples (87%) assigned to SNE and 6 samples (13%) assigned to MAB.

Variable importance for the RF analysis differed slightly from the LDFA (Table 3.6). The mean decrease in Gini coefficients showed that Ba:Ca remained the most influential variable, followed by d18O, for population discrimination of SNE and MAB. Mg:Ca, Cu:Ca,

and Mn:Ca all remained in the top five variables of importance, Zn:Ca was higher than d13C, and Sr:Ca contributed the least to classification. OOB error rates for each of the eight models analyzed using RF are in Table 3.7. The model using all isotopes except Sr:Ca (model 6) resulted in the lowest error rate (13%) and was used to assign samples of unknown origin (GOM). Default values for *ntree* and *mtry* were 500 and 2, respectively. At a classification threshold of 0.50 (i.e. 50% chance that a sample belongs to a certain region), 41 GOM samples (87%) were classified to SNE and 6 (13%) to MAB. For samples assigned to SNE, there was a maximum probability of 0.98, an overall average probability of 0.83, and three-quarters had a probability of 0.80 or above. The maximum probability of samples assigned to MAB was 0.75, with an overall average probability of 0.66.

The LDFA and RF assigned the same number of GOM samples to each region (41 to SNE and 6 to MAB); however, two samples switched regions between models, i.e. one sample assigned to MAB in the LDFA was assigned to SNE in the RF analysis, and the opposite for the other sample. The probabilities of assignment reported in the RF analysis were near the 0.50 cutoff for both samples.

Discussion

Otolith Core Chemistry

This was the first study to use otolith microchemistry as an approach to study black sea bass. The results of this work provide insight on the population composition in the upper GOM, a region to which this species recently expanded (McMahan et al. 2020). Elements are indicators of different processes and their abundance in the environment can be influenced by

many factors. Incorporation of elements into otolith material is shown to vary with exogenous and endogenous processes, many times interactively, and they differ between element, location, and fish species (Kalish 1989; Fowler et al. 1995a, 1995b; Thorrold et al. 1997b; Hamer and Jenkins 2007; Barnes and Gillanders 2013; Sturrock et al. 2015). Despite the uncertainty in the mechanism of incorporation, these elements are useful in discrimination studies because they differ among groups of fish (Campana et al. 2000).

Microchemical analyses revealed significant differences in the otolith core chemical signatures between SNE and MAB, indicating that these spawning populations present unique core signatures. Discrimination models were largely driven by elements that were statistically significantly different between regions, i.e. Ba:Ca, Mg:Ca, Mn:Ca, Cu:Ca, and d18O (Table 3.3). Although the results of each classification method were the same (i.e. 41 GOM samples assigned to SNE and 6 to MAB), variable importance differed between each analysis (Tables 3.4 and 3.6). For example, Ba:Ca and Mg:Ca exhibited similar patterns between regions, but Mg:Ca was the fifth most important variable in the LDFA and third in the RF. Post-hoc analyses of these elements among regions showed that SNE had significantly higher concentrations of Ba:Ca and Mg:Ca in otolith cores than MAB (Figure 3.4). Additionally, the GOM samples were not significantly different from SNE for either of these ratios, suggesting they may have been spawned in the same environment.

Water temperature could explain the differences in Ba:Ca and Mg:Ca concentrations observed between SNE and MAB. An inverse relationship between temperature and incorporation of Ba and Mg into otoliths is described in several studies (Fowler et al. 1995b, 1995a; Sturrock et al. 2015; Régnier et al. 2017; Moreira et al. 2018). The lower levels of

Ba:Ca and Mg:Ca observed in the cores of fish from MAB, which typically has warmer water than SNE, would follow this trend. The exact mechanism of regional differentiation was difficult to ascertain due to a variety of other factors that can cause these elements to vary in the environment. For instance, temperature's relationship to Ba and Mg incorporation into otoliths is inconsistent (Fowler et al. 1995a; Hoff and Fuiman 1995; Bath et al. 2000; Elsdon and Gillanders 2002; Barnes and Gillanders 2013). These elements can also vary with salinity (Fowler et al. 1995a; Sturrock et al. 2015; Moreira et al. 2018), overall environmental availability (Bath et al. 2000; Campana et al. 2000; Elsdon and Gillanders 2002; Hamer and Jenkins 2007), and, in the case of Mg, physiological regulation (Hamer and Jenkins 2007; Barnes and Gillanders 2013).

Discrimination between SNE and MAB in the models was heavily influenced by d18O. Average d18O values were highest in MAB, significantly different from GOM and SNE. SNE had the lowest values but was not significantly different from GOM. Oxygen isotopes are deposited in otoliths directly proportional to its abundance in the surrounding water (Kalish 1991; Thorrold et al. 1997a) and, thus, are influenced by environmental availability. Temperature has a well-documented, negative relationship with d18O in otoliths (Kalish 1991; Thorrold et al. 1997a; Elsdon and Gillanders 2002; Dorval et al. 2011; Carvalho et al. 2017a). The expectation was that d18O levels in MAB would be more depleted (generally higher temperatures) and higher in SNE (generally lower temperatures); however, the opposite was observed in this study. There did not appear to be any impact of sample source influencing extreme values in any region; samples at the lowest and highest

ends of each region were from different collaborative sources/states and caught using a variety of capture methods.

Compiled bottom temperature data from collaborative black sea bass sampling (acquired in Chapter 2) shows considerable overlap in temperature regimes between regions (Supplemental Materials, Table 3.8). The temperature range at sites from May to September in SNE was between 7.0ºC to 22.3ºC with an overall average of 15.3ºC. MAB ranged from 9.1ºC to 22.5ºC with an overall average of 16.6ºC, though data were limited for some months and statistical areas. Caruso (1995) noted spawning in Nantucket Sound peaked as water temperatures approached 20ºC in 1993 and 18ºC in 1994. McBride et al.'s (2018) collection of age 0 black sea bass in 2006-2007 reported bottom temperatures ranging from 6ºC to 20ºC in Nantucket Sound, as well as surface temperatures in Buzzards Bay from 14ºC to 23ºC. This information demonstrates the large amount of variability in temperature between black sea bass spawning areas within each region, as well as high recorded temperatures in Massachusetts waters. Additionally, Able et al. (1995) noted higher water temperatures at stations in Massachusetts than in the MAB where age 0 black sea bass were captured. A high number of SNE spawning adults in this study were sampled from Buzzards Bay and Nantucket Sound, where temperatures can be over 20ºC, and may explain the unexpected results for d18O observed in this study. Additionally, half of the MAB samples in this study came from statistical area 614 in July, where the average temperature was 16ºC. Thus, it is possible SNE caught black sea bass were spawned in warmer waters than MAB caught fish, which would support the observed d18O results.

Mn:Ca and Cu:Ca were also important variables used to discriminate regions in this study. Factors that influence Mn and Cu incorporation into otoliths include temperature, salinity, and environmental availability (Fowler et al. 1995a; Sturrock et al. 2015). Additionally, these elements are biologically important (Kremling 1985; Hamer and Jenkins 2007) and physiologically regulated (Thorrold et al. 1998). The average concentrations for both ratios were highest in MAB and lowest in GOM, with SNE falling between the two (Figure 3.4). Though GOM concentrations for these elements were not as similar to SNE, they were clearly more closely related to SNE than MAB.

The main sources for Mn and Cu in marine environments are river outflow, anthropogenic runoff, and sediment disturbance (Kremling 1985; Shiller 1997; Van Hulten et al. 2017). Many of the fish captured in MAB were located near the Hudson and Delaware river outflows during the spawning season (Figure 3.1). The expectation was that these rivers contributed to high levels of these elements in the samples studied; however, the direction of the Hudson River outflow changes seasonally. Chant (2008) models how oceanographic conditions in the winter allow for the expected river outflow transport along the New Jersey coast; but, during the summer months, a freshwater bulge is created and forced north along the Long Island coast. If this is the case, black sea bass larvae off the coast of New Jersey in the summer were unlikely to experience an influx of elemental compounds from the Hudson River outflow. Still, physiological regulation, uptake, and incorporation of these elements into otolith material remains unclear (Hamer and Jenkins 2007; Loewen et al. 2015); and, an in-depth analysis of why elemental concentrations differed between regions in this study was not possible.

Though there were no statistically significant differences within otolith cores, average values for d13C and Sr:Ca in MAB were slightly lower than SNE (Figure 3.4). GOM and SNE averages for both these elements were almost identical, adding to the similarity between these two regions observed in these analyses. The inclusion of d13C in the RF analysis reduced error and it was the third most important variable in the LDFA; however, the same was not true for Sr:Ca (Tables 3.4 and 3.6). Sr:Ca did not change the LDFA model's accuracy (Table 3.5) and inclusion in the RF analysis raised the OOB error rate (Table 3.7). Though these elements followed similar patterns, the reason d13C had a bigger impact on the discrimination of these regions was unclear.

Despite the diverging impacts on error rates, the lack of significant differences between SNE and MAB for d13C and Sr:Ca were not surprising. Dissolved inorganic carbon (DIC) in the surrounding environment is the main source of carbon incorporation into the otolith structure; however, carbon incorporation is also heavily influenced by dietary sources (Kalish 1991; Thorrold et al. 1997a). Black sea bass are opportunistic omnivores (Mercer 1989; Steimle et al. 1999; McMahan et al. 2020); therefore, similar d13C values between regions were expected. However, the slight difference in d13C in the MAB samples could be due to prey type available in one region and not in the other (McMahan et al. 2020). Temperature and salinity influences on d13C incorporation into otoliths are inconsistent (Kalish 1991; Elsdon and Gillanders 2002; Carvalho et al. 2017a); and, as a result, it was difficult to postulate whether temperature differences between SNE and MAB impacted d13C values in these otoliths.

The concentration of Sr in the marine environment remains relatively constant (Thorrold et al. 1997b; Elsdon et al. 2008); therefore, a significant difference between regions for Sr:Ca in otoliths was not expected. The slight depression in Sr:Ca values in MAB may be related to the freshwater outputs near those sampling regions, as seen in other studies (Carvalho et al. 2017a; Moreira et al. 2018). Salinity (and temperature) effects on the incorporation of Sr into otoliths are inconsistent (Townsend et al. 1995; Kalish 1989, 1990; Townsend et al. 1989, 1992; Sadovy and Severin 1992; Fowler et al. 1995a; Hoff and Fuiman 1995; Bath et al. 2000; Elsdon and Gillanders 2002; Sturrock et al. 2015); thus, it was unclear whether the magnitude of the Hudson and Delaware River outflows impacted Sr:Ca ratios in these samples. Additionally, the summer freshwater bulge pushed north into the Long Island coast from the Hudson Canyon discussed above would reduce expected impacts to salinity along the mid-Atlantic coast (Chant et al. 2008).

Zn incorporation into otoliths is impacted by temperature (Fowler et al. 1995b, 1995a; Sturrock et al. 2015); however, as a biologically important element (Conway and John 2014; Middag et al. 2019) its uptake, regulation, and incorporation into otolith material is less understood (Loewen et al. 2015). Similar to Mn and Cu, riverine input and anthropogenic activities are important sources of Zn in the marine environment (Thorrold et al. 1997b; Conway and John 2014). A slightly higher mean value of Zn:Ca was observed in SNE (Figure 3.4), though inspection of raw data better displays the dispersion and lack of significant difference between regions (Supplemental Material, Figure 3.6). Including this variable resulted in lower accuracy for the LDFA model (Table 3.5), but, conversely, it lowered OOB error rate in the RF model (Table 3.7). Zn:Ca was included in the RF model;

however, since the final assignment of GOM samples was the same for both models (i.e. 41 samples assigned to SNE, 6 to MAB), Zn:Ca was likely not essential in delineating the GOM samples.

Despite the limitations surrounding the understanding of otolith element regulation and incorporation, otolith microchemistry is useful to infer population structure (Elsdon et al. 2008; Steer et al. 2009) and to identify natal origin (Campana et al. 1994, 2000). The exact mechanisms driving the chemical differences observed in otoliths between SNE and MAB in this study remain unclear; however, classification of unknown origin fish (GOM) was possible using these unique fingerprints.

Hypotheses and Classification

The hypothesis that the GOM otolith core chemical signatures would match with SNE's was based on the proximity of these two regions, as well as on colloquial theories and tagging studies. One theory is that fish or larvae are transported through the Cape Cod Canal, from spawning activity in Buzzards Bay, and advected north. McBride et al. (2018), however, notes that there are no ichthyoplankton data to support this idea. Alternatively, it is thought that fish in the GOM could be SNE spawned individuals that strayed north when migrating back from offshore overwintering grounds. Moser and Shepherd (2009) tagged black sea bass from Massachusetts to North Carolina and found that black sea bass returned to previous spawning areas. The high percentage of tag returns to each spawning region can be seen in the Supplementary Materials, Table 3.9 (Table 2 from SARC 2016); however, Moser and Shepherd (2009) observed straying behavior more prevalent in fish tagged north of the Hudson Canyon. Six percent of the fish from north of the Hudson Canyon were

captured 1 degree square from the release location, versus 0.005% of fish from south of the Hudson Canyon exhibiting the same behavior (Moser and Shepherd 2009). This, in addition to a low rate of fish tagged in the south but recovered in the north (0.70%; Supplementary Materials, Table 3.9), supports the theory that SNE fish may have strayed to the GOM.

Though there are few documented occurrences of MAB fish straying north, this study aimed to look at the possibility of GOM fish originating from this region. A change in migration pattern or behavior could have major implications for the management of this species, thus highlighting the importance of exploring this possibility. Also, there are no published tagging studies completed in recent years to track these fish or record any changes. LDFA and RF analyses both assigned 41 (87%) of the GOM samples to SNE and 6 (13%) to MAB. The overall average probability of samples assigned to MAB from the RF model was 0.60, with a maximum probability of 0.75. These values were lower than those for fish assigned to SNE, which had an overall probability of 0.83 and a maximum probability of 0.98. This indicates that there was less certainty that the samples assigned to MAB truly originated from this region, compared to the samples assigned to SNE. Additionally, there were two GOM samples that were assigned to different regions in each model (i.e. one sample assigned to MAB in the LDFA was assigned to SNE in the RF analysis, and vice versa). Both GOM samples had assignment probabilities very close to 0.50; therefore, it was not surprising that there was a difference in these samples between models.

Overall, most of the GOM samples were assigned to SNE with a high probability of origin from that region. This confirmed the pattern observed in individual isotope ANOVA's; where, for most elements, GOM otolith chemical concentrations aligned more closely to the

concentrations measured in SNE samples. Based on these results, future stock assessments could assume life history traits of GOM fish align with those of the SNE sub-stock; however, recent work by McMahan et al. (2020) suggests differently. Their work found that black sea bass caught in Maine waters grew faster and reached maturity at a younger age than those caught in northern and southern Massachusetts. This finding as well as the assignment of several samples to the MAB in the current study, highlight the need for more research on black sea bass movement and possible residency in the upper GOM.

Assumptions and Other Considerations

No Spawning in GOM

The aim of this study was to determine the source of fish caught in the upper GOM to assess the possibility of unexpected MAB contribution to this region. This objective assumed no black sea bass spawn within the GOM, particularly in Maine where these samples were captured. Although there is evidence of YOY, juveniles, and mature adults present within the lower GOM, the assumption that spawning was not occurring appears to be sound given the current information available. McBride et al.'s (2018) analysis of bottom-trawl survey data from the Northeast Fisheries Science Center (NEFSC) and Massachusetts Division of Marine Fisheries indicated that nursery grounds, YOY, and spawning adults have moved northward over the last 40 years. YOY black sea bass were more abundant in Cape Cod and Massachusetts Bay waters from 2008-2016 (n = 1,233) than from 1978-1987 (n = 121; McBride et al. 2018). However, few spawning condition (or spent) females were found in these areas, which “would provide the most direct evidence of spawning” in the GOM (McBride et al. 2018). Additionally, the NEFSC survey extends to mid-coast Maine (~44ºN),

but the northernmost occurrence of black sea bass YOY or developing females was 42ºN (off Gloucester, MA). McMahan (2017) also observed black sea bass YOY in Massachusetts waters, though they were significantly more abundant south of Cape Cod, and no YOY were found in Maine. Conversely, 10 out of the 47 GOM black sea bass used in the current study were in 'ripe' spawning condition. This information, McMahan's observations, and McBride's prediction that spawning will eventually be seen in the GOM highlights the possibility that spawning within this region is beginning to occur or will in the future. The ripe GOM samples in this study were from year classes 2011-2014; thus, based on the information available, it is unlikely that spawning in the GOM, especially in the upper GOM, was occurring during these years.

Representative Spawning Regions

In natal origin studies, acquiring fish from all spawning or larval sources to represent each natal region can be difficult (Miller et al. 2005; Gibb et al. 2017). Black sea bass exhibit a general continuum of spawning activity along the Atlantic coast versus discrete locations (G. Shepherd, personal communication, 2017), which can be represented by age-0 black sea bass fall distributions seen in the Supplemental Materials, Figure 3.7 (Supplemental Figure 4 from McBride et al. 2018). The objective of this study was formulated considering this behavior and used the recent spatial population split at the Hudson Canyon (NEFSC 2017) to discern regions; looking at a wide spatial range versus attempting to split the populations further into arbitrary segments.

Spawning condition black sea bass from SNE and MAB were selected based on the assumption that this species returns to natal regions for spawning and would, therefore,

characterize these regions. A violation of this assumption would mean, for example, that the fish used to represent SNE actually represented MAB (Campana et al. 1994). Natal homing and spawning site fidelity are well documented for black sea bass. As previously discussed, the Moser and Shepherd (2009) tagging study observed a high rate of return to spawning locations the following spring (>90%; Supplementary Materials, Table 3.9). Kolek (1990) and Fabrizio et al. (2013) also observed returning fish to tagged locations the year following release, indicating homing behavior. Additionally, the distinct regional differences observed in otolith core elemental concentrations and overall chemical signatures in this study support the assumption that these fish represented separate regions.

Interannual Variation

Microchemical studies often aim to match exact year classes for comparison to avoid the assumption of non-significant interannual variation in chemical fingerprints. Data limitations for the black sea bass samples acquired for this study (i.e. availability of maturity data) led to the use of a range of year classes (Table 3.2). Though most of the year classes overlap, there was one year (2016) represented in the GOM samples that was not available for SNE and MAB. Annual variation in elemental concentrations, or misrepresentation of a year class, can impact the accuracy of classification models (Tanner et al. 2012; Maguffee et al. 2019). Figure 3.8 (Supplemental Materials) shows each element concentration by year class and region. Not only was the 2016 GOM year class only one sample, it appeared to lie within normal ranges for all elements. These plots show some interannual variation among elemental concentrations within regions, which was expected; however, no major trends or outliers appear to influence the overall chemical signature in each region. A possible

exception may include d13C for the GOM, but factors influencing this element in otoliths was discussed above and described that variability is common.

Analysis of multiple year classes and identification of multi-year regional chemical fingerprints in this study may give the opportunity for further use in the future. Several studies showed good classification and re-assignment accuracies when using multi-annual signatures (Brown 2006; Tournois et al. 2013). The work in this study may be possible to use as baseline data for future microchemical analyses; however, Tournois et al. (2013) suggests connectivity studies should be completed annually to track any deviations in elemental concentrations.

Maternal Elemental Transfer

Microchemistry studies show there can be an elevated concentration of certain elements in the otolith primordium (Laugier et al. 2015; Artetxe-Arrate et al. 2019; Maguffee et al. 2019), often attributed to maternal transfer during egg development (Ruttenberg et al. 2005). There is concern that primordia concentrations do not accurately reflect the natal region and instead represent the water chemistry surrounding the female during gonadal development (Ben-Tzvi et al. 2007; Artetxe-Arrate et al. 2019). Black sea bass begin inshore migration to spawning locations from offshore overwintering grounds by April, when water temperatures begin to warm (Drohan et al. 2007). Wilk et al. (1990) found that peak GSI occurs in July (only 4% ripe in May) in the New York Bight, and Wuenschel et al. (2011) found that peak GSI occurred in May and June in Massachusetts and Rhode Island. Yet, this work does not portray when development of ovaries and eggs begin. Mercer's (1978) histological work showed that stage 3 of oogenesis, representing the start of ovarian activity,

began in May for black sea bass in the MAB. This suggests that ovary development does not occur until after the spring migration inshore has begun.

Compiled fish maturity information (females only) for otolith samples collected for work described in Chapter 1 is shown in the Supplemental Material (Table 3.10). In SNE, developing females were present starting in April, though data were limited for this month and months prior. MAB data show a few developing females in February and March, though most were identified as resting in those months. Even though there were black sea bass in the developing stage before April in the MAB, these fish were caught inshore; therefore, any maternal elemental influence caused by incorporation from the surrounding environment would be from the region of interest.

Maguffee et al. (2019) measured otoliths starting 100 microns from the primordia, estimating the timing of exogenous feeding. Identification of the primordia within the opaque core of black sea bass otoliths was difficult with the camera resolution and lighting options on the LA-ICPMS; therefore, it was not feasible to follow a similar method accurately. Despite this, the information presented above suggests that ovary development does not begin to occur until inshore migration has begun. This would mean that elemental incorporation from the environment by the female would occur within the spawning regions identified in this study. If future microchemical studies are conducted to look at finer spatial detail, however, a method avoiding the primordium should be considered.

Opaque Core Size Variability

Otolith core measurements (opaque region only) in this study were slightly smaller than those measured by Wenner et al. (1986) for the southern stock of black sea bass. Growth

rates for fish in the northern stock are faster than farther south (Mercer 1978; Kolek 1990), though Mercer (1978) does note that growth for ages 1 and 2 is faster in the south. Variability in the size of the opaque region of the otolith core was likely an artifact of spawning date (Wenner et al. 1986; Laugier et al. 2015). Black sea bass in the northern stock spawn from April through October, peaking in June-July (Mercer 1978; Kolek 1990; Wuenschel et al. 2013; McBride et al. 2018). A fish spawned earlier in the season has a longer time to grow before migrating in the fall; therefore, the core measurement for that fish would be larger.

Otolith microchemistry studies often use a fixed transect length for all samples; however, the aim of this study was to target the area prior to fall migration out of natal regions. Thus, the difference in spawning dates influences the amount of time fish spend in these areas. Important chemical data could be missed if the transect was too short for some samples, or material associated with regions outside the natal area could be included if the transect was too long. Wenner et al. (1986) notes that the central opaque region in black sea bass otoliths represents the first 1-4 months of life. Age 0 juveniles display a high degree of site fidelity (Able and Hales 1997), remaining in natal regions from 1 to 6 months until fall migration (Fabrizio et al. 2013). Therefore, the central opaque region was targeted for analysis as it was believed to represent the period prior to fall migration.

Not using a fixed transect length questions whether this variability impacts elemental concentrations due to the amount of material analyzed per sample. Although there was a significant effect of core measurement by region, there was very low correlation and no patterns observed for isotope values (Figures 3.3 and A.1). Therefore, even though the use of

a standardized transect length is recommended, there was little concern of systematic effects on chemical concentrations attributable to this factor in this study.

Recommendations

The population separation at the Hudson Canyon was a result of observed differences between MAB and SNE populations from tagging studies, fisheries independent trawl surveys, commercial and recreational fisheries data, and oceanographic conditions between each region (Cadrin et al. 2016; Miller et al. 2016b; SARC 2016). Based on results from this study, in conjunction with these differences, a substantial number of black sea bass spawned in the MAB and traveling to the GOM is unlikely. Nonetheless, the MAB natal origin assignment of several GOM individuals in this study highlights the need for additional research. These fish are possible strays, or were misclassified (lower associated assignment probabilities), but additional research is required to answer this question. Black sea bass tagging studies are limited to Cape Cod and farther south (Kolek 1990; Able et al. 1995; Able and Hales 1997; Moser and Shepherd 2009; Fabrizio et al. 2014); therefore, a GOM tagging study is prudent and overdue.

Additional otolith microchemistry studies are also warranted. A natal origin analysis with finer spatial detail could help elucidate how black sea bass are moving from SNE into the GOM. This was the first otolith microchemistry study completed for this species, thus, there is a wide range of opportunities to use this technique to learn more about black sea bass stock structure and migration patterns. Supplementing this work with genetic analyses would also contribute more detailed information about population structure in this region.

Conclusion

This study identified unique core elemental fingerprints for SNE and MAB that were used to successfully discriminate known samples between these regions. Statistically significant variations in Ba:Ca, Mg:Ca, Mn:Ca, Cu:Ca, and d18O contributed most to discrimination models; though, d13C was also an important variable in both LDFA and RF models. Zn:Ca and Sr:Ca were less important for discrimination, although, Zn:Ca reduced error in the RF model. GOM classification analyses resulted in 41 samples assigned to SNE as the region of natal origin and 6 to MAB. These results were largely as expected (i.e. most samples were assigned to SNE); however, the few samples assigned to MAB may highlight a need for further research or continued monitoring.

Not much is known about black sea bass' movement, interactions, or potential for long-term success in the GOM. Distribution shifts of a species into a new region can have cascading effects and major implications for management (Fogarty et al. 2007; Bell et al. 2015; Pershing et al. 2015). Differences in life history characteristics, e.g. growth rates (Kolek 1990; Caruso 1995; McMahan et al. 2020), between the populations north and south of the Hudson Canyon could influence proliferation in this new region or response to exploitation. Identifying the natal origin of individuals caught in the upper GOM gives insight on their movement into this region and indicates what life history characteristics they may possess. This study confirms hypotheses that the black sea bass observed in the GOM largely come from SNE; however, additional research is needed to determine whether the evidence of MAB individuals in the GOM is a rare occurrence, or if there are changes in this species' migratory behavior occurring.

This work supplies information to managers for use in future stock assessments. The data suggested that most of the fish from GOM are of SNE origin and, until further work is completed on this species, life history traits of these fish are more likely similar to those of fish from SNE, rather than MAB. Recent trends show black sea bass continuing to propagate into the GOM and additional work should be completed to learn more about this species' movement, residency, and potential for spawning in this new region.

References

Able, K. W., M. P. Fahay, and G. R. Shepherd. 1995. Early life history of black sea bass, Centropristis striata, in the mid-Atlantic Bight and a New Jersey estuary. Fishery Bulletin 93:429–445.

Able, K. W., and L. S. Hales. 1997. Movements of juvenile black sea bass Centropristis striata (Linnaeus) in a southern New Jersey estuary. Journal of Experimental Marine Biology and Ecology 213:153–167.

Arslan, Z., and D. H. Secor. 2008. High resolution micromill sampling for analysis of fish otoliths by ICP-MS: Effects of sampling and specimen preparation on trace element fingerprints. Marine Environmental Research 66:364–371.

Artetxe-Arrate, I., I. Fraile, D. A. Crook, I. Zudaire, H. Arrizabalaga, A. Greig, and H. Murua. 2019. Otolith microchemistry: a useful tool for investigating stock structure of yellowfin tuna (Thunnus albacares) in the Indian Ocean. Marine and Freshwater Research 70:1708–1721.

Ateş, C., Ö. Kaymaz, H. E. Kale, and M. A. Tekindal. 2019. Comparison of test statistics of nonnormal and unbalanced samples for multivariate analysis of variance in terms of type-I error rates. Computational and Mathematical Methods in Medicine:1–8.

Barnes, T. C., and B. M. Gillanders. 2013. Combined effects of extrinsic and intrinsic factors on otolith chemistry: implications for environmental reconstructions. Canadian Journal of Fisheries and Aquatic Sciences 70:1159–1166.

Bath, G. E., S. R. Thorrold, C. M. Jones, S. E. Campana, J. W. McLaren, and J. W. H. Lam. 2000. Strontium and barium uptake in aragonitic otoliths of marine fish. Geochimica et Cosmochimica Acta 64(10):1705–1714.

Bell, R. J., D. E. Richardson, J. A. Hare, P. D. Lynch, and P. S. Fratantoni. 2015. Disentangling the effects of climate, abundance, and size on the distribution of marine fish: an example based on four stocks from the Northeast US shelf. ICES Journal of Marine Science 72(5):1311–1322.

Ben-Tzvi, O., A. Abelson, S. D. Gaines, M. S. Sheehy, G. L. Paradis, and M. Kiflawi. 2007. The inclusion of sub-detection limit LA-ICPMS data, in the analysis of otolith microchemistry, by use of a palindrome sequence analysis (PaSA). Limnology and Oceanography: Methods 5:97–105.

Bigelow, H. B., and W. C. Schroeder. 1953. Black sea bass, Centropristis striata. Pages 407–409 Fishes of the Gulf of Maine. Vol 53. Fishery Bulletin of the Fish and Wildlife Service.

Breiman, L. 2001. Random forests. Machine Learning 45:5–32.

Brown, J. A. 2006. Classification of juvenile flatfishes to estuarine and coastal habitats based on the elemental composition of otoliths. Estuarine, Coastal and Shelf Science 66:594–611.

Burnett, J., L. O'Brien, R. K. Mayo, J. A. Darde, and M. Bohan. 1989. Finfish maturity sampling and classification schemes used during Northeast Fisheries Center bottom trawl surveys, 1963-89. NOAA Technical Memorandum NMFS-F/NEC:1–14.

Cadrin, S., R. Leaf, and O. Jensen. 2016. Contributions to the SAW62 black sea bass stock assessment. Science Center for Marine Fisheries:1–6.

Campana, S. E. 1999. Chemistry and composition of fish otoliths: pathways, mechanisms and applications. Marine Ecology Progress Series 188:263–297.

Campana, S. E. 2005. Otolith elemental composition as a natural marker of fish stocks. Pages 227–245 in S. X. Cadrin, K. D. Friedland, and J. R. Waldman, editors. Stock Identification Methods: Applications in Fishery Science.

Campana, S. E., G. A. Chouinard, J. M. Hanson, A. Frechet, and J. Brattey. 2000. Otolith elemental fingerprints as biological tracers of fish stocks. Fisheries Research 46:343–357.

Campana, S. E., A. J. Fowler, and C. M. Jones. 1994. Otolith elemental fingerprinting for stock identification of Atlantic Cod (Gadus morhua) using laser ablation ICPMS. Canadian Journal of Fisheries & Aquatic Sciences 51:1942–1950.

Campana, S. E., and D. Neilsson. 1985. Microstructure of fish otoliths. Canadian Journal of Fisheries & Aquatic Sciences 42:1014–1032.

Campana, S. E., and S. R. Thorrold. 2001. Otoliths, increments, and elements: keys to a comprehensive understanding of fish populations? Canadian Journal of Fisheries & Aquatic Sciences 58(1):30–38.

Campana, S. E., S. R. Thorrold, C. M. Jones, D. Günther, M. Tubrett, H. Longerich, S. Jackson, N. M. Halden, J. M. Kalish, P. Piccoli, H. De Pontual, H. Troadec, J. Panfili, D. H. Secor, K. P. Severin, S. H. Sie, R. Thresher, W. J. Teesdale, and J. L. Campbell. 1997. Comparison of accuracy, precision, and sensitivity in elemental assays of fish otoliths using the electron microprobe, proton-induced X-ray emission, and laser ablation inductively coupled plasma mass spectrometry. Canadian Journal of Fisheries & Aquatic Sciences 54:2068–2079.

Caruso, P. G. 1995. The age, growth, and spawning of black sea bass (Centropristis striata, Linneaus) in Massachusetts waters. MADMF Black Sea Bass Investigations Internal Report:11–25.

Carvalho, M. G., C. Moreira, J. F. M. F. Cardoso, G. J. A. Brummer, P. van Gaever, H. W. van der Veer, H. Queiroga, P. T. Santos, and A. T. Correia. 2017. Movement, connectivity and population structure of the intertidal fish Lipophrys pholis as revealed by otolith oxygen and carbon stable isotopes. Marine Biology Research 13(7):764–773.

Chant, R. J., J. Wilkin, W. Zhang, B.-J. Choi, E. Hunter, R. Castelao, S. Glenn, J. Jurisa, O. Schofield, R. Houghton, J. Kohut, T. K. Frazer, and M. A. Moline. 2008. Dispersal of the Hudson River plume in the New York Bight. Ocenography 21(4):148–161.

Conway, T. M., and S. G. John. 2014. The biogeochemical cycling of zinc and zinc isotopes in the North Atlantic Ocean. Global Biogeochemical Cycles 28:1111–1128.

Denoyer, E. R., K. J. Fredeen, and J. W. Hager. 1991. Laser solid sampling for inductively coupled plasma mass spectrometry. Analytical Chemistry 63(8):445–457.

Díaz-Uriarte, R., and S. Alvarez de Andrés. 2006. Gene selection and classification of microarray data using random forest. BMC Bioinformatics 7(3):1–13.

Dorval, E., K. Piner, L. Robertson, C. S. Reiss, B. Javor, and R. Vetter. 2011. Temperature record in the oxygen stable isotopes of Pacific sardine otoliths: experimental vs. wild stocks from the Southern California Bight. Journal of Experimental Marine Biology and Ecology 397:136–143.

Drohan, A. F., J. P. Manderson, and D. B. Packer. 2007. Essential fish habitat source document: black sea bass, Centropristis striata, life history and habitat characteristics. NOAA Technical Memorandum NMFS-NE-200. Woods Hole, MA.

Edmonds, J. S., M. J. Moran, N. Caputi, and M. Morita. 1989. Trace element analysis of fish sagittae as an aid to stock identification: pink snapper (Chrysophrys auratus) in Western Australian waters. Canadian Journal of Fisheries and Aquatic Sciences 46:50–54.

Elsdon, T. S., and B. M. Gillanders. 2002. Interactive effects of temperature and salinity on otolith chemistry: challenges for determining environmental histories of fish. Canadian Journal of Fisheries and Aquatic Sciences 59:1796–1808.

Elsdon, T. S., B. K. Wells, S. E. Campana, B. M. Gillanders, C. M. Jones, K. E. Limburg, D. H. Secor, S. R. Thorrold, and B. D. Walther. 2008. Otolith chemistry to describe movements and life-history parameters of fishes: hypotheses, assumptions, limitations and inferences. Oceanography and Marine Biology 46:297–330.

Fabrizio, M. C., J. P. Manderson, and J. P. Pessutti. 2013. Habitat associations and dispersal of black sea bass from a mid-Atlantic Bight reef. Marine Ecology Progress Series 482:241–253.

Fabrizio, M. C., J. P. Manderson, and J. P. Pessutti. 2014. Home range and seasonal movements of black sea bass (Centropristis striata) during their inshore residency at a reef in the mid-Atlantic Bight. Fishery Bulletin 112:82–97.

Farrell, J., and S. E. Campana. 1996. Regulation of calcium and strontium deposition on the otoliths of juvenile tilapia, Oreochromis niloticus. Comparative Biochemistry and Physiology 115A(2):103–109.

Fogarty, M., L. Incze, R. Wahle, D. Mountain, A. Robinson, A. Pershing, K. Hayhoe, A. Richards, and J. Manning. 2007. Potential climate change impacts on marine resources of the northeastern United States. Climate Change and Marine Resources Impacts:1–33.

Fowler, A. J., S. E. Campana, C. M. Jones, and S. . Thorrold. 1995a. Experimental assessment of the effect of temperature and salinity on elemental composition of otoliths using solution-based ICPMS. Canadian Journal of Fisheries & Aquatic Sciences 52:1421–1430.

Fowler, A. J., S. E. Campana, C. M. Jones, and S. R. Thorrold. 1995b. Experimental assessment of the effect of temperature and salinity on elemental composition of otoliths using laser ablation ICPMS. Canadian Journal of Fisheries and Aquatic Sciences 52:1431–1441.

Fox, J., and S. Weisberg. 2019. An {R} Companion to Applied Regression.

Gallahar, N. K., and M. J. Kingsford. 1992. Patterns of increment width and strontium: calcium ratios in otoliths of juvenile rock blackfish, Girella elevata (M.). Journal of Fish Biology 41:749–763.

Gibb, F. M., T. Régnier, K. Donald, and P. J. Wright. 2017. Connectivity in the early life history of sandeel inferred from otolith microchemistry. Journal of Sea Research 119:8–16.

Gillanders, B. M. 2002. Connectivity between juvenile and adult fish populations: Do adults remain near their recruitment estuaries? Marine Ecology Progress Series 240:215–223.

Hamer, P. A., and G. P. Jenkins. 2007. Comparison of spatial variation in otolith chemistry of two fish species and relationships with water chemistry and otolith growth. Journal of Fish Biology 71:1035–1055.

Hoff, G. R., and L. A. Fuiman. 1995. Environmentally induced variation in elemental composition of red drum (Sciaenops ocellatus) otoliths. Bulletin of Marine Science 56(2):578–591.

Hothorn, T., F. Bretz, and P. Westfall. 2008. Simultaneous inference in general parametric models. Biometrical Journal 50(3):346–363.

Van Hulten, M., R. Middag, J.-C. Dutay, H. De Baar, M. Roy-Barman, M. Gehlen, A. Tagliabue, and A. Sterl. 2017. Manganese in the west Atlantic Ocean in the context of the first global ocean circulation model of manganese. Biogeosciences 14:1123–1152.

Javor, B., and E. Dorval. 2014. Geography and ontogeny influence the stable oxygen and carbon isotopes of otoliths of Pacific sardine in the California Current. Fisheries Research 154:1–10.

Jones, C. M., M. Palmer, and J. J. Schaffler. 2017. Beyond Zar: the use and abuse of classification statistics for otolith chemistry. Journal of Fish Biology 90:492–504.

Kalish, J. M. 1989. Otolith microchemistry: validation of the effects of physiology, age and environment on otolith composition. Journal of Experimental Marine Biology and Ecology 132:151–178.

Kalish, J. M. 1990. Use of otolith microchemistry to distinguish the progeny of sympatric anadromous and non-anadromous salmonids. Fishery Bulletin 88(4):657–666.

Kalish, J. M. 1991. 13C and 18O isotopic disequilibria in fish otoliths: metabolic and kinetic effects. Marine Ecology Progress Series 75:191–203.

Kerr, L. A., Z. T. Whitener, S. X. Cadrin, M. R. Morse, D. H. Secor, and W. Golet. 2020. Mixed stock origin of Atlantic bluefin tuna in the U.S. rod and reel fishery (Gulf of Maine) and implications for fisheries management. Fisheries Research 224:1–11.

Kleisner, K. M., M. J. Fogarty, S. McGee, J. A. Hare, S. Moret, C. T. Perretti, and V. S. Saba. 2017. Marine species distribution shifts on the U.S. Northeast Continental Shelf under continued ocean warming. Progress in Oceanography 153:24–36.

Kolek, D. 1990. Homing of black sea bass, Centropristis striata, in Nantucket Sound, with comments on seasonal distribution, growth rates, and fisheries of the species. MADMF Black Sea Bass Investigations Internal Report:2–9.

Kremling, K. 1985. The distribution of cadmium, copper, nickel, manganese, and aluminium in surface waters of the open Atlantic and European shelf area. Deep Sea Research 32(5):531–555.

Laugier, F., E. Feunteun, C. Pecheyran, and A. Carpentier. 2015. Life history of the small sandeel, Ammodytes tobianus, inferred from otolith microchemistry. A methodological approach. Estuarine, Coastal and Shelf Science 165:237–246.

Lenth, R. 2019. Emmeans: estimated marginal means, aka least-squares means. R package version 1.4.3.01.

Liaw, A., and M. Wiener. 2002a. Classification and Regression by randomForest. R News 2(3):18–22.

Loewen, T. N., J. D. Reist, P. Yang, A. Koleszar, J. A. Babaluk, N. Mochnacz, and N. M. Halden. 2015. Discrimination of northern form dolly varden char (Salvelinus malma malma) stocks of the North Slope, Yukon and Northwest Territories, Canada via otolith trace elements and 87Sr/86Sr isotopes. Fisheries Research 170:116–124.

Maguffee, A. C., R. Reilly, R. Clark, and M. L. Jones. 2019. Examining the potential of otolith chemistry to determine natal origins of wild Lake Michigan Chinook Salmon. Canadian Journal of Fisheries and Aquatic Sciences 76:2035–2044.

Manel, S., O. Gaggiotti, and R. Waples. 2005. Assignment methods: matching biological questions with appropriate techniques. Trends in Ecology and Evolution 20(3):136–142.

McBride, R. S., M. K. Tweedie, and K. Oliveira. 2018. Reproduction, first-year growth, and expansion of spawning and nursery grounds of black sea bass (Centropristis striata) into a warming Gulf of Maine. Fishery Bulletin 116:323–336.

McMahan, M. D. 2017. Ecological and socioeconomic implications of a northern range expansion of black sea bass, Centropristis striata. Northeastern University.

McMahan, M. D., G. D. Sherwood, and J. H. Grabowski. 2020. Geographic variation in life-history traits of black sea bass (Centropristis striata) during a rapid range expansion. Frontiers in Marine Science 7(567758):1–15.

Mercer, L. P. 1978. The reproductive biology and population dynamics of black sea bass, Centropristis striata. The College of William and Mary.

Mercer, L. P. 1989. Species profiles: life histories and environmental requirements of coastal fishes and invertebrates (South Atlantic): Black Sea Bass. U.S. Fish Wildlife Service Biological Report 82, Morehead City, NC.

Mercier, L., A. M. Darnaude, O. Bruguier, R. P. Vasconcelos, H. N. Cabral, M. J. Costa, M. Lara, D. L. Jones, and D. Mouillot. 2011. Selecting statistical models and variable combinations for optimal classification using otolith microchemistry. Ecological Applications 21(4):1352–1364.

Middag, R., H. J. W. de Baar, and K. W. Bruland. 2019. The relationships between dissolved zinc and major nutrients phosphate and silicate along the GEOTRACES GA02 transect in the West Atlantic Ocean. Global Biogeochemical Cycles 33:63–84.

Miller, A. S., G. R. Shepherd, and P. S. Fratantoni. 2016a. Offshore habitat preference of overwintering juvenile and adult black sea bass, Centropristis striata, and the relationship to year-class success. PLoS ONE 11(1):1–19.

Miller, J. A., M. A. Banks, D. Gomez-Uchida, and A. L. Shanks. 2005. A comparison of population structure in black rockfish (Sebastes melanops) as determine with otolith microchemistry and microsatellite DNA. Canadian Journal of Fisheries and Aquatic Sciences 62:2189–2198.

Miller, T. J., R. J. Latour, K. Drew, and J. Wiedenmann. 2016b. Proposed partitioning of northern black sea bass stock for purposes of developing spatial stock assessment models. Report to the Mid-Atlantic Fishery Management Council's Scientific and Statistical Committee:1–5.

Moreira, C., E. Froufe, A. N. Sial, A. Caeiro, P. Vaz-Pires, and A. T. Correia. 2018. Population structure of the blue jack mackerel (Trachurus picturatus) in the NE Atlantic inferred from otolith microchemistry. Fisheries Research 197:113–122.

Moser, J., and G. R. Shepherd. 2009. Seasonal distribution and movement of black sea bass (Centropristis striata) in the northwest Atlantic as determined from a mark-recapture experiment. Journal of Northwest Atlantic Fishery Science 40:17–28. Northwest Atlantic Fisheries Organization.

Musick, J. A., and L. P. Mercer. 1977. Seasonal distribution of black sea bass, Centropristis striata, in the Mid-Atlantic Bight with comments on the ecology and fisheries of the species. Transactions of the American Fisheries Society 106(1):12–25.

NEFSC. 2017. 62nd Northeast regional stock assessment workshop. Northeast Fisheries Science Center Reference Assessment Summary Report:1–36.

Pershing, A. J., M. A. Alexander, C. M. Hernandez, L. A. Kerr, A. Le Bris, K. E. Mills, J. A. Nye, N. R. Record, H. A. Scannell, J. D. Scott, G. D. Sherwood, and A. C. Thomas. 2015. Slow adaptation in the face of rapid warming leads to collapse of the Gulf of Maine cod fishery. Science 350(6262):809–812.

Radtke, R. L. 1989. Strontium-calcium concentration ratios in fish otoliths as environmental indicators. Comparative Biochemical Physiology 92A(2):189–193.

Régnier, T., J. Augley, S. Devalla, C. D. Robinson, P. J. Wright, and F. C. Neat. 2017. Otolith chemistry reveals seamount fidelity in a deepwater fish. Deep-Sea Research Part I 121:183–189.

Ruttenberg, B. I., S. L. Hamilton, M. J. H. Hickford, G. L. Paradis, M. S. Sheehy, J. D. Standish, O. Ben-Tzvi, and R. R. Warner. 2005. Elevated levels of trace elements in cores of otoliths and their potential for use as natural tags. Marine Ecology Progress Series 297:273–281.

Sadovy, Y., and K. P. Severin. 1992. Trace elements in biogenic aragonite: correlation of body growth rate and strontium levels in the otoliths of the white grunt, Haemulon Plumieri (Pisces: Haemulidae). Bulletin of Marine Science 50(2):237–257.

Sadovy, Y., and K. P. Severin. 1994. Elemental patterns in red hind (Epinephelus guftatus) otoliths from Bermuda and Puerto Rico reflect growth rate, not temperature. Canadian Journal of Fisheries and Aquatic Sciences 51:133–141.

SARC. 2016. Proposed partitioning of northern black sea bass stock for purposes of developing spatial stock assessment models. Black Sea Bass Benchmark Stock Assessment Review Term of Reference - Spatial Issues:1–40.

Secor, D. H. 1999. Specifying divergent migrations in the concept of stock: the contingent hypothesis. Fisheries Research 43:13–34.

Shiller, A. M. 1997. Manganese in surface waters of the Atlantic Ocean. Geophysical Research Letters 24(12):1495–1498.

Steer, M. A., A. J. Fowler, and B. M. Gillanders. 2009. Age-related movement patterns and population structuring in southern garfish, Hyporhamphus melanochir, inferred from otolith chemistry. Fisheries Management and Ecology 16:265–278.

Steimle, F. W., C. A. Zetlin, P. L. Berrien, and S. Chang. 1999. Essential fish habitat source document: life history and habitat characteristics. NOAA Technical Memorandum NMFS-NE-143:1–42.

Sturrock, A. M., E. Hunter, J. A. Milton, R. C. Johnson, C. P. Waring, and C. N. Trueman. 2015. Quantifying physiological influences on otolith microchemistry. Methods in Ecology and Evolution 6:806–816.

Tanner, S. E., P. Reis-Santos, and H. N. Cabral. 2016. Otolith chemistry in stock delineation: a brief overview, current challenges and future prospects. Fisheries Research 173:206–213.

Tanner, S. E., P. Reis-Santos, R. P. Vasconcelos, S. França, S. R. Thorrold, and H. N. Cabral. 2012. Otolith geochemistry discriminates among estuarine nursery areas of Solea solea and S. senegalensis over time. Marine Ecology Progress Series 452:193–203.

Thomas, D. R., and B. D. Zumbo. 1996. Using a measure of variable importance to investigate the standardization of discriminant coefficients. Journal of Educational and Behavioral Statistics 21(2):110–130.

Thorrold, S. R., S. E. Campana, C. M. Jones, and P. K. Swart. 1997a. Factors determining δ 13C and δ 18O fractionation in aragonitic otoliths of marine fish. Geochimica et Cosmochimica Acta 61(14):2909–2919.

Thorrold, S. R., C. M. Jones, and S. E. Campana. 1997b. Response of otolith microchemistry to environmental variations experienced by larval and juvenile Atlantic croaker (Micropogonias undulatus). Limnology and Oceanography 42(1):102–111.

Thorrold, S. R., C. M. Jones, P. K. Swart, and T. E. Targett. 1998. Accurate classification of juvenile weakfish Cynoscion regalis to estuarine nursery areas based on chemical signatures in otoliths. Marine Ecology Progress Series 173:253–265.

Thresher, R. E. 1999. Elemental composition of otoliths as a stock delineator in fishes. Fisheries Research 43:165–204.

Tournois, J., F. Ferraton, L. Velez, D. J. McKenzie, C. Aliaume, L. Mercier, and A. M. Darnaude. 2013. Temporal stability of otolith elemental fingerprints discriminates among lagoon nursery habitats. Estuarine, Coastal and Shelf Science 131:182–193.

Townsend, D. W., R. L. Radtke, S. Corwin, and D. A. Libby. 1992. Strontium:calcium ratios in juvenile Atlantic herring Clupea harengus L. otoliths as a function of water temperature. Journal of Experimental Marine Biology and Ecology 160:131–140.

Townsend, D. W., R. L. Radtke, D. P. Malone, and J. P. Wallinga. 1995. Use of otolith strontium:calcium ratios for hindcasting larval cod Gadus morhua distributions relative to water masses on Georges Bank. Marine Ecology Progress Series 119:37–44.

Townsend, D. W., R. L. Radtke, M. A. Morrison, and S. D. Folsom. 1989. Recruitment implications of larval herring overwintering distributions in the Gulf of Maine, inferred using a new otolith technique. Marine Ecology Progress Series 55:1–13.

Venables, W, and B. D. Ripley. 2002. Modern applied statistics. Fourth Ed. Springer, New York.

Wenner, C. A., W. A. Roumillat, and C. W. Waltz. 1986. Contributions to the life history of black sea bass, Centropristis striata, off the Southeastern United States. Fishery Bulletin 84(3):723–741.

Wickham, H. 2016. ggplot2: elegant graphics for data analysis. Springer-Verlag, New York.

Wilk, S. J., W. W. Morse, and L. L. Stehlik. 1990. Annual cycles of gonad-somatic indices as indicators of spawning activity for selected species of finfish collected from the New York Bight. Fishery Bulletin 88:775–786.

Wuenschel, M. J., R. S. McBride, and G. R. Fitzhugh. 2013. Relations between total gonad energy and physiological measures of condition in the period leading up to spawning: results of a laboratory experiment on black sea bass (Centropristis striata). Fisheries Research 138:110–119.

Wuenschel, M. J., G. R. Shepherd, R. S. McBride, R. Jorgensen, K. Oliverira, E. Robillard, and J. Dayton. 2011. Sex and maturity of black sea bass collected in Massachusetts and Rhode Island waters; preliminary results based on macroscopic staging of gonads with a comparison to survey data. Working Paper for SARC 53-Black Sea Bass Meeting:529–559.

Figures

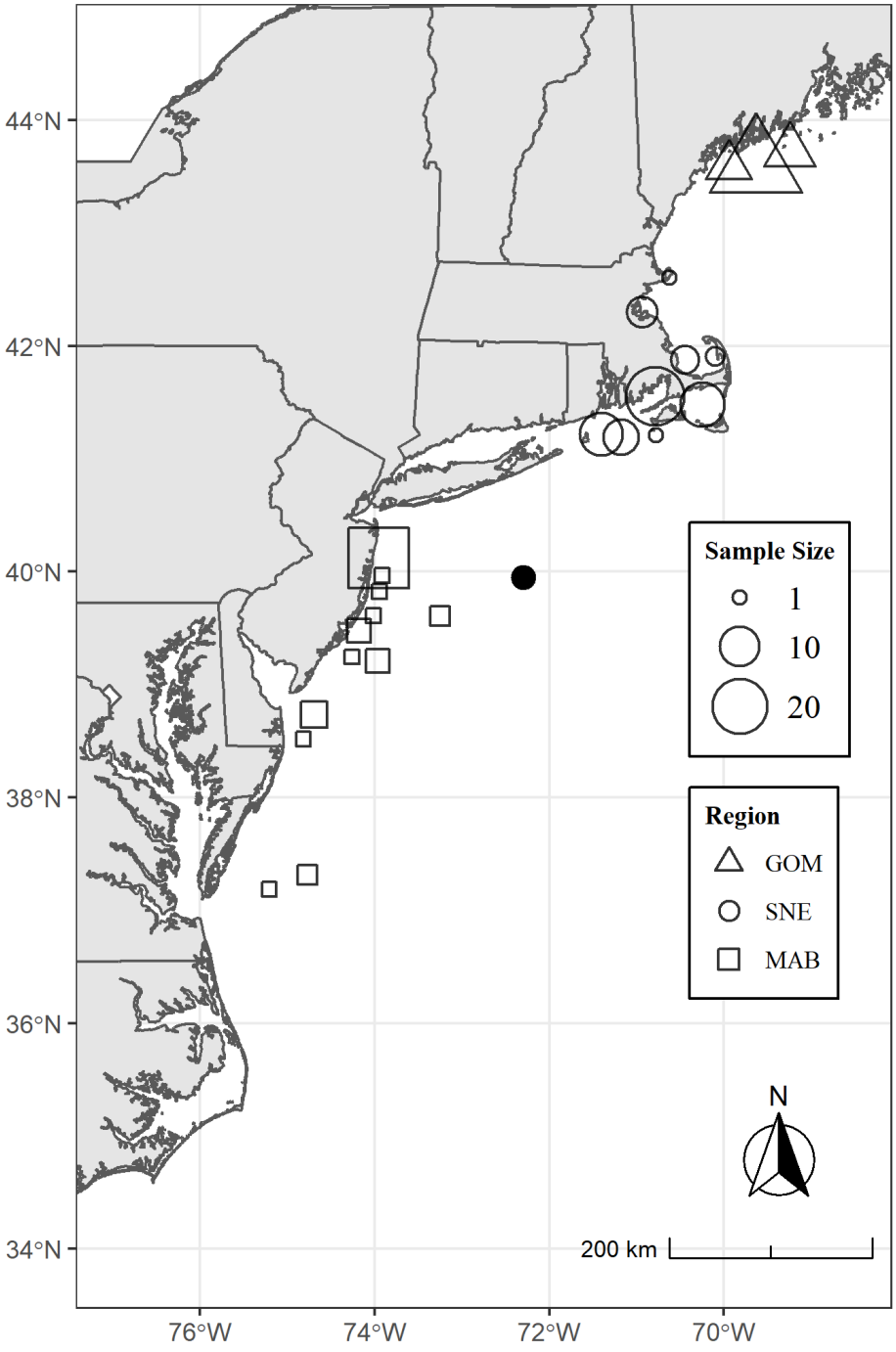

Figure 3.1: Map of samples used for LA-ICPMS and GB-IRMS. Triangles represent GOM, circles are SNE, and squares are MAB. Size of symbols are weighted by sample size. Dark circle represents samples (n = 3) designated to SNE (based on the Northeast Statistical Area separation in SARC 2016) removed from analyses because of proximity to MAB.

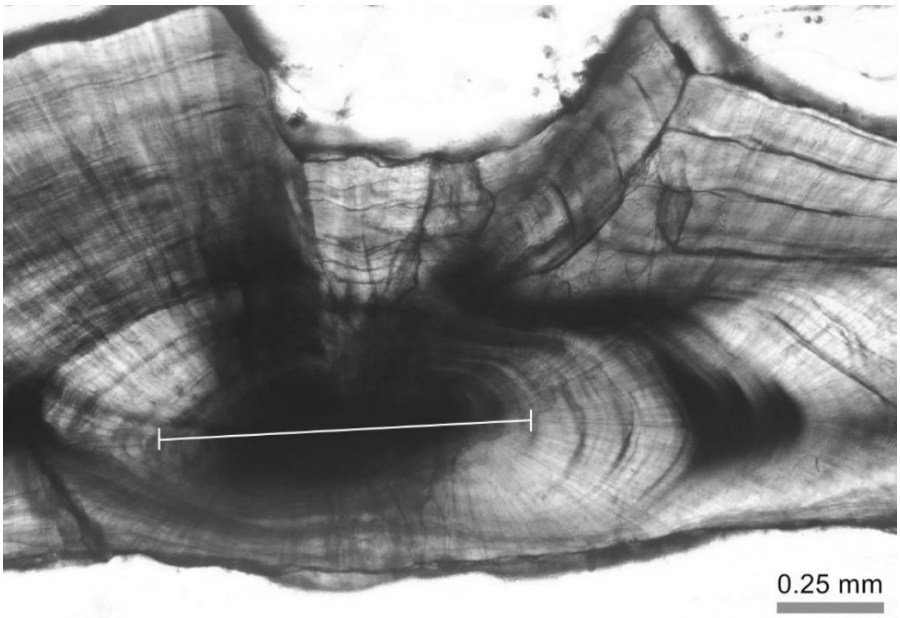

Figure 3.2: Sectioned black sea bass otolith with core transect for microchemical analyses. White solid line indicates the sampling transect through the opaque region of otolith core for LA-ICPMS and GB-IRMS.

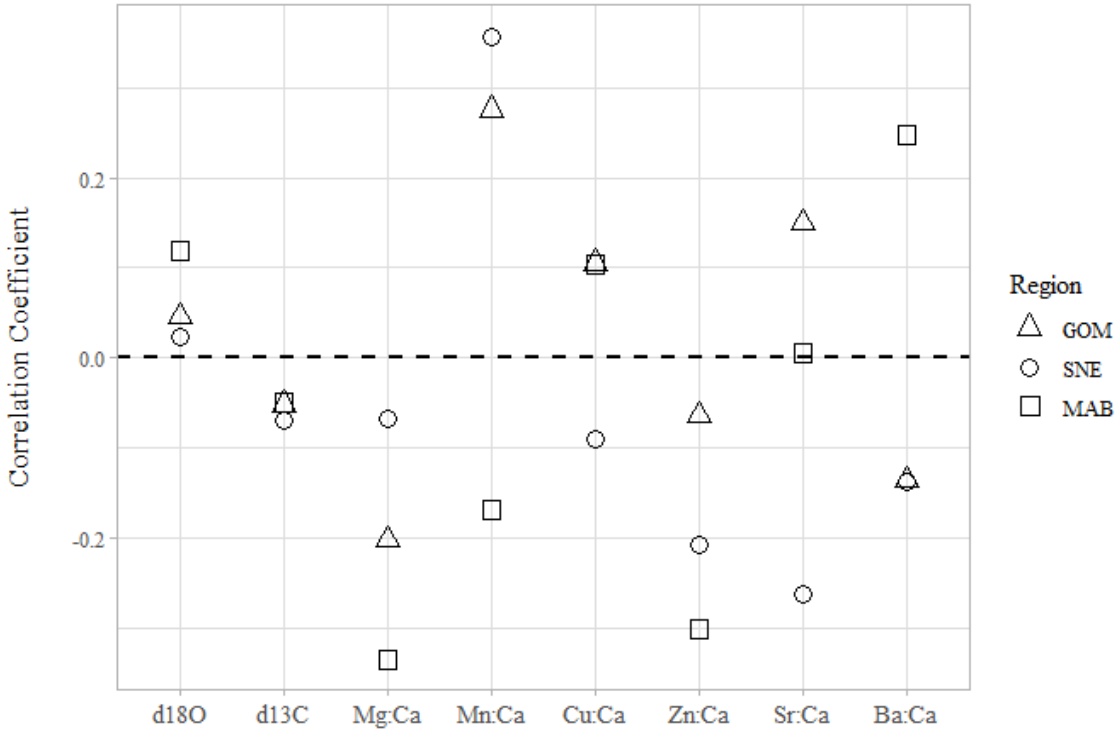

Figure 3.3: Correlation coefficients between core measurements and isotopic variables for each region (Pearson's correlation, alpha = 0.05).

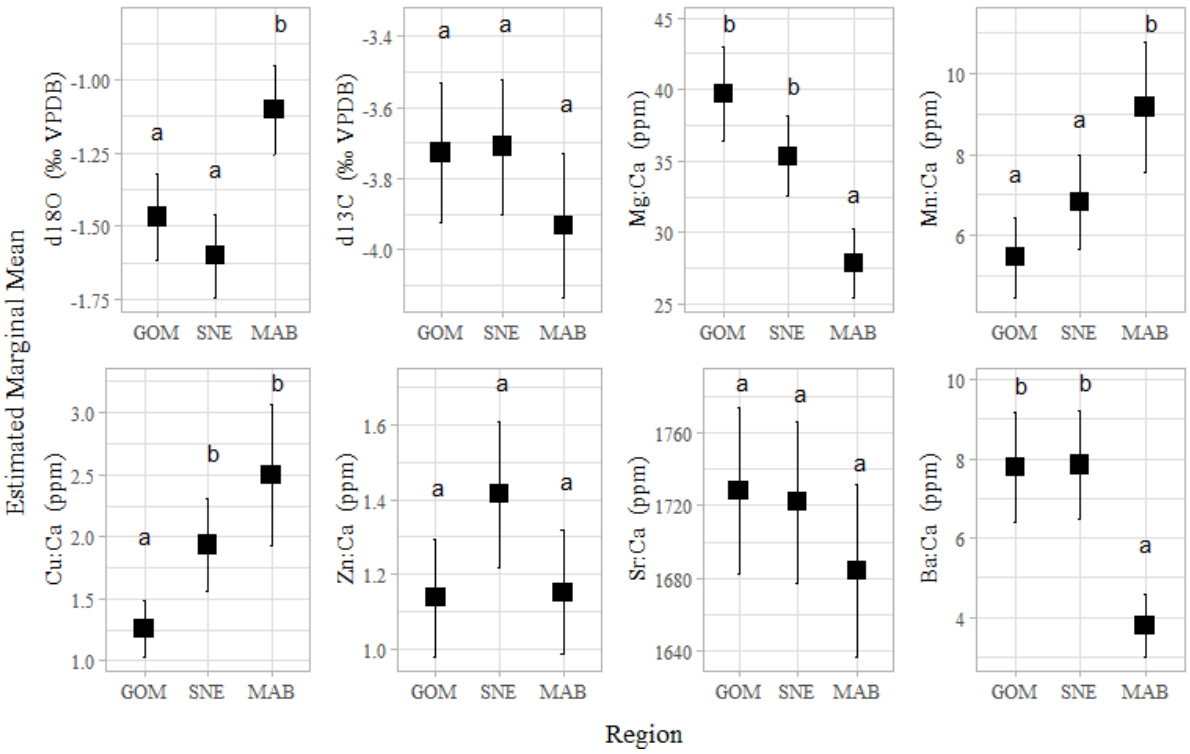

Figure 3.4: Estimated marginal means of each isotope by Region. Letters denote significant differences (Tukey's HSD; alpha = 0.05). Error bars represent two standard errors of the estimated marginal mean.

Tables

Table 3.1: Pearson's correlation coefficients between isotopes (alpha = 0.05). Gray highlighted values are within-element correlations used for comparisons. Mn55 was removed from correlation analysis because no other manganese isotope was evaluated.

	Mg24	Mg25	Mg26	Cu63	Cu65	Zn64	Zn66	Sr86	Sr87	Sr88	Ba136	Ba137	Ba138
Mg24	1	0.99	0.99	0.19	0.18	0.48	0.42	0.11	0.17	0.1	0.03	0.03	0.04
Mg25		1	0.99	0.19	0.18	0.47	0.4	0.12	0.19	0.11	0.01	0.01	0.03
Mg26			1	0.18	0.17	0.49	0.43	0.1	0.15	0.07	0.01	0.01	0.03
Cu63				1	0.98	0.24	0.25	0.11	0.08	0.04	-0.04	-0.01	-0.02
Cu65					1	0.26	0.28	0.09	0.07	0.03	-0.04	-0.01	-0.01
Zn64						1	0.89	0.08	0.07	0.04	0.04	0.09	0.16
Zn66							1	0.05	0.07	0.01	0.03	0.08	0.13
Sr86								1	0.86	0.79	0.22	0.23	0.21
Sr87									1	0.79	0.15	0.17	0.17
Sr88										1	0.23	0.24	0.24
Ba136											1	0.98	0.96
Ba137												1	0.98
Ba138													1

Table 3.2: Sample data for otoliths used in microchemical analyses. F = female; M = male; Unk = unknown sex.

Region	Age Range (years)	Year Classes	F	M	Unk	Gear Type	Total
GOM 'Mixed Stock'	2 - 4	2010 - 2016	30	16	1	Trap; Trawl; Hook & Line	47
SNE 'Spawning Adults'	2 - 6	2010 - 2015	26	24	0	Trap; Trawl; Hook & Line	50
MAB 'Spawning Adults'	2 - 6	2010 - 2015	17	27	0	Trap; Trawl	44

Table 3.3: ANOVA results examining the effect of Region on each isotope. Asterisk denotes that one outlier was removed from analysis.

Isotope	F-value	df	p-value
d18O	12.169	2	< 0.0001
d13C	1.540	2	0.2180
Mg:Ca*	18.543	2	< 0.0001
Mn:Ca	8.474	2	< 0.001
Cu:Ca	12.223	2	< 0.0001
Zn:Ca	3.134	2	0.0467
Sr:Ca	1.043	2	0.3553
Ba:Ca	19.154	2	< 0.0001

Table 3.4: Standardized LDFA coefficients to assess variable importance. Values are listed in decreasing order. Zn:Ca and Sr:Ca left out of model output due to low importance.

Isotope	LD1 Coefficients
Ba:Ca	-1.0109
d18O	0.5404
d13C	-0.5124
Mn:Ca	0.4334
Mg:Ca	-0.3564
Cu:Ca	-0.3023

Table 3.5: LDFA percent accuracy for candidate models. Model with highest accuracy chosen for analysis (Model 4).

No.	Candidate Model	Accuracy
1	Region ~ all isotopes	84.04%
2	Region ~ significant isotopes (sig)	81.91%
3	Region ~ sig + Zn:Ca	81.91%
4	Region ~ sig + d13C	85.11%
5	Region ~ sig + Sr:Ca	81.91%
6	Region ~ sig + Zn:Ca + d13C	84.04%
7	Region ~ sig + Zn:Ca + Sr:Ca	80.85%
8	Region ~ sig + d13C + Sr:Ca	84.04%

Table 3.6: RF mean decrease in Gini coefficient for variable importance. Values are listed in decreasing order of importance.

Isotope	Gini Mean Decrease
Ba:Ca	10.88
d18O	7.83
Mg:Ca	5.70
Cu:Ca	5.63
Mn:Ca	4.73
Zn:Ca	4.15
d13C	3.85
Sr:Ca	3.54

Table 3.7: RF OOB error rate for candidate models. Model with lowest error rate chosen for analysis (Model 6).

No.	Candidate Model	OOB Error Rate
1	Region ~ all isotopes	15.96%
2	Region ~ significant isotopes (sig)	26.60%
3	Region ~ sig + Zn:Ca	18.09%
4	Region ~ sig + d13C	21.28%
5	Region ~ sig + Sr:Ca	23.40%
6	Region ~ sig + Zn:Ca + d13C	12.77%
7	Region ~ sig + Zn:Ca + Sr:Ca	20.21%
8	Region ~ sig + d13C + Sr:Ca	20.21%

Supplemental Materials

Additional Figures and Tables

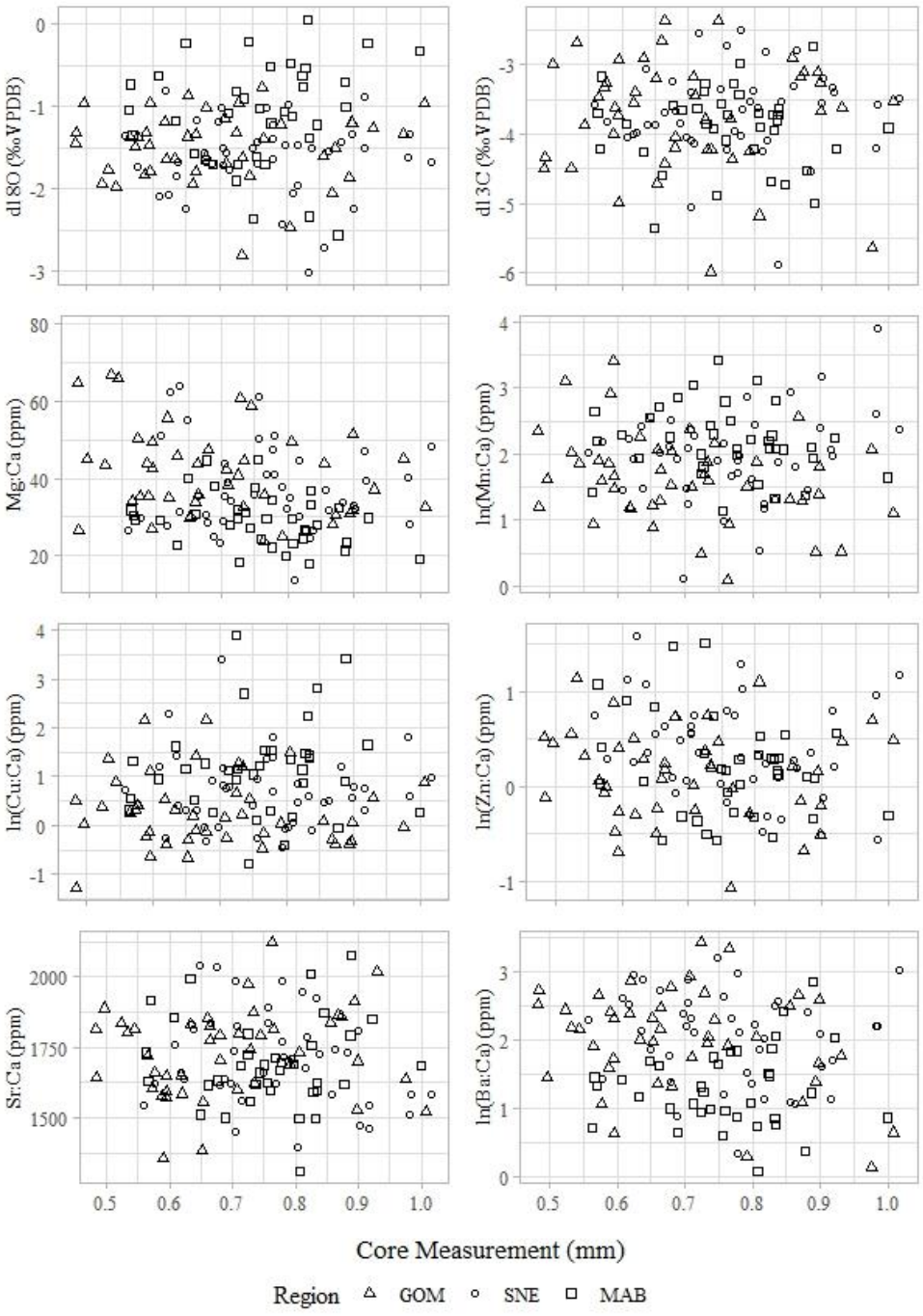

Figure 3.5: Isotope concentration by core measurements for each region (raw data). Triangles represent GOM, circles SNE, and squares MAB.

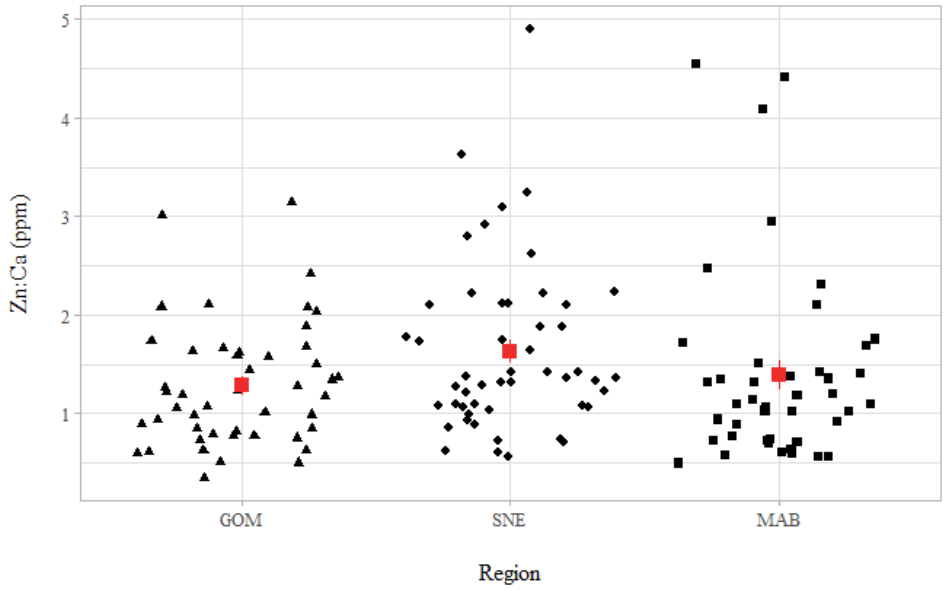

Figure 3.6: Zn:Ca raw data by each region. Red squares are region means; red lines are 1 standard error of the mean.

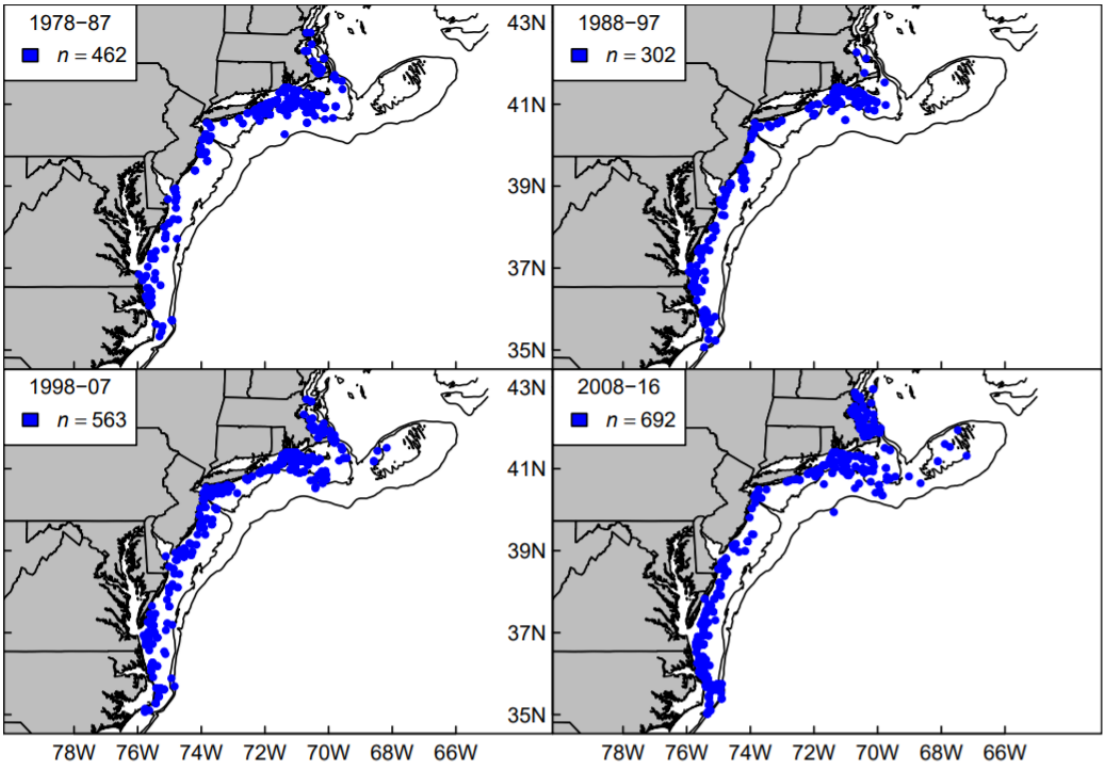

Figure 3.7: Age 0 black sea bass (≤ 12 cm) distribution in the fall Northeast Fisheries Science Center bottom trawl survey from 1978-2016 (Supplemental Figure 4 from McBride et al. 2018). The isobars are 50 and 100 m; sample sizes indicated by n.

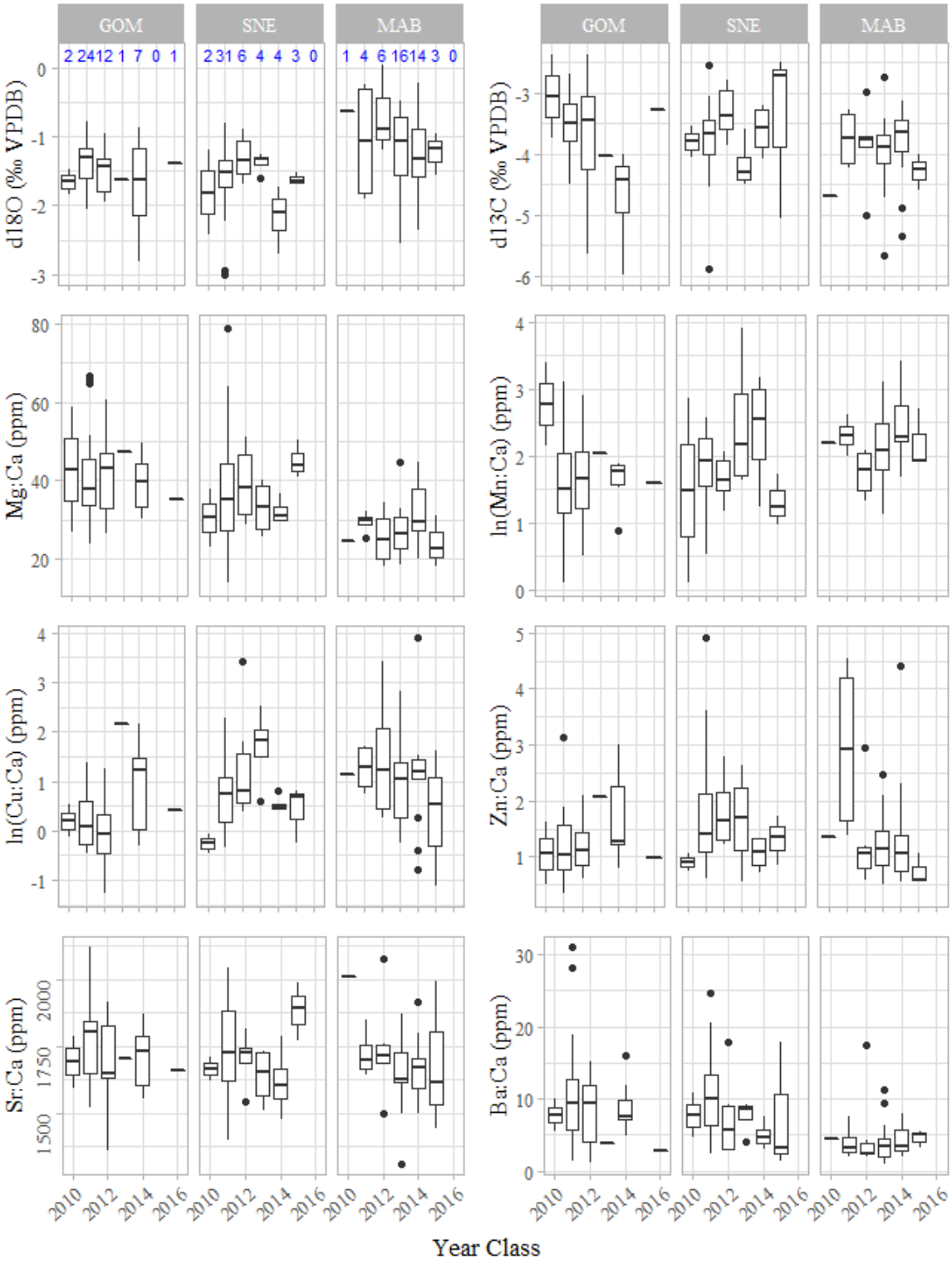

Figure 3.8: Boxplots for each isotope by region and year class. Blue numbers indicate sample sizes and apply to all isotopes.

Table 3.8: Average bottom water temperature (ºC) for SNE and MAB from collaborative black sea bass data (Chapter 2). SNE data was from MA-DMF Resource Assessment and Ventless Trap Surveys. MAB data was from NEFSC bottom trawl survey and NJ Ventless Trap Survey (Rutgers University). Cells highlighted in gray are the months in which microchemical samples were used, for each region. Northeast statistical areas are ordered from north to south.

	Statistical Area	May	Jun	Jul	Aug	Sept	Region Average
SNE	514	7.8	7.0			19.3	15.3
	537	9.9	17.1	14.5	16.5	17.8	
	538	13.1	17.7	20.3	22.3	20.9	
	539	8.3				17.3	
	Monthly Average	9.8	13.9	17.4	19.4	18.9	

	Statistical Area	May	Jun	Jul	Aug	Sept	Region Average
MAB	614		13.5	16.0	22.5	18.7	16.6
	615	9.1				18.3	
	621					17.6	
	625					21.1	
	626					12.7	
	Monthly Average	9.1	13.5	16.0	22.5	17.7	

Table 3.9: Black sea bass NEFSC tag recoveries by region, north and south of the Hudson Canyon from 2002-2007 (Table 2 from SARC 2016).

	Recovery location	
Release location	North	South
North	93.1%	6.9%
South	0.7%	99.3%

Table 3.10: Compiled fish maturity information (females only) for samples collected in Chapter 1 (n = 1,411): (a) SNE and (b) MAB. Maturity codes: T = resting; D = developing; R = ripe; U = running ripe; S = spent.

(a)

Month	T	D	R	U	S	Count
Jan	75%				25%	8
Feb						NA
Mar	100%					1
Apr		89%	11%			9
May	1%	84%	12%	3%		457
Jun	0%	70%	27%	2%		252
Jul	8%	38%	27%	18%	9%	179
Aug	12%	23%	16%	33%	17%	129
Sep	73%	5%	1%	1%	20%	282
Oct	69%	3%			28%	32
Nov						NA
Dec						NA

(b)

Month	T	D	R	U	S	Count
Jan						NA
Feb	89%	7%			4%	27
Mar	91%	9%				11
Apr		100%				6
May						NA
Jun						NA
Jul						NA
Aug				100%		2
Sep			100%			16
Oct						NA
Nov						NA
Dec						NA

SNE YOY and SNE Spawning Adult Comparisons

YOY from SNE were collected from the Massachusetts Division of Marine Fisheries (MA-DMF) Fall Resource Assessment Survey in 2017 (n = 29). One additional YOY sample was used from the MA-DMF otolith archive from 2016. Otoliths were embedded using West System® epoxy resin and hardener in silicone molds. Transverse sections (0.5mm) along the dorsoventral plane, containing the otolith core were removed using a low speed Buehler® Iso-Met^{TM} diamond blade saw. Otoliths were mounted, photographed, measured, and analyzed for core elemental concentrations as described in the study above. Nine samples were removed due to issues of broken otolith sections or instrumentation error.

Skewed isotopic distributions required data transformations for SNE YOY and SNE spawning adults. Mg:Ca, Mn:Ca and Ba:Ca were log10 transformed, Cu:Ca and Zn:Ca were inverse transformed, and Sr:Ca, d18O, and d13C were not transformed. Normality, homogeneity of variance and covariance, and outliers were assessed using diagnostic plots, the Shapiro-Wilk test (alpha = 0.05), and Levene's test (alpha = 0.05). Mg:Ca did not pass the Shapiro-Wilk test ($p = 0.0055$), and Cu:Ca did not pass Levene's test ($p = 0.015$); however, inspection of diagnostic plots showed very little departure from normality and homogeneity, respectively, and parametric tests were considered suitable for these isotopes.

The elemental fingerprints differed significantly between each of these groups (MANOVA, Pillai's Trace = 0.77, $F = 25.82$, $df = 8$, $p < 0.0001$). Individual elemental ANOVAs showed significant differences in the estimated marginal means for d18O ($F = 34.488$, $df = 1$, $p < 0.0001$), d13C ($F = 14.852$, $df = 1$, $p < 0.001$), Mg:Ca ($F = 114.17$, $df = 1$, $p < 0.0001$), Cu:Ca ($F = 17.719$, $df = 1$, $p < 0.0001$), Zn:Ca ($F = 8.853$, $df = 1$, $p < 0.01$), and

Ba:Ca ($F = 14.938$, $df = 1$, $p < 0.001$). No significant differences were seen in Mn:Ca ($F = 0.2432$, $df = 1$, $p = 0.6235$), or Sr:Ca ($F = 0.3413$, $df = 1$, $p = 0.561$). These results are shown visually in Figure 3.9.

The comparisons between SNE spawning adults and SNE YOY show significantly different core elemental compositions, except for Mn:Ca and Sr:Ca. Though the YOY samples were expected to corroborate the elemental fingerprint in the SNE spawning region, discrepancies in years and areas sampled between each group could result in the differences observed. The year classes sampled for SNE spawning adults were from 2010-2015 compared to the 2016-2017 range for SNE YOY. Additionally, YOY largely came from Buzzards Bay and the Vineyard Sound (Figure 3.10); whereas, SNE spawning adults were sampled from a larger area of the region (Figure 3.1). As shown in Figure 3.8, interannual variation is common for elements within regions. Upon closer inspection, all the SNE YOY isotopes lie within the ranges of variability for SNE adults observed in this figure, except for Mg:Ca. The average concentration for Mg:Ca in SNE YOY is approximately five times higher than the average for SNE adults. The reason for this magnitude of a difference is unclear.

The true source of disparity between elemental fingerprints is difficult to discern; however, most elemental concentrations for SNE YOY were within the interannual variation observed in SNE adults. Nevertheless, SNE YOY data were excluded from the mixed stock classification analysis because they represented years not accounted for in the other regions. Additionally, no YOY were collected from MAB to include in conjunction with SNE YOY. The use of spawning condition adults in the mixed stock classification analysis was

representative of all spawning locations and years and, thus, were more reliable proxies for regional chemical fingerprints.

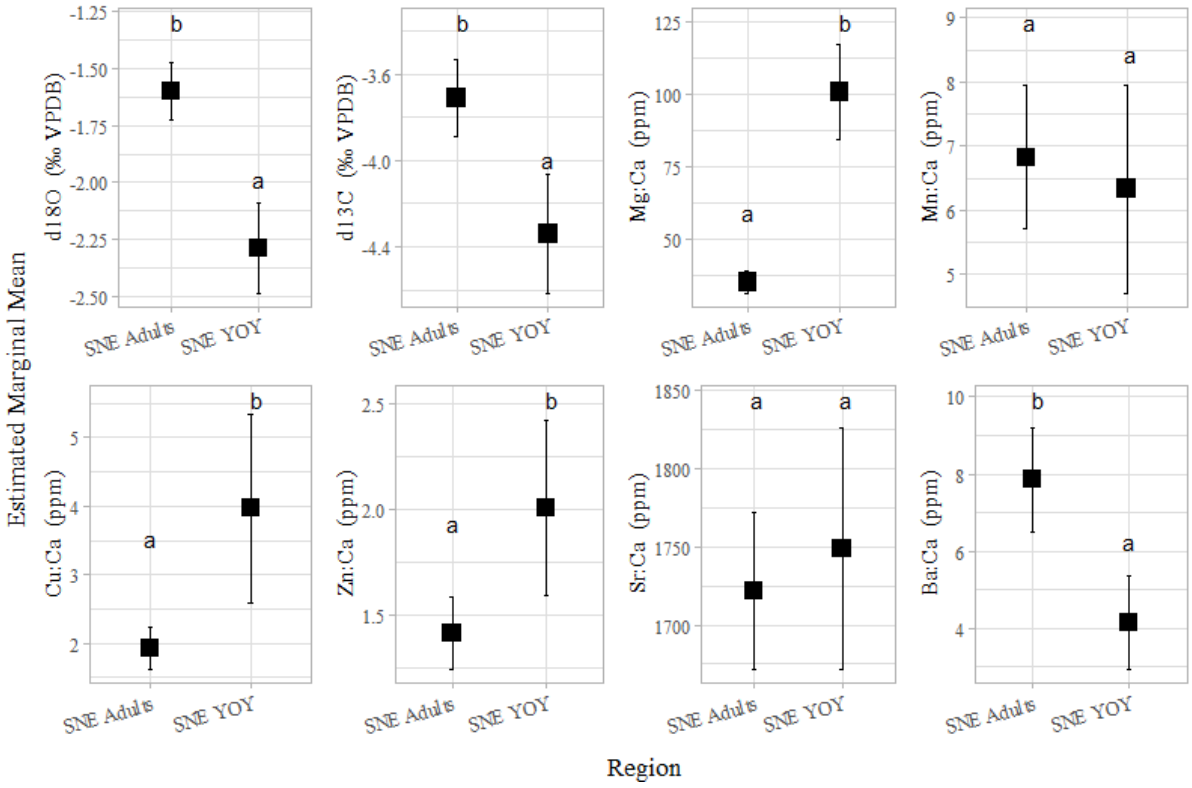

Figure 3.9: SNE spawning adult (n = 50) and SNE YOY (n = 21) estimated marginal means for each isotope. Letters denote significant differences (ANOVA; alpha = 0.05). Error bars represent two standard errors of the estimated marginal mean.

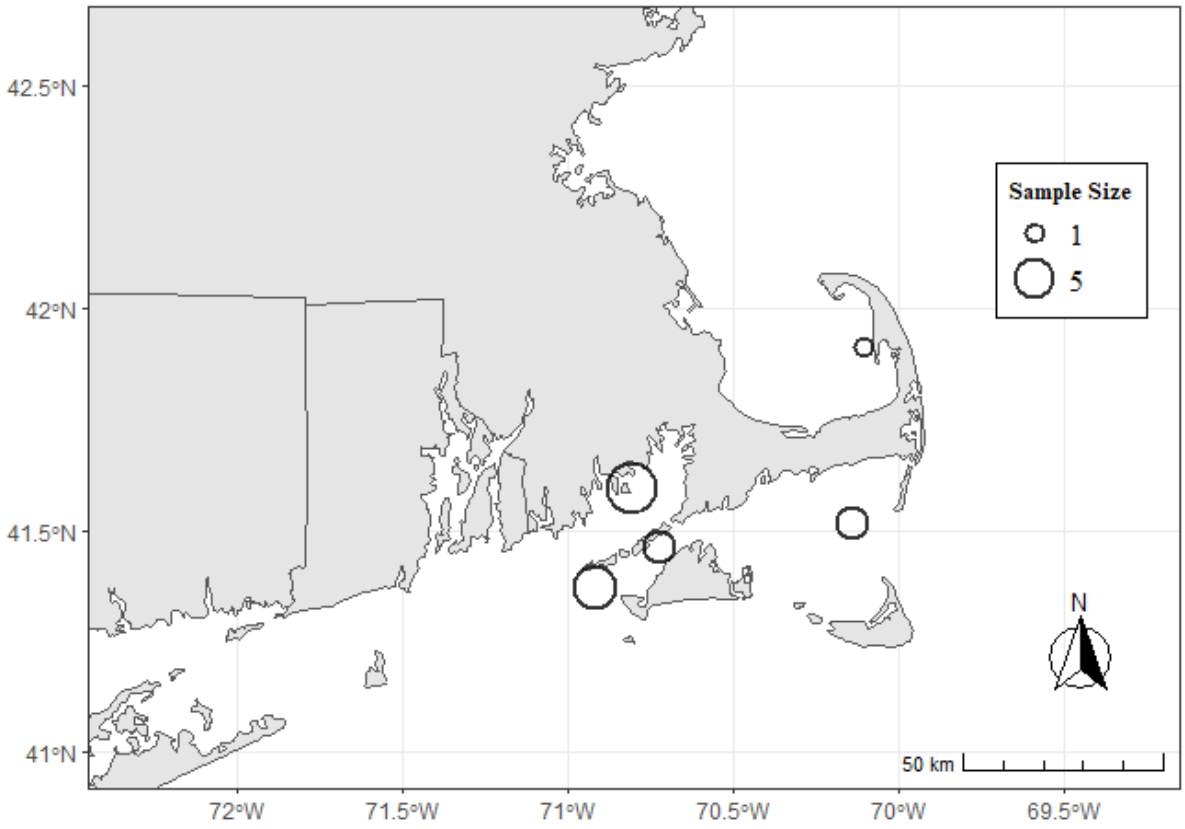

Figure 3.10: Map of SNE YOY samples used for microchemical analyses (n = 21).

Additional Random Forest Probability Threshold Levels

Additional RF probability levels were analyzed to look at the effects on GOM sample assignment. A threshold probability level of 0.50 allowed for all samples to be assigned and no data were lost from the analysis; however, those samples just above the 0.50 level were allocated to a group despite a large amount of uncertainty. Figure 3.11 shows that increasing the probability threshold increased the number of samples that were not assigned to either group. One sample from SNE becomes unassigned at a level of 0.55, followed by the removal of two samples from MAB at 0.60. Ultimately, six samples were removed from SNE

and four samples from MAB at a probability threshold of 0.70. At this threshold, the overall average probability of samples assigned to SNE was 0.87 versus 0.73 for MAB. Though some samples were removed from each region as the threshold was increased, the pattern of assignment remained the same. A large percentage of the GOM samples were assigned to SNE and these samples had a high probability of originating from this region. Few samples appeared to originate from MAB and the average probability of those samples was lower.

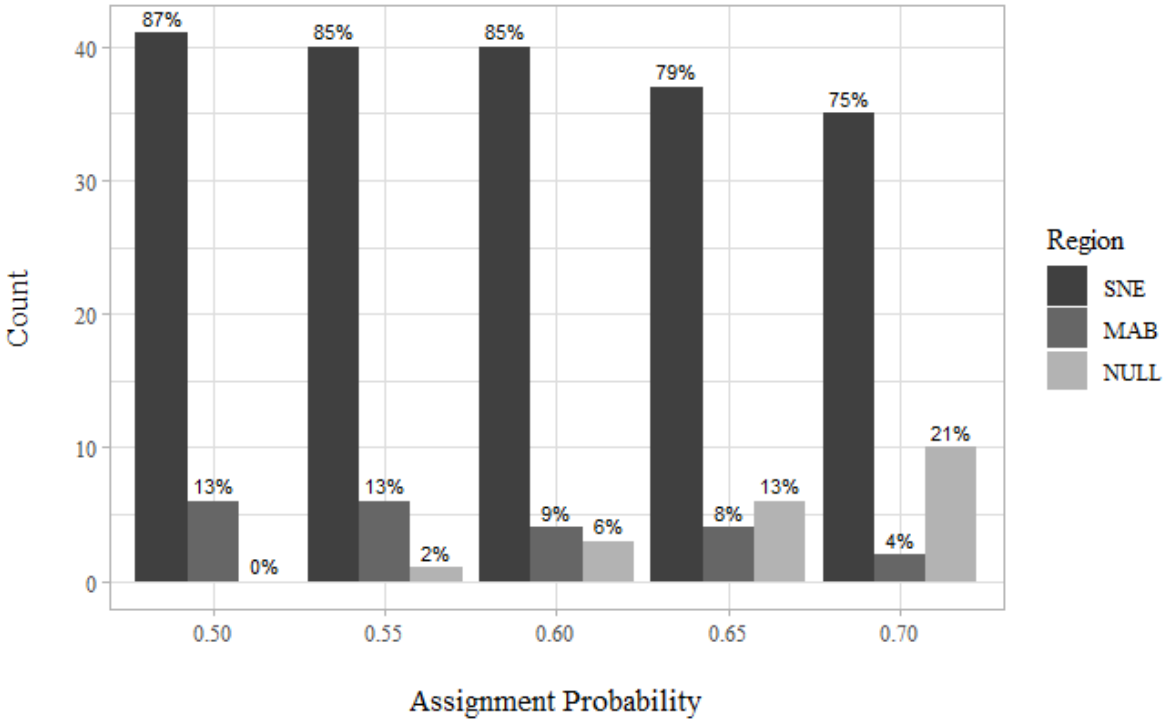

Figure 3.11: Bar chart of GOM samples assigned to each region for assignment probabilities between 0.50 and 0.70. Numbers above bars are the percentages of GOM samples assigned to each region within each probability level.

CHAPTER 4

CONCLUSION

This thesis provided important conclusions regarding the validity of the otolith ageing method for the northern stock of black sea bass. Further, for the first time, otolith microchemical analyses were used to elucidate the natal origin of black sea bass caught in the upper Gulf of Maine (GOM). These results contributed insights into the species' life history in the northern Atlantic stock, particularly age, migration, and population structure.

Validating the otolith ageing method for the northern stock of black sea bass increases the confidence in the quality and accuracy of age data used in stock assessments. This study demonstrated that one opaque annulus is deposited per year in late spring or early summer. This finding was consistent throughout the age range of this species, as well as for the populations north and south of the Hudson Canyon. This study also validated the location of the first annulus, a region that often leads to high rates of ageing error and had not previously been completed in the published literature. Additionally, this was the first ageing project for this species that utilized samples representing the entire spatial range of the northern stock, as well as included a variety of capture methods and fishery types. Based on this study, use of otoliths for future ageing is recommended, particularly for data contributed to upcoming stock assessments.

Information gathered from otolith microchemistry in this study identified unique core chemical signatures for the two known spawning regions of black sea bass in the northern stock, Southern New England (SNE) and the mid-Atlantic Bight (MAB). The differences between these two regions were largely driven by Ba:Ca, Mg:Ca, d18O, Mn:Ca, and Cu:Ca, though d13C was also useful for discrimination. Comparing otolith core chemical signatures of black sea bass caught in Maine waters (grouped as GOM) to these two regions showed that most elemental concentrations were closer to SNE than MAB. Further analyses assigned 87% of the GOM samples to SNE as the region of natal origin and 13% to MAB. This study confirmed the assumption that GOM fish have travelled from SNE; however, the presence of possible MAB spawned black sea bass was surprising. Future stock assessments should presume that most fish in the GOM are of SNE origin; however, additional studies are needed to track and monitor migration and residency in the GOM.

Movement of the northern stock of black sea bass into Maine waters has raised many questions about changes to life history, behavior, and migration. This body of work utilized methodology not previously employed to study this species and presented insights into impacts this movement has had on regional populations. Additional research on this species in the GOM is needed - first, to better understand the current movement of black sea bass into this region, but also to monitor its long-term success, formation of new potential spawning groups, and influences on other species.

BIOGRAPHICAL SKETCH OF AUTHOR

Elise Koob's interest in marine science somewhat ironically began as a child living in a land-locked, midwestern state. The desire to learn about the ocean never waned and she eventually attended college at the University of New Hampshire in Durham and received a B.S. in Marine Biology with a minor in Environmental Science. Elise pursued an opportunity to study abroad in New Zealand, which gave her an incredible education in environmental conservation. She then traveled to Brisbane, Australia for an internship with the Commonwealth Scientific and Industrial Research Organization and worked on an age and growth project on golden trevally, a large marine fish. This was her first otolith-focused project and the experience she gained led to a position at the Gulf of Maine Research Institute for a study on bluefin tuna and swordfish otoliths. From there, Elise secured a position with the Massachusetts Division of Marine Fisheries Age and Growth Laboratory and shortly after began working on her graduate degree. She hopes to continue her career in fisheries science research.